Screens for Components of AC Invasion and Establishment of the Anchorage of the Egg-Laying System

and

Studying Candidate Genes for their Involvement in Associative Learning in *C. elegans*

Dissertation

zur

Erlangung der naturwissenschaftlichen Doktorwürde

(Dr. sc.nat.)

vorgelegt der

Mathematisch-naturwissenschaftlichen Fakultät

der

Universität Zürich

von

Sara M. Vassalli

aus

Riva San Vitale TI

Promotionskomitee:

Prof. Dr. Alex Hajnal, Universität Zürich

(Vorsitz, Leitung der Dissertation)

Prof. Dr. Michael Hengartner, Universität Zürich

Prof. Dr. Urs Greber, Universität Zürich

Dr. Michel Labouesse, IGBMC, Illkirch Cedex, France

Zürich 2009

To my Family

Summary

Part I

During the development of multicellular organisms, cells must divide and differentiate. Differentiated cell clusters undergo morphogenesis to form organs that together eventually build the entire organism's body. Developmental processes are controlled by a complex network of protein interactions that are currently being unravelled through the study of model organisms. The development of the egg-laying organ of the *C. elegans* hermaphrodite serves as an ideal process in which these complex interactions can analysed. This organ consists of the vulva connected to the uterus via a subset of specialised ventral uterine cells. One single cell with a ventral uterine identity, the anchor cell, serves as the key organizer during the synchronisation of development of the vulva and the ventral uterine cells. The anchor cell builds the connection between the two tissues by inducing specific cell fates in the vulval tissue and in the ventral uterine tissue. Furthermore, by attaching to and invading the vulval tissue, the AC makes the first close physical contact between the two tissues.

During my thesis, I first wanted to find new molecular components of AC attachment, and invasion but also new genes that would be involved in the differentiation of the ventral uterine cells that finally build the connection between the vulva and the uterus. Therefore, I first studied the attachment of the AC to the vulval tissue in wild-type animals and in different mutant backgrounds. Second, I performed a forward EMS mutagenesis screen and identified a handful of interesting mutants. The isolated mutants were grouped into three classes. The first class contains mutants that seem to have a defect in ventral uterine cell differentiation. Interestingly, the second group consists of mutants that in addition of the previously mentioned phenotype also seem to have a defect in AC fate specification. The third group contains two new alleles, of *fos-1* and *lin-28* that show an AC invasion defect.

Furthermore, in a reverse genetics approach, carried through RNA interference, I studied the role of heterotrimeric G proteins during AC invasion and attachment. None of the genes that were downregulated by RNAi showed an interesting phenotype. Lastly, I tested the putative role of the RAS/MAPK pathway in the AC. From the results that I obtained, it would seem that this pathway is not involved in AC attachment or invasion.

Part II

Memory is the ability of higher organisms to store information and to recall it during a later period of life. Interestingly, *C. elegans* has evolved a conserved mechanism that is defined as memory performance. This leads to the striking advantage that candidate genes that are involved in memory performance in humans can be analysed for their suggested function during memory performance in the worm. It was previously shown in our laboratory that GLR-1 could be involved in memory perfomance. I tested the three PDZ encoding genes, *lin-10, lin-2* and *lin-7* for their involvement in memory performance by performing chemotactic associative memory assays in *C. elegans*. These genes are putative candidates that might be involved in the localisation of the GLR-1 receptor subunit to the postsynaptic densities during associative memory performances. Unfortunately, the mutants that are deficient for these genes show a defect in olfaction. This makes it impossible to study the defect in memory performance with the chemotactic associative memory assay that I employed, since this test relies on adequate olfaction of the subject animals.

Zusammenfassung

Teil I

Während der Entwicklung von multizellulären Organismen teilen sich Zellen und differenzieren zu bestimmten Zelltypen. Diese differenzierten Zellen durchlaufen Morphgenese und bilden in Folge verschiedene Organe. Organe bilden zusammen schlussendlich einen vollständigen Organismus. Dieser Entwicklungsprozess basiert auf einem komplexen Netzwerk von Protein-Interaktionen, die mittels Gebrauch von Modelorganismen entschlüsselt werden können Die Entwicklung der Ei-lege-organs des Modelorganismus *C. elegans*, das für die Eiablage und die Befruchtung verantwortlich ist, dient als ideales Modell um diese komplexen Prozesse zu studieren. Das Organ besteht aus der Vulva, welche in engem Kontakt mit spezialisierten ventralen uterinen Zellen steht. Die Ankerzelle, eine spezifische Zelle des ventralen Uterus, kontrolliert die Synchronisation der Entwicklung der Vulva und die Entwicklung der ventralen uterinen Zellen. Die Ankerzelle bildet die Verbindung zwischen der Vulva und dem Uterus, indem sie in beiden Gewebetypen Differenzierungsschritte induziert. Darüber hinaus bildet die Ankerzelle eine direkte Verbindung zwischen der Vulva und dem Uterus indem sie die Vulva invadiert.

Ein Ziel meiner Doktorarbeit war, neue molekulare Komponenten zu identifizieren, die zur Verbindung von Uterus und Vulva beitragen und die insbesondere in die Invasion der Ankerzelle ins Vulva Gewebe involviert sind. Ich studierte den frühen Kontakt der Anker Zelle mit der sich entwickelnden Vulva in Wildtyp-Tieren und verschiedenen Mutanten. Zusätzlich habe ich einen mutagenese Screen ausgeführt und habe verschiedene Mutanten isoliert. Diese Mutanten wurden anhand ihres Phenotypes in drei Gruppen unterteilt. Die erste Gruppe enthält Mutanten, die wahrscheinlich einen Defekt der Differenzierung der ventralen uterinen Zellen zeigen. Die zweite Gruppe enthält Mutanten, die zusätzlich zum Defekt der ersten Gruppe einen Defekt in der Spezifizierung der Ankerzelle aufweisen und die dritte Gruppe enthält neue Allele der Gene *fos-1* und *lin-28*, welche beide einen Defekt der Ankerzell-Invasion aufzeigen.

Des Weiteren habe ich in einem RNAi Screen die Rolle von heterochronischen G-Proteinen im Bezug auf die Invasion der Ankerzelle studiert. Keines der erwähnten Gene hat durch die Herunterregulation einen interessanten Phenotypen gezeigt. Letztendlich habe ich die vermeintliche Rolle der RAS/MAPK Signalkaskade in der

Ankerzelle studiert. Die Resultate zeigen, dass es nicht wahrscheinlich ist, dass die Invasion durch diese Signalkaskade reguliert wird.

Teil II

Erinnerung ist die Fähigkeit von höheren Organismen, Informationen zu speichern und diese später zu einem späteren Zeitpunkt des Lebens wieder abzurufen. Auch *C. elegans* weist einen solch konservierten Mechanismus vor. Das hat den Vorteil, dass man Gene, von denen man annimmt, dass sie zur Erinnerungsfähigkeit beitragen, in *C. elegans* analisieren kann, um ihre molekulare Rolle zu ermitteln. Resultate in unserem Labor zeigen, dass GLR-1, eine Glutamat- Rezeptor-Einheit, möglicherweise in den Mechanismus des Erinnerungsaufbaus involviert ist. Ich habe mich mit drei PDZ-codierende Genen, *lin-10*, *lin-2* und *lin-7* befasst, um eine mögliche Funktion während dieses Prozesses festzustellen. Dementsprechend habe ich die Mutanten mittels eines Experiments, welches auf chemotaktischer Assoziation basiert, getestet. Die drei Gene tragen möglicherweise während des Aufbaus von Erinnerung zur korrekten Lokalisation des GLR-1 Proteins an der postsynaptischen Membran bei. Leider zeigen die erwähnten Mutanten einen starken olfaktorischen Defekt. Dies macht es unmöglich, die Leistung im Bezug auf Erinnerung mittels des oben erwähnten Experiments zu testen, da dieses auf Olfaktion beruht.

Table of contents

1 Abbreviations

1°	primary
2°	secondary
3°	tertiary
AC	anchor cell
ACEL	anchor cell specific enhancer of *lin-3*
AP-1	activator protein 1
Chr	Chromosome
CI	chemotactic index
CSL	CBF1/su(H)/LAG-1
Dpy	Dumpy
DTC	distal tip cell
DU	dorsal uterine
ECM	extra cellular matrix
EGF	epidermal growth factor
Egl	egg-lying defective
EMS	ethane methyl sulfonate
Evi-1	ectotropic viral integration site 1
FLP	fragment length polymorphism
FRE	*fos-1* responsive element
GCPR	G protein-coupled receptor
GNEF	guanine nucleotide exchange factor
GFP	green fluorescent protein
GPCR	G protein coupled receptor
hrs	hours
HSN	hermaphrodite specific neuron
hyp	hypodermis
LI	learning index
Lin	lineage defective
L1-4	larval stages 1-4
MAPK	mitogen-activated protein kinase
Muv	multivulva

NICD	Notch intracellular domain
Pvl	protruding vulva
RAS	rat sarcoma
RNAi	RNA interference
RTK	receptor tyrosine kinase signalling pathway
SNP	single nucleotide polymorphism
Unc	uncoordinated
ut	toroidal uterine
utse	uterine seam cell
uv1	uterine ventral cell 1
VPC	vulval precursor cell
VU	ventral uterine

Part I

2 Introduction

2.1 *C. elegans*, a Model to Study Biological Processes

The body of higher eukaryotes is made of organs that ensure that the organism is able to grow and produce new offspring. These organs, which perform diverse highly specialised functions, are formed from many differently specified cells, the fundamental components of life. It is fascinating that, every cell in an organism's body is produced from a single cell that originates from the fertilisation of an egg. This cell starts proliferating giving rise to many daughter cells that differentiate and eventually form different tissues and organs. The development of the different organs and tissues of an organism is defined as pattern formation. Pattern formation is a process by which initially equivalent cells in a developing tissue assume complex forms resulting in a perfect interaction and coordination between the cells that form the functional organs.

These processes are genetically controlled, and are based on a complex network of protein interactions known as signalling pathways. Signalling pathways govern basic cellular activities and coordinate these cell actions. In accordance, cells differentiate for example, along a morphogen gradient or adopt a specific cell fate through short distance cell-to-cell communication.

How cells grow, differentiate and how cell clusters undergo morphogenesis to eventually form a unity and organ are fundamental questions that developmental biologists study.

These basic questions are of high interest, since besides pure interest and fascination they are also the key of understanding the processes that are involved in genetically encoded diseases, such as cancer, congenital deformations and premature aging. These questions cannot be studied in humans for obvious ethical reasons. Fortunately, the underlying molecular mechanisms have been wonderfully conserved throughout the natural kingdom, and can thus be studied in simple model organisms such as the nematode *Caenorhabditis elegans.*

It is important to note that the extent to which these molecular mechanisms were conserved throughout evolution, to quote Jaques Monod: *“What is true for E. coli is*

also true for the elephant" is probably one of the biggest and nicest surprises of modern biology.

Examples of universal mechanisms include the universality of the genetic code, the syntax of genetic regulation, and finally the principles of pattern formation of organs through morphogens and other developmental genes. Without these universal mechanisms, it would be almost impossible to transfer the knowledge gained in model organism into human therapies.

The most popular current model organisms are the already mentioned nematode *C. elegans*, the fruitfly *D.melanogaster*, the zebrafish *D. rerio* and the mouse *M.musculus.* All model organisms have their advantages and disadvantages.

The mouse is the most commonly employed model organism in biomedical research since its genetics and physiology are those that resemble humans most closely. However the mouse is not a universally ideal model organism. The same qualities that make it a desirable model for biomedical research hinder its widespread usage in fundamental research. Mouse development and genetics are very complex. Moreover, since it is a mammal, only a limited amount of offspring are obtained with each generation, after a relatively long rearing time –from the researcher's point of view at least- of ten weeks. These elements combine to make mice a too expensive and complex model organism for fundamental research.

In contrast, the nematode *C. elegans*, - the main actor in this thesis – has a generation cycle of approximately three days during which it undergoes four larval stages (L1-L4). It easy to handle and its maintenance on plates covered with a layer of *E.coli* is cheap and practical. In 1974, Sydney Brenner started studying this 1 mm long soil worm and since then it had been used extensively to decipher molecular and developmental biology mechanisms (Brenner, 1974).

But what exactly makes *C. elegans* such a popular model organism and what are its striking highlights ?

First, the nematode is comprised of a finite and identified number of cells (959 somatic cells in the adult hermaphrodite) that follow a stereotyped pattern of cell divisions during development. Thus, *C. elegans* is famous for its invariant somatic cell lineage, which makes it possible to study the impact of mutations affecting a specific mother cell on the differentiation pattern that defines its well-characterised progeny or other surrounding cells. One example of a famous cell lineage is the one that leads from vulval precursor cells to the mature vulva. The analysis of this

process constituted the background of this thesis and its development is described in the following section.

Moreover, the fact that *C. elegans* is sexually dimorphic makes it highly attractive. *C. elegans* mostly appears in the hermaphrodite form, that is able to self fertilise and give genetically identical progeny. Nevertheless, in case of necessity, we can take the advantage of sexual reproduction and cross different strains together to study the outcome of the combined features.

There are many other, more broadly used tools that lead to a better understanding of cellular interaction and in accordance its molecular pathways in *C. elegans* such as the possibility to down regulate genes by performing RNA interference experiments or the use of genetic reporters to analyze the expression of specific genes. The use of some of these tools is described in this thesis.

2.2 A model Organ to Study Organogenesis and Cell Signaling

One of the main interests of the laboratory of Prof. Dr. A. Hajnal, is the development of the hermaphrodite's vulva, a part of the worm's egg-laying and mating apparatus of *C. elegans*. It is located on the ventral side of the mid section of the body, and consists of 22 cells only. The vulva's functionality depends on its precise anchorage in the body of the animal. It must be in close cellular connection with the uterine tissue with which it forms the unity of the egg-laying system and which in addition serves as a base to anchor the vulva.

The cells that form the vulva and the uterus adopt an invariant pattern of cell fates. Disruption of this pattern by the creation of mutations within genes involved in vulva formation leads to the development of misshaped vulvae. Vulval development is genetically amenable because mutations that affect vulval development are often viable and the corresponding phenotypes are easily discernable under the microscope making it a practical model to study organogenesis.

Besides from being a practical model organ that is easy to examine, the organogenesis of the egg-laying apparatus is relevant for developmental biologists since it is based on conserved signalling pathways that are known to have an impact on human biology such as cancer progression. Furthermore, communication between different tissues during their development with the goal to form a functional

unit, is a fundamental process that raises many questions that must be answered for the better understanding of developmental biology.

Such developmental step takes place during the establishment of the connection between the vulva and the uterus. To form the entire functional egg-laying system, the individual developmental steps of the two tissues need to be very tightly regulated. This involves bidirectional signaling between different tissues to synchronize their individual development, cell migration events, the proteolysis of extra-cellular matrix (ECM), cell invasion and tubulogenesis, all together describing the process of organogenesis.

2.3 Overview of the Development of the Egg-Laying Organ in *C. elegans*

The uterine and the vulval tissue develop from two different germ layers. The vulval tissue is a specialised epidermis tissue, while the uterine tissue derives from a part of coordinated lineage formation mostly, the mesoderm.

Despite this fact, they eventually develop in a fashion to build together one organ. The developmental steps that underlie this process will be explained here briefly to give the reader a first overview.

The development of the vulva can be divided into several steps (see Fig.1). During the first step, the establishment of the six vulval precursor cells (VPCs) takes place. The VPCs are cells that have the potential to adopt vulval cell fates. Nevertheless, only three of these VPCs are induced to adopt the two different vulval cell types (see Fig. 1B). As a consequence of their induction, they start dividing in a stereotypic fashion to finally form 22 descendants (see Fig. 1C). These descendants execute cell fate decisions, undergo migration and cell fusion events, finally forming the mature vulva (see Fig.1D).

Meanwhile, the gonad and with it the uterus develops in parallel to the vulva. To accomplish the connection between the vulva and the uterus and to anchor the egg-laying system in the animal's body, six cells of the ventral uterine tissue are induced to adopt the π cell fate (see Fig. 2/3). One round of cell division follows the induction step and the cells differentiate further to adopt uv1 (uterine ventral 1) (four cells) and uterine seam cell fate (utse) (syncytium with eight nuclei). While the uv1 cells build

the connection between the uterus and the vulva, the utse anchorages the uterus and the vulva to the body of the animal.
One single cell, the anchor cell (AC), belonging to uterine tissue, is the main organizer of the development of the vulva and ventral uterine tissue. It is responsible for inductive steps in both developing tissues, thereby synchronising the development of the vulva and the ventral uterus. Furthermore, by invading the vulval tissue, the AC makes the first close contact between the two tissues.
To be able to understand in detail the way the connections are built, one has to understand the individual differentiation of the organs that are connected later during development. Therefore, I will first describe the development of the vulva followed by the description of the developmental steps of the uterine tissue and finally concentrate on how the two organs are united.

2.4 Establishment of the Tripotent Vulval Equivalence Group

At hatching, 12 P postembryonic blast cells are arranged along the sides of the body in 2 symmetrical longitudinal rows of 6 cells (Sulston, 1977 #1) (Fig. 1). These cells migrate during the first larval stage to form a single row of 12 cells that are situated ventrally in the animal and are denoted from P1 to P12 from anterior to the posterior. Further, the P cells all divide once to form an anterior daughter cell (Pn.a) and a posterior daughter cell (Pn.p) (Sommer et al., 1994). While the anterior daughters give rise to neuroblasts, the hypodermal cells P1.p, P2.p, P9.p P10.p and P11.p fuse during the L1 stage with the syncytial hypodermal cell hyp7 and P12.p fuses to syncytial hypodermal cell hyp12.
The P(3-8).p cells remain unfused and form the vulval equivalence group also known as vulval precursor cells (VPCs) (Clark, 1993 #2). The VPCs are tripotent and can be induced to form 1° or 2° vulval cells, or they adopt the 3° cell fate, in which case they fuse to the hypodermal tissue and do not contribute to the vulval tissue (Ambros, 1999). Although P3.p belongs to the equivalence group, it remains un-fused in only 51% of the animals probably due to its location at the very edge of the gradient that is responsible for keeping the cells unfused. It is believed that as long as the VPCs do not have fused to the hypodermis cell hyp7 they are competent to be induced. Therefore, one mechanism that maintains the equivalence group competent until the induction, is the inhibition of their fusion.

In *lin-39* loss-of-function mutants, P3.p to P8.p fuse to hyp7 and fail to become VPCs, in a manner similar to the anterior and posterior Pn.p cells. LIN-39 HOX, a homeotic mid-body specific gene maintains the unfused status of VPCs by repressing *eff-1*, a membrane protein responsible for most cell fusions during *C. elegans* development (Shemer, 2002 #4). A LIN-3 EGF signal produced by the gonad and WNT signaling are two identified factors that are suggested to prevent the VPCs from fusion and maintain their competence via LIN-39 during the second larval stage L2 (Myers, 2007 #3).

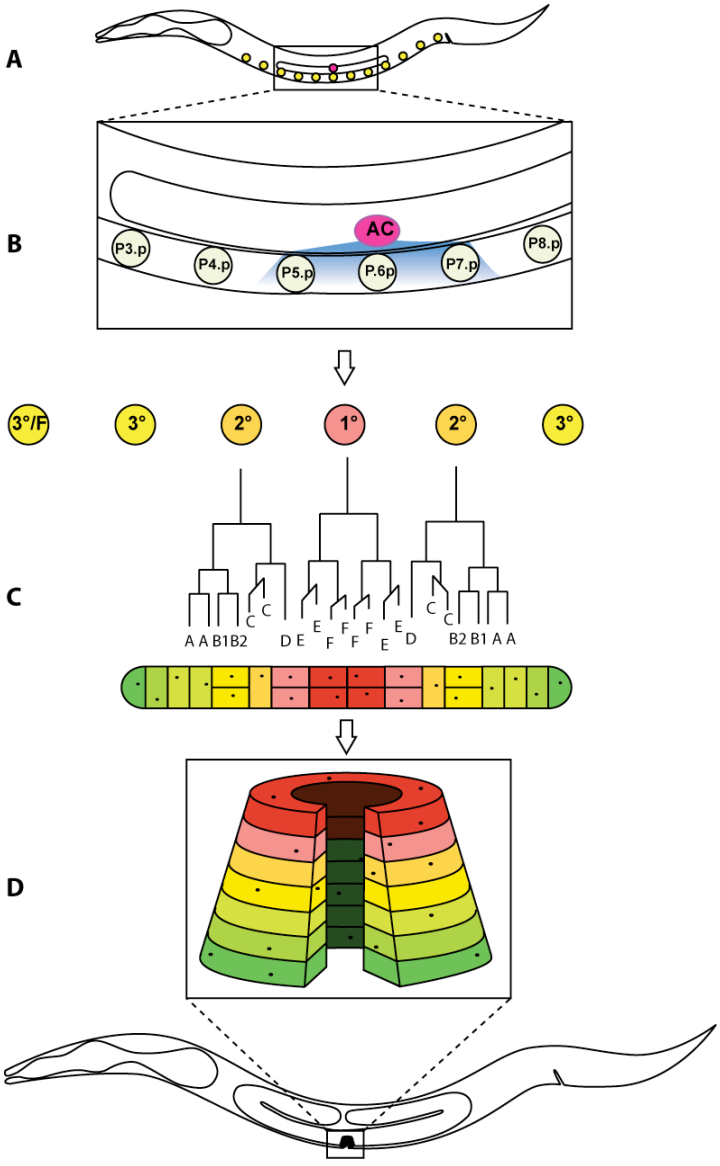

Fig. 1 Schematic representation of vulval development. (A) During the L1 larval stage the six vulval precursor cells (VPCs) develop from twelve Pn.p cells (P1.p to P12.p) located on the

ventral side of the animal. P3.p to P6.p form the vulval equivalence group, which means that they all have the potential to adopt vulval cell fate. P3.p, a member of the vulval equivalence group, remains fuses (F) in 49% of the animals to the hyp7. (B) During the late L2 to early L3 larval stage, the anchor cell (AC), a cell of the somatic lineage of the gonad induces the VPCs P5.p P6.p and P7.p to adopt vulval cell fates. P6.p, the cell closest to the AC adopts 1° cell fate, while the two cells adjacent to the 1° cell both adopt 2° cell fate. P3.p, P4.p and P8.p adopt 3° cell fate and after one cell division fuse to hyp7. (C) The 1° cell and the two 2° cells start dividing in a stereotypic fashion. The 2° cells produce seven progeny each, while the 1° cell produces eight progeny. During the first two round of division, 1° and 2° cells divide identically, while during the third round of division, the 1° cells divide transversally and the 2° cells divide asymmetrically. The outer 2° cells divide longitudinally, while the neighboring 2° cells divides transversally. The inner most 2° cell does not divide. The 1° cells form vulF and vulE cells and the 2° cells form vulA, vulB1/B2 vulC and vulD cells which are depicted by different colours. (D) During the L4 stage, vulval cells of identical sub-fates form toroidal rings by forming cellular extensions and fusions. Thereby, a stack of seven rings is formed (a slice was cut off to show the central lumen). The dots depict the nuclei of the fused cells within the different rings. Anterior is to the left.

2.5 Vulval Induction

Around the late L2 and early L3 larval stage, three important steps take place that lead to the further development of the VPCs (Hill and Sternberg, 1992; Kimble, 1981) (Fig. 1).

First, P6.p is induced to adopt 1° vulval cell fate. The signal that leads to induction is released from the AC (Hill and Sternberg, 1992). P6.p is located closest to the AC and therefore receives the highest amount of the inductive protein, which leads to 1° fate adoption.

Second, the induction of P5.p and P7.p to adopt 2° cell fates takes place and finally, the remaining VPCs that were not induced, P3.p, P4.p and P8.p, adopt 3° cell fate, a non-vulval cell fate. After one round of cell division, the 3° cells fuse with their surrounding hypodermis hyp7.

The vulval inductive signal is LIN-3 EGF (Hill and Sternberg, 1992). It is released by the AC and binds to its receptor LET-23, an orthologous of the EGF receptor that is located on the surface of the VPCs . The receptor is restricted to the basolateral cell-membrane, by a protein-scaffolding complex containing LIN-2 CASK, LIN-7 VELIS and LIN-10 MINT (Whitfield et al., 1999, Kaech, 1998 #29). LET-23 EGFR transduces the signal intra-cellularly through SEM-5 GRB2 and further to SOS-1,

(Chang et al., 2000) a RAS guanine nucleotide exchange factor (GNEF) that interacts with LET-60, the homolog of a RAS protein. The signal is further transmitted through LIN-45 RAF (Han et al., 1993), MEK-2, MPKK MEK (Wu et al., 1995) and MPK-1 MAPK (Lackner et al., 1994) to the nucleus where it induces expression changes of its targets LIN-1 and LIN-31 (Beitel et al., 1990; Han and Sternberg, 1990). Both, LIN-1 an ETS domain containing transcription factor and LIN-31 HNF3 a forkhead transcription factor act downstream of MPK-1 to specify 1° fate (Tan et al., 1998). When RAS signaling is inactive, the two proteins form a complex that has been suggested to inhibit vulval induction. As soon as the Ras pathway is induced, LIN-31 HNF3 is phosphorylated by MPK-1 MAPK and consequently, LIN-1 and LIN-31 dissociate from each other to promote the expression of 1° cell fate specific genes, (Beitel et al., 1995; Miller et al., 1993).

Subsequently, the induced P6.p signals through the LIN-12 NOTCH signaling pathway to its direct neighbors P5.p and P7.p, in order to force them to adopt to adopt the 2° cell fate. This pathway is composed of LIN-12 NOTCH, the receptor, and its ligands APX-1, LAG-2 and DSL-1, DELTA/SERRATE/LAG-2 proteins (DSL), that were identified as lateral signaling compounds (Chen and Greenwald, 2004). The EGFR/MAPK signaling pathway regulates the expression of these ligands. The DSL ligands are expressed in P6.p, the future 1° cell, while the receptor LIN-12 NOTCH is expressed in the two cells adjacent to P6.p (P5.p and P7.p) (Chen and Greenwald, 2004). It is known that upon activation, the intracellular domain of LIN-12 NOTCH is cleaved (Struhl and Adachi, 2000). The cleaved moiety of the receptor, NICD, translocates into the nucleus of the future 2° cells where it changes the transcriptional state of downstream targets by interacting with the transcription factor LAG-1. LAG-1 is a member of the Notch family of transcription factors (CBF1, Suppressor of Hairless, LAG-1) (CSL). It has been shown that LAG-1 CSL prevents P5.p and P7.p from adopting the 1° cell fate by inhibiting the EGF signaling pathway. Two examples of such genes are *lip-1* and *ark-1,* which both exhibit CSL sites in their enhancer regions. (Berset et al., 2001; Hopper et al., 2000; Yoo et al., 2004). Further, LAG-1 is suggested to induce genes involved in 2° cell fate specification (Ambros, 1999; Greenwald and Seydoux, 1990; Seydoux and Greenwald, 1989). Surprisingly, so far no genes that are involved in specification of the 2° cell fate have been identified

2.6 Execution of Vulval Cell Fate and Vulval Morphogenesis

The induction of vulva development described above ensures that P3.p to P8.p adopt a 3°-3°-2°-1°-2°-3° cell fate pattern (see Fig. 1) It is the basis for the development of a wild-type vulva, which is followed by the divisions of P5.p (2°), P6.p (1°) and P7.p. (2°) in a mirror symmetrical pattern along the anterior-posterior axis. During the L3 stage, these cells undergo three rounds of division to generate 22 cells. While the 1° cell is the precursor of 8 descendants, the two 2° cells give rise to 7 cells each. The last division round is executed in a stereotypic fashion that shows different division planes. Cells in the 1° lineage divide transversally to the anterior-posterior axis of the animal. In the 2° lineage the two most distal cells divide longitudinally, whereas the next proximal cell divides transversally and finally, the most distal cell does not divide further (Sharma-Kishore et al., 1999).

Once these cells are born, they undergo morphogenetic rearrangements to form the mature vulva. This process can be split into three parts.

In the first part, the cells migrate to their final position and build a tube-like structure of seven rings that are located between the endothelium of the uterus and the external epithelium.

During the second step that occurs at the L4 larval stage, the vulval cells fuse in a homotypic fashion to form seven multinuclear cells that form the aforementioned rings. This generates the toroid rings that line the vulval cavity. The two uppermost rings are formed by the 1° cells, VulE and VulF. The other five rings are formed by the 2° cells VulA, VulB1, B2, C and VulD (see Fig. 1D). The VulF cells attach to the uv1 uterine cells to form a stable connection between the uterus and the vulva.

Lastly, the process ends when the vulva everts during the L4 to adult molt. The lumen that was present earlier, during the formation of the seven stacks, disappears. Henceforth, the eversion event leads to a block of the vulval opening that lasts until the vulval muscles open it, as the eggs are laid (Sharma-Kishore et al., 1999).

2.7 Development of the Somatic Gonad

At hatching, the hermaphrodite's gonadal primordium consists of four cells (Z1-Z4). This tissue is situated in the middle of the animal, in the region of the future vulval cells (Kimble and White, 1981; Seydoux and Greenwald, 1989).

Z2 and Z3 are the primordial germ cells that grow further during development. While, on the other hand, Z1 and Z4, the somatic germline precursors generate twelve descendants during the early L2. During development, these twelve somatic germline precursors give rise to multiple tissues such as the uterus, the distal tip cells (DTC), the gonadal sheat, the distal constriction of the spermatheca, the spermatheca-uterine valve (also called the spermathecal-uterine junction) and the spermatheca.

The gonad is bi-lobed, with germ line maturing in both arms (Hirsh et al., 1976). The DTCs are responsible for the proliferation and for the guidance of the growing gonad arms posteriorly and anteriorly along the ventral part of the animal during earlier development and later growing the distance back on the dorsal side of the animal.

Further, three of the cells become ventral uterine (VU) cells and one adopts AC fate (Z1.ppa, Z4.aap, Z4aaa, Z1.ppp) (see Fig. 2). The VUs will form the ventral part of the uterus and the spermathecal and the spermathcal-uterine valve cells. In contrast to the germ cells and the DTCs, the uterus is situated still at the position where the primordium was born, close to the developing vulva.

Dorsal to the VU cells, there are two dorsal uterine (DU) cells (Z1.pap and Z4.apa) (Fig. 2). These two DU cells will form a part of the dorsal uterus wall, the spermathecal and spermathecal-uterine valve cells. The uterine cells are flanked by two pairs of somatic sheat cells and spermatheca precursor cells (Kimble and Hirsh, 1979).

Most cells of the uterus are descendants of the two dorsal precursor cells (DU) cells, and the three ventral uterine precursor cells (VU) (Kimble and Hirsh, 1979). Each of the two DU cells produces 24 descendants that are symmetrical to each other. Of these 48 cells, 28 of them give rise to uterine tissue while the remaining 20 contribute partly to the anterior and posterior spermatheca. The three VU cells (Z1.ppa/Z4aap/Z4aaa or Z1.ppp) divide into 36 descendants, of which 32 contribute to the uterus. Z1.ppp or Z4.aaa adopt AC fate (see Fig. 2).

Finally, the VU and DU cells differentiate, and build the adult uterus from several different cell types. In summary, there are three mononucleate cells on both sides of the animal uterine ventral cells (uv1-3), a single DU cell opposite of the ventral uterine junction, the utse syncytium, four multinucleate toroidal uterine cells (ut1-4) and the toroidal spermathecal valve cell.

The utse syncytium attaches the uterus to specialised lateral epithelial seam cells. The ut1-4 cells are followed by the toroidal spermathecal valve cell (TSVC). The TSVC contains a ring of four nuclei, which has microfilaments that wrap around the inner face of the torus and presumably acts as a sphincter to close the spermathecal valve in the adults. The cells of the spermatheca are situated distally to the spermathecal valve (Kimble and Hirsh, 1979).

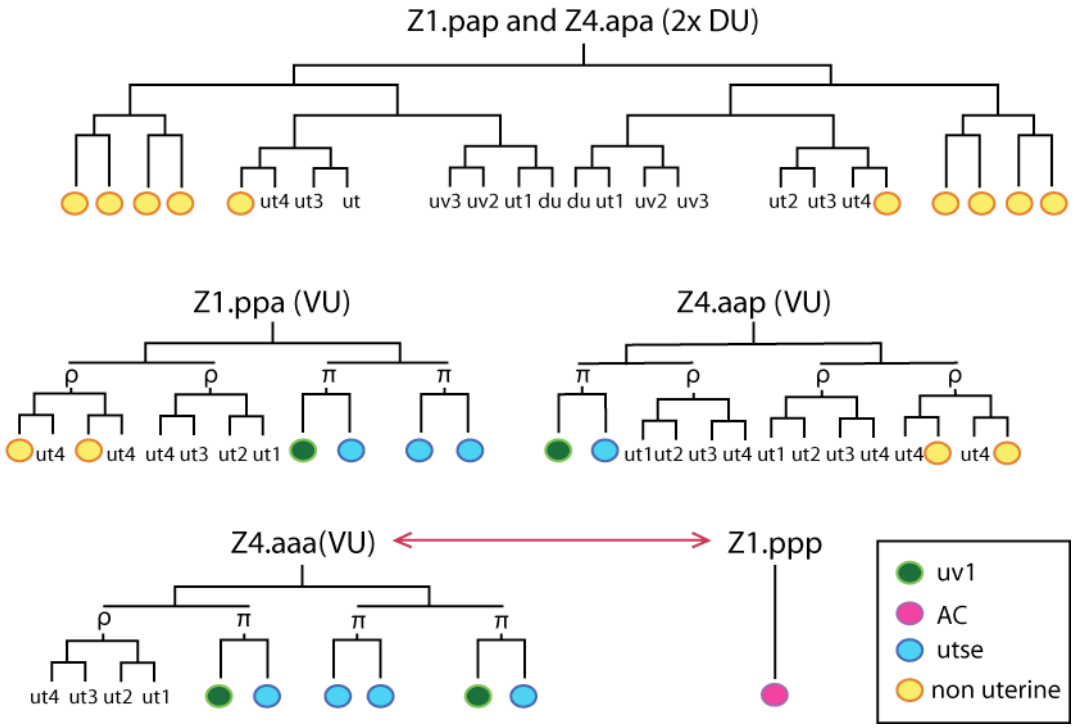

Fig. 2 Uterine cell lineages adopted form Newman et al., and Kimble and Hirsh. The figure depicts the cell lineages of the three ventral uterine (VU) cells and the two dorsal uterine (DU) cells. The lineages of the two DU cells Z1.pap and Z4.apa are symmetric and therefore only illustrated once.

During the early to mid L3 stage, three VU cells divide twice and six of them adopt the π cell fate from the VU lineage, intermediate precursor cells. The π cells divide further to produce eight precursor utse cells (blue) and four uv1 cells (green).

Cells that contribute to the spermatheca and spermathecal-uterine junction are depicted in yellow. du, dorsal uterine cells are forming the dorsal epithelium in the central region of the uterus; utse, uterine seam cell; uv1, uterine vulval cell 1; ut, uterine toroidal epithelial cells that constitute the bulk of the uterus; The VU cells Z4.aaa and Z1.ppp have both the potential to become AC (pink) or alternatively to divide further.

2.8 Birth of the AC

As mentioned previously, the AC is a specialised ventral uterine cell of the gonadal tissue of the hermaphrodite that has a pivotal role in vulval and gonadal patterning and in the morphogenesis of the egg-laying apparatus.

Z1.ppp and Z4.aaa, two of the VU cells are born during the first larval stage (Hirsh et al., 1976). During the mid L2, they are in direct contact with each other and form an equivalence group (Greenwald and Seydoux, 1990; Wilkinson et al., 1994). One of them adopts the AC fate, while the other one adopts the VU cell fate, supposedly in an arbitrary fashion (see Fig.2/3A).

After birth, the AC moves to a central position in the gonad where it is surrounded by three VU and two DU cells. In contrast to VU and DU cells, the AC does not proliferate hereafter. At the beginning of vulval development, the AC is directly adjacent to the future 1° vulval cell, where it is ready to organise the surrounding tissue (see Fig. 3B).

It has been suggested that at the molecular level, AC specification is mediated via LIN-12 NOTCH signaling in a laterally inhibitory manner (Kimble, 1981; Newman et al., 2000, Wilkinson, 1994 #69) (see Fig. 4).

Initially, both cells produce the ligand LAG-2 DELTA and the receptor LIN-12 NOTCH.

It has been suggested that small differences of LIN-12 NOTCH signalling between the two cells are amplified via feedback loops, thereby determining the cell fate of the two cells in such a way that *lag-2* expression is restricted to the AC, while *lin-12* expression becomes restricted to the presumptive VU (Karp, 2004 #134).

HLH-2, a class I helix-loop-helix (bHLH) transcription factor, the ortholog of the mammalian E and Drosophila Daughterless transcriptional activators, is responsible for the transcription of *lag-2* Dsl.

The first identified difference between the two cells is HLH-2 translation only in the AC, although *hlh-2* is transcribed in both the pre-VU and the pre-AC, (Karp, 2004 #134). It is thought that the uneven distribution of HLH-2 DAUGHTERLESS between the two cells is due to a negative feedback loop of LIN-12 NOTCH signalling acting on HLH-2 (Karp and Greenwald, 2003).

In sharp contrast to the model that depicts the AC/VU decision as being arbitrary, detailed analysis has shown that, in most cases, the cell that is born first adopts AC fate (Karp, 2004 #134).

Interestingly, Hwang et al., suggest that *egl-43* is also involved in AC/VU specification (Hwang et al., 2007). This hypothesis is based on the hereunder observations. First, EGL-43 downregulation leads generation of supernumerary ACs in the gonadal tissue. Second, *egl-43 evi-1* elimination, in a *lin-12 Notch* hypermorphic mutant, reverses the AC deficient phenotype, which suggests the involvement of EGL-43, downstream or in parallel of LIN-12 NOTCH signalling during the AC/VU specification (Hwang et al., 2007).

2.9 The Connection between the Vulva and the Uterus

In order to mate and to lay eggs, *C. elegans* depends on a properly formed egg-laying system that contains the vulva and a part of the uterus. In consequence, not only the proper development of both the vulva and the uterus has to be guarantied, but also the synchronisation and connection between these two tissues is of importance.

The lack of connection between the vulva and the uterus is referred as connection of gonad (Cog) phenotype and leads to the fact that the mature vulva is not properly anchored to the animal (Palmer et al., 2002). In some cases, the vulva even everts and forms a protuberance that is very well visible. This phenotype is then termed protruding vulva (Pvl). Furthermore, if in addition to a Pvl, the mutation does not lead to sterility due pleiotropic effects, the larvae hatch inside of the animal. This leads to a phenotype known as egg-laying defective (Egl) and forms a bag of worms. The following three sections describe two basic developmental steps that are crucial in establishing the connection between the vulva, the uterus and the whole animal, leading to such phenotypes in case of misregulation.

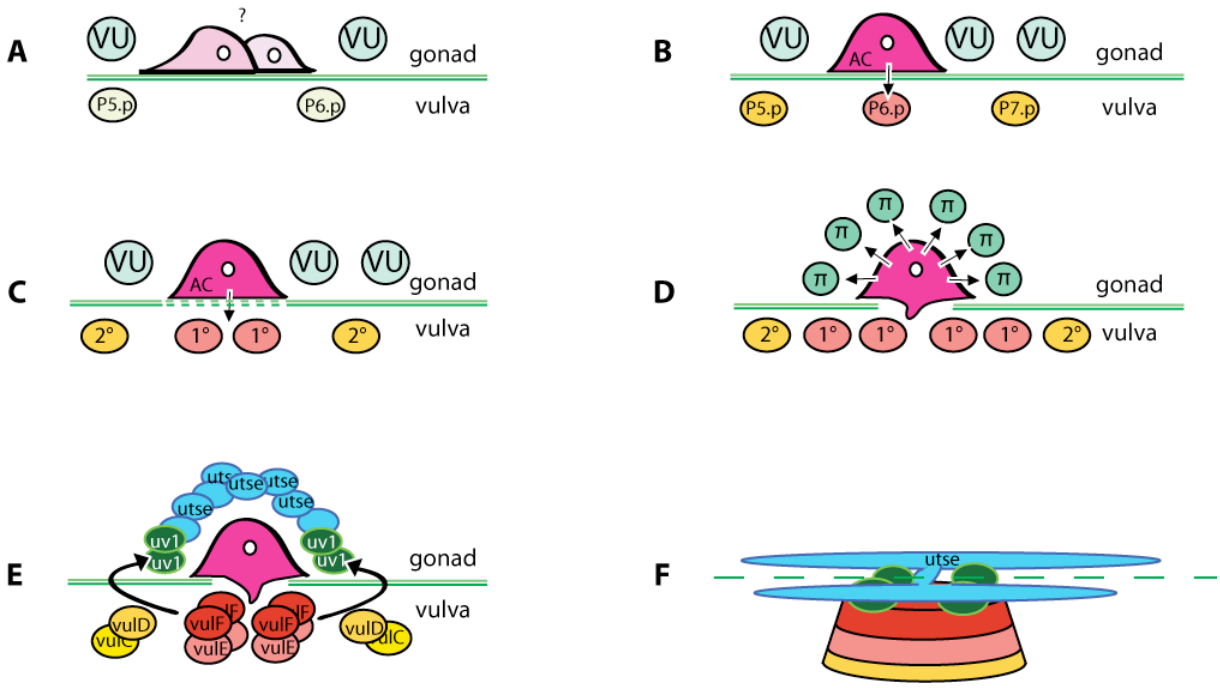

Fig. 3. The AC coordinates the development of the vulval and the uterine tissue. (A) During the mid L2, the AC is specified the VU cells of the developing gonad by LIN-12 NOTCH in a laterally inhibitory manner and has migrated to the basal laminae. The two pink cells represent the two VU cells with the potential to adopt AC fate (pre-AC/pre-VU cells). The basal laminae are represented by green lines that separate the gonadal and vulval tissue. (B) By the early L3 stage, the AC has attached to the basal laminae in closest vicinity of the nucleus of P6.p and induces vulval development by LIN-3 EGF signalling. (C) The AC dissolves the basal laminae and starts invading the vulval tissue, a mechanism controlled by FOS-1. (D) The two basal laminae underlying the AC have dissolved. Meanwhile, the AC induces six out of twelve VU cells in the gonadal tissue to adopt π cell fate by LIN-12 NOTCH. (E) After one round of cell division, a subgroup of the π cells receives a signal from the vulF cells, a subgroup of the 1°cell progeny that are closest to the gonadal tissue. As a result, four of the twelve π adopt the uv1 cell fate by LIN-3 EGF LET-23 EGFR signaling. (F) The remaining 8 π cells become utse cells, change cell shape and migrate away from the site of induction. Furthermore, these cells undergo homotypic cell fusion and fuse with the AC in a heterotypic fashion to form an "H" shaped syncytium. The dashed line represents the ventral midline of the animal. Anterior is to the left.

2.9.1 Attachment and Invasion of the AC to the Vulval Tissue

The invasion of the AC is the most prominent step during the consolidation between the vulva and the uterus. Prior to induction during the L2 larval stage, the gonadal tissue and the VPCs are demarcated by two basal laminae covering the gonadal and the vulval tissue (see Fig. 3). Whenever the animal moves, the position of the developing gonad relative to the vulval precursor cells and with it the distance between P6.p and the AC changes (Kramer, 1994). From the late L2 to early L3, the time of induction of vulval development, the AC attaches to the vulval tissue and thereby gains a stable position above P6.p or 1° cell. Whether P6.p has already adopted the 1° cell fate has not been determined yet. From this position on, the AC is disposed to invasion through the two basal laminae. During the mid-L3 larval stage, the two basal laminae become dissolved precisely underneath the attached AC that is centred above the P6.p descendants establishes a direct contact with the 1° vulval cells (see Fig.3).

The mechanism that cells use to attach to and cross trough extracellular matrices (ECMs) to invade the another tissue is of high interest since it occurs during many natural developmental processes such as trophoplast implantation in mammels (Ozanne et al., 2006). Furthermore, cell invasion is also described as an important step during the transformation of a sessile tumour into a malignant, metastasizing tumour (Yamaguchi et al., 2005). Despite the importance to achieve more understanding about the process of general cellular invasion, little is known about its mechanism, a reason to elucidate the invasion of the AC in *C. elegans*.

Recently, investigators could show that an attractive cue endows the 1° vulval cells with the potential to direct the AC its way of invasion. Up till now, the nature of the attractive protein has not been identified (Sherwood and Sternberg, 2003).

The AC seems not only to be attracted generally by the cell with 1° cell fate but makes direct hits between the middle most 1° cells, suggesting that there is a signal that leads the AC to this position, supposedly during invasion or/and during attachment before the division of the induced P6.p cell (Sherwood and Sternberg, 2003).

Ablation experiments, removing P5.p, P6.p and P7.p have shown that isolated 1° cells originating from P8.p that are in distance to the AC, provoke an extension of the AC when they start dividing. This extension moves towards the 1° cell regardless of

the distance between the two cells and often even crosses the basement membranes before reaching its destination. This suggests that there is a diffusible invasion cue released from 1° cells (Sherwood and Sternberg, 2003). Moreover, in 20% of vulvaless (Vul) animals, the AC invades the vulval tissue during the expected time frame of mid-to-late L3, suggesting that there is a signal coming form induced vulval cells and another less strong invasion stimulus that is independent from the 1° cell signal. Additionally, in animals containing only 2° cells, invasion takes place in 20% of the animals, supporting the model of the two signals, one having its origin in the 1° vulval cells (Sherwood and Sternberg, 2003).

However, to invade the vulval tissue, the AC has first to dissolve the extracellular matrix (ECM) that locates between the gonad and the vulva to gain access to the vulval tissue.

ECMs are well studied in *C. elegans* because of its conserved identity corresponding compositions and function being similar to the vertebrate's basal lamina. ECM is made of many different components as for example collagen and glycoproteins such as laminin, fibronection and nidogen, and proteoglycans, proteins with attached glycosaminoglycan chains (Kramer, 1994). ECMs give mechanical stability, keep cells in position and are involved in signaling to obtain cell polarity. Furthermore, ECMs are known to be involved in cell and axon migration (Kramer, 2005). Most probably, studies of matrix proteins that compose basement membranes will elucidate components of AC attachment and invasion.

Recently, several genes involved in dissolving the ECMs between the uterine and the vulval tissue have shed some first light on the mechanism of AC invasion (Sherwood et al., 2005).

FOS-1, the orthologous of the c-FOS proto-oncogene was identified to induce genes expressed in the AC to accomplish invasion (see Fig. 4). In *fos-1* loss-of-function animals, the AC invades only very occasionally and delayed during the early L4 (Sherwood et al., 2005). It is suggested, that the invasion is not accomplished in *fos-1* animals during the expected time due to the inability of the disruption of the basement membranes.

c-FOS is a basic leucine zipper (bZIP) transcription factor that is known to form together with c-JUN the dimeric transcription factor Activator Protein-1 (AP-1) (Chinenov and Kerppola, 2001). The dimeric complex binds to AP-1 regulatory elements that are found in many promoter and enhancer regions of downstream

targets (Chinenov and Kerppola, 2001). Furthermore, AP-1 was identified to be involved in tumour invasion mechanisms (Lamb et al., 1997).

Nevertheless, c-FOS can form homodimers though they are a less stable then c-FOS/c-JUN heterodimers (O'Shea et al., 1992).

Recently, JUN-1 has been identified as the closest homolgous of *D.melanogaster* and human Jun (Fox et al; 2005 International Worm Meeting). It remains to be elucidated whether JUN-1, the homolog of c-JUN, is involved in AC invasion. But RNAi downregulation of *jun-1* did not lead to a Pvl phenotype, which rather states against the involvment of *jun-1* in AC invasion.

FOS-1A, one of the two fos-1 transcripts, was shown to regulate three matrix related components through EGL-43, the homolog of EVI-1, a mammalian proto-oncogene (Rimann and Hajnal, 2007, Hwang, 2007 #59). EGL-43 encodes a Zn-finger transcription factor that exists as two isoforms. The longer one controls AC invasion, while the shorter is involved in neuron migration (Garriga et al., 1993).

Moreover, three effector proteins, a cadherin, a hemicentin and zinc metalloproteinase homologue were identified to be located downstream of EGL-43 (see Fig. 4).

CDH-3 is expressed in different tissues that are involved in the formation of the egg-laying apparatus such as the AC, the seam cells, a subgroup of vulval cells and the neurons that innervate the vulval muscles (Li and Chalfie, 1990, Garriga, 1993 #116). CDH-3 is suggested to function as cell recognition molecule that is involved in establishment of de novo cell interactions of epithelial cells (Pettitt et al., 1996).

Second, ZMP-1 a metalloproteinase is expressed simultaneously with CDH-3 in the AC. Metalloproteinases were identified to degrade the constituent of proteins of the extracellular matrix (Wada et al., 1998).

Finally, HIM-4 is homologous to the vertebrate extracellular matrix component hemicentin (Vogel and Hedgecock, 2001). It is found in the ECM and in addition is secreted from the AC to the ECM during invasion.

Interestingly, the triple mutant *cdh-3; him-4; zmp-1* does not exhibit a penetrant invasion phenotype in contrast to *fos-1* and *egl-43* mutants. This leads to the conclusion that other components are involved in breaking the ECM between the vulva and the uterus (see Fig. 4).

2.9.2 Establishment of Connection between the Vulva, the Uterus and the Seam Cells via Defined Uterine Cells

There are two identified uterine tissues types that are responsible to obtain structural integrity of the egg-laying system.

First, the utse is a syncytium that is believed to be involved in anchorage of the uterus inside of the animal's body by attaching the uterus to the seam cells, a specialised lateral hypodermis. Moreover, the utse is suggested to form a planar surface that helps the vulval lips to separate during development (see Fig 3F). Most likely, the utse is important for the proper establishment of the uterine-vulval connection but it is probable that it is not be critical within the final structure because it is destroyed when the first egg is laid.

Second, the uv1 cells, mononucleate interfacial cells build the intimate contacts between vulval and uterine cells, thereby attaching the vulva to the uterine tissue (see Fig. 3F). Both cell types, the uv1 cells and the utse derive from the intermediate precursor VU cells, the VU granddaughters. Around four hours after vulval induction, during the mid L3 stage, these cells are induced by a signal from the AC to adopt the π cell fate (Newman et al., 2000). The six intermediate precursor VU cells closest to the AC are induced to adopt π cell fate rather then keeping the ground state, which is termed ρ fate. ρ and π cells are distinguishable by their stereotype division pattern (see Fig. 2)

The π cells divide once in a dorsal-ventral division plane during the L3 lethargus. In contrast, the ρ cells divide twice, mostly in an anterior-posterior plane. The six ρ give rise to other types of differentiated cells, the uterine toroidal epithelial cells that constitute the bulk of the uterus (see Fig. 2)

The six π divided cells produce larger dorsal and smaller ventral cells. After further differentiation, they give rise to four uv1 cells and 8 utse precursor cells that will fuse to form the utse syncytium. Using Normarski optics, Newman observed that the two cell types are easily distinguished since the uv1 cells remain closely associated with the vulva, whereas the cells that later form the utse undergo long-range migrations after specification (Newman et al., 1996). The time, when the eight precursor utse cells fuse to build a syncytium has so far not been clearly defined. Most likely, the AC fuses with the utse prior to the time of extensive nuclear migrations and appears to be engulfed by the utse. Further, it is described by the Newmann laboratory, that

prior to these migration events during the mid L4, the AC becomes less round, its nucleus begins to look like the nucleus of migrating cells and its starts to migrate with the migrating cells (Newman et al., 1996).

After completed differentiation, the utse shapes a thin multinucleate process with the form of the letter “H”, containing nine nuclei (8 cells derived form π cells and the AC nucleus) (see Fig 3F).

Interestingly, the utse has two apical surfaces that endow the cells to establish adherens junctions with the seam cells, the lateral epidermal cells and uv2 cells. (Newman et al., 1996) The two sides of the H run along each side of the animal attaching these to the specialised lateral epidermis.

The four uv1 cells, form adherens junctions with the vulF cells, the innermost vulval cells deriving from the 1° vulval cells. Further they form adherens junctions with the utse cells (Newman et al., 1996).

Transformation of π to ρ cell fate can be caused by either ablation of the AC after the time of induction during the early L3 stage or by the introduction of a mutation that leads the loss-of-function of *lin-12,* showing relevance of LIN-12 NOTCH signaling during π cell fate adoption (Newman et al., 1995). The receptor LIN-12 NOTCH is found on the surface of all VU intermediate precursor cells whereas its ligand DELTA LAG-2 is expressed in the AC (see Fig 4). In accordance, the VU intermediate precursor cells with a close cellular contact to the AC are induced to adopt π cell fate, suggesting that both ligand and receptor are membrane-bound (Wilkinson and Greenwald, 1995).

During π cell fate specification, LIN-12 NOTCH signaling acts in an instructive manner unlike LIN-12 NOTCH signaling during the AC/VU decision which is described as lateral inhibition (Seydoux and Greenwald, 1989). Obviously, for both mechanisms the presence of LAG-2 DSL in the AC is crucial. However, in contrast to AC versus VU decision, the expression of LAG-2 in the AC during the π cell fate adoption is regulated in a cell autonomous fashion in the AC by LIN-29, a zinc finger transcription factor (Newman et al., 2000). Thus, LIN-29 seems to be important to regulate the transition of lateral inhibition of the AC/VU decision to inductive signaling to induce the VU cells to adopt π cell fate (Newman et al., 2000). LIN-29 was previously identified as a member of the heterochronic pathway, believed to synchronise seam cell development with the molting cycle (Bettinger et al., 1996). Here, LIN-29 acts independently of the heterochronic pathway (Bettinger et al.,

1996). *lin-29* defective animals exhibit a thick layer of tissue between the uterine and the vulval lumen due to a lack of uv1 and utse cells. As a concomitant feature, the AC shows a migration defective phenotype and remains un-fused. A very similar defect can be observed in *lin-11* loss-of-function animals. LIN-11 encodes a LIM homeodomain transcription factor. Its expression is downregulated in the VU cells in a *lin-29* loss-of-function background (Newman et al., 2000) (see Fig 4).

Initially, there is no significant change in number of cell division and no change in axis of division in *lin-11* mutants (Newman et al., 1999). Nevertheless, few cells undergo an additional round of cell divisions, indicating ρ cell fate adoption. Later during development, the migration process of a subset of π cells, the future utse cells in direction of the ut2 cells is abrogated, and the cells do not reach their destination suggesting a abnormal differentiation of utse cells in *lin-11* mutants (Newman et al., 1999). Interestingly, it was recently stated that *lin-11* mutants show in addition to an utse defect improperly formed uv1 cells (Nelms and Hanna-Rose, 2006, L. Huang W. Hanna-Rose).

Further, LIN-11 is dependent on sumoylation by SMO-1 in order to be functional for proper π cell specification and migration (Broday et al., 2004)) (see Fig 4). SMO-1 is the homolog of the small ubiquitin-like modifier (SUMO), a member of the ubiquitin-like superfamily. SUMO conjugation is known to be involved in subcellular localisation of target proteins, thereby affecting its stabilities and activities (Muller et al., 2004).

Moreover, the CSL binding sites present in the *lin-11* locus are sufficient to drive uterine expression, corroborating the belief of direct regulation of LIN-11 by LIN-12 NOTCH signaling (Gupta, 2002 #122). *egl-13*, previously known under the name *cog-2*, encoding a SOX domain transcription factor was identified to be crucial for the mechanism of π cell development (Hanna-Rose and Han, 1999). In *egl-13* mutants, the intermediate ventral uterine precursor cells divide dorso-ventrally as seen in wild-type animals during π cell fate adoption, but then often divide again (Cinar et al., 2003).

The persistence of expression during the differentiation of uv1 and utse cells suggests that *egl-13* is involved in several distinct processes during cell fate specification of the π cell lineage or might not be necessary for π cell induction but more involved in the maintenance of π cell fate (Hanna-Rose and Han, 1999). Investigators observed that uv1 cell execution is mediated properly in *egl-13* mutants

leading to a model that rather suggests that only utse cell fate is impaired and not π cell fate (Nelms and Hanna-Rose, 2006). However, this is contradictory to the observation of other investigators that suggested that π cell descendents lacking uv1 induction adopt utse cells by default (Chang et al., 1999). To decipher the mechanisms of *egl-13* and *lin-11* an other new components during uv1 and utse cell fate adoption, I suggest the description of *ida-1* expression in the two mutant backgrounds. *ida-1* encodes a protein tyrosine phosphatase-like receptor, orthologous to the mammalian type I diabetes autoantigens IA-2 and phogrin, which are expressed in dense core vesicles of neuroendocrine tissue and involved in regulated protein secretion. IDA-1 appears to be required for regulating presynaptic neurotransmission. *ida-1* expression is detected in a subset of neurons. Further, *ida-1* is also detected in the vulval uv1 cells, which contain neurosecretory-like vesicles (Zahn et al., 2001).

Recently, it has been shown that the identified CSL and Fos/Jun cis-enhancer elements of *egl-13* are essential for proper expression of *egl-13* in the π cells (see Fig 4). It is suggested that JUN-1 and FOS-1 form a dimer to regulate *egl-13* expression (Oommen and Newman, 2007). It is important to note that the collaboration of the NOTCH and AP-1 is conserved for many steps of development. In our laboratory, Ivo Rimann identified *egl-43 Evi-1* another gene that is in addition to its importance during AC invasion, involved in the specification of π cell fate. *egl-43* cis-regulatory elements contain multiple putative Notch responsive CSL binding sites in addition to Fos/Jun sites. Performing egl-43 downregulation via RNAi experiments in *lin-12* gain-of-function mutations, reduced the amount of overinduced additional π cells due to the *lin-12* gain-of-function. From this can be concluded that EGL-43 is located downstream or in parallel of LIN-12 NOTCH during π cell induction (Rimann and Hajnal, 2007).

As already mentioned, it has been suggested that lack in uv1 induction, leads to utse cell fate adoption (Chang et al., 1999). This leads to the hypothesis that there is, in addition to the pathway responsible to prevent the four future uv1 π cells from forming utse cells, and another signal that ensures correct uv1 differentiation (Huang and Hanna-Rose, 2006).

So far, only a few factors involved specifically in uv1 cell fate differentiation have been identified. One of them is EGL-38. EGL-38 encodes a transcription factor, homologous to PAX5 that is expressed in the vulF cells and in the uv1 cells (see Fig

4). Lack of *egl-38* expression leads to abrogated vulF separation and further to the lack of uv1 cells. In the vulF cells, *egl-38* positively regulates the expression of LIN-3 EGF that induces uv1 induction through LET-23 EGFR expressed in the uv1 cells (Chang et al., 1999). The additional *egl-38* expression in the uv1 cells is suggested to be required as well for uv1 development. Since ectopic *let-23* expression in the uv1 cells can bypass the uv1 defects in *egl-38* mutants and *egl-38* does not eliminate *let-23* expression, one possible explanation is that EGL-38 works in parallel to LIN-3 EGF LET-23 EGFR signaling (Rajakumar and Chamberlin, 2007). Not surprising, the components of the vulval induction pathway downstream of LET-23 such as LET-60 RAS are suggested to be involved during the uv1 induction again (Chang et al., 1999).

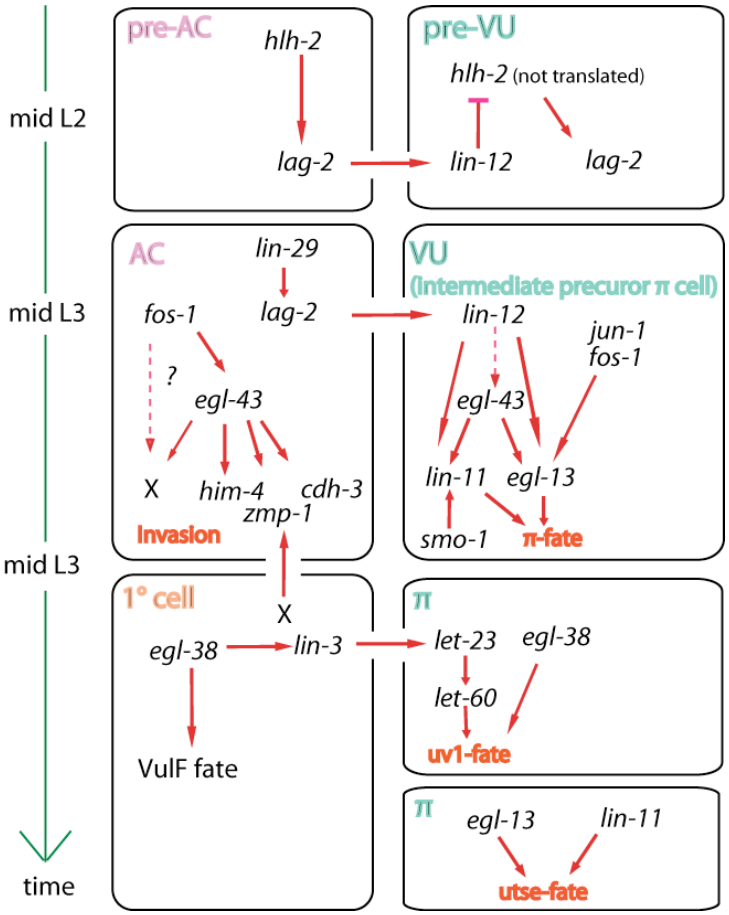

Fig. 4 This model gives an overview of the genes that are involved in the specification of the AC and the induction steps that are performed during the establishment of the uterus-vulva

connection. The induction of vulval development via EGF LIN-3 is not shown here. AC, anchor cell; VU, ventral uterine; utse uterine seam; uv1, uterine ventral 1. uv1 and utse differentiation.

2.9.3 Synchronised Development of the Uterus and the Vulva

The different induction events and the reciprocal signaling between the future vulva and the future uterus during development ensure that the developmental steps are synchronised. There are known genes, as for instance *lin-28* a member of the heterochronic pathway that disrupts drastically the communication between the two tissues drastically. LIN-28 is required for events specific to the L2 stage that are left out in *lin-28* mutants (Euling and Ambros, 1996). In accordance, *lin-28* mutants have a precocious vulval induction during the second larval stage. Due to this timing defect, the invasion of the AC is abrogated and all inductive signals are asynchronous, leading to a strong Pvl phenotype due to a lack of connection between the uterus and the vulva through AC invasion .

Another example is *cog-3,* a so far uncloned gene. The uv1 cells in mutants for *cog-3* exhibit an intermediate precursor cell fate, ready to adopt π cell fate. Due to abrogation of developmental timing, the *let-23* expression is late in relation to the vulva and the *lin-3* inductive signal coming from this tissue is missed. As a result, the uv1 cells then undergo cell death (Huang and Hanna-Rose, 2006).

2.10 Fusion of the AC to the Utse

In the last chapters, the odysee of the AC and its role in the proper establishment of the egg-laying system were presented. After all the duties are accomplished, the AC goes into retirement by fusing to the utse. The fusion of the utse and the AC takes place during the mid L4 stage. Before, thick uterine tissue is localised dorsal from the vulva. Fusion between these cells and the AC removes this bulky tissue, replacing it by the thin utse syncytium.

It is believed the utse hymen is destroyed, when the first egg is laid, opening a direct channel between the two tissues (Newman et al., 1996).

In general, cell-cell fusions are a very important process during development. The first cell-cell fusion event during the development of every organism is the sperm-egg fusion during fertilization giving raise to the development of a new organism.

In *C. elegans*, the *eff-1* (epithelial-fusion-failure-1) gene has been identified by Mohler et al to be required for epithelial cell fusions (Mohler et al., 2002).
Interestingly, loss-of-function of *eff-1* does not impede the fusion between the utse and the AC. In support of this result, an additional fusion protein, a predicted type-I transmembrane protein with ectodomain structure similar to *eff-1* has been identified in the genome of *C. elegans* (Sapir et al., 2007).
In an *aff-1* loss-of-function mutant background, the AC-utse fusion is blocked. In contrast, ectopic expression of *aff-1* results in fusion of cells that normally do not fuse. *aff-1* expression is observed in both, the utse and the AC just before fusion.
Moreover, *aff-1* expression in the AC is suggested to be regulated by FOS-1 the same transcription factor that is involved in AC invasion earlier during development, thereby coordinating the timing between the AC invasion and fusion. In *fos-1* defective animals, *aff-1* expression is strongly reduced or even not detectable in the AC. A direct regulation of *aff-1* by *fos-1* is supported by the identification of a consensus Fos-binding site in the *aff-1* promoter (Sapir et al., 2007).
Further, *nsf-1* encoding a N-ethylmaleinide-sensitive factor, an intracellular membrane fusion factor was identified to be crucial for AC fusion (Choi et al., 2006). *nsf-1* is expressed and required cell-autonomously in the AC and its expression was so far not observed in the utse.
NSF is a known and well studied protein required for vesicular fusion by binding to SNARE complexes (Sollner et al., 1993). NSF has also been reported to associate with non-SNARE receptors and influence their transport (Huang et al., 2005). However, the mode of interaction between the fusogen AFF-1 and NSF-1 remains to be elucidated.

2.11 Egg-laying Muscles and its Innervating Neurons

A young and healthy hermaphrodite animal carries on average 12 eggs in its uterus at any given time. To expel the fertilised eggs, the development of specialised uterine and vulval muscles and neurons that innervate the vulva and contribute in the end to an effective function of the organ, have to be established (Newman and Sternberg, 1996). Their development has to be synchronised relative to the vulva and uterus development.

A total of 16 muscle cells are likely to be involved in the mechanism of the egg-laying process. Of these, four vm2 vulval muscles have been shown to be particularly critical. They are arranged in a cross shape, with their apical ends attached to the vulva. In addition, 4 vm1 vulval muscles are arranged in a X-shaped pattern similarly to the vm2 muscles, also suggested to be involved in opening the vulva in order to lay eggs (White et al., 1976).
Furthermore, there are eight uterine muscles. They form bands that frame the anterior and the posterior arms of the uterus. The uterine muscles are also suggested to promote egg-laying. However their ablation does not result in the similar severe egg-laying defects as when ablating the vm2 neurons.

The HSN motorneurons, hermaphrodite specific neurons play a central role in egg-laying behaviour. Its cell bodies are located lateral and slightly posterior to the vulva making extensive neuromuscular junctions with the vm2 vulval muscles.
Moreover, 6 VC motorneurons have been identified, hermaphrodite specific neurons in the ventral nerve cord that are most likely also involved in egg-laying. They can be subdivided into two classes, being located proximally to the vulva (VC4 and VC5) and distally to the vulva (VC1-3 and VC6).
Particularly, the VC5 neurons receive significant synaptic input form the HSNs. The involvement of VC neurons in egg-laying is assessed by neuronal ablation experiments showing that the VC neurons are involved in egg-laying but less striking than the effects of the HSN ablation (Schafer, 2005).

2.12 Putative Roles of Heterotrimeric G Proteins in *C. elegans*

During my thesis, I performed experiments to identify a possible role of heterotrimeric G proteins during AC attachment and invasion. The next paragraph thus contains an introduction to heterotrimeric G proteins that that will serve as a guide for the corresponding section in experimental scection.

2.12.1 Heterotrimeric G Proteins

GPCRs, the largest group of cell surface receptors, belong to a large family of seven-pass trans-membrane proteins. They mediate extracellular signals of cellular responses that are involved in many very different cellular responses that cover

neurotransmitters, hormones, chemoattractants, taste ligands, pheromones and growth factors (Hamm, 1998).

The interaction with the activated GPCR and a heterotrimeric G-protein complex leads to the exchange of GDP against GTP in the G alpha subunit.

This protein complex is inactive in GDP bound form but upon exchange with GTP, Galpha-GTP and the G ß gamma heterodimer dissociate and have both the potential to interact with its effectors. Hydrolysis of GTP restores Galpha-GDP that reassociates with G ß gamma and signalling terminates (reviewed by Bastiani, 2006 #137, Battu, 2003 #143).

There are four identified classes of G alpha proteins known as Gi/o, Gi, Gq and G12, each controlling the activity of different second messengers. Gi/o for example is known to activate adenylyl cyclase to produce AMP, which activates Protein kinase A (PKA) and modulates cyclic nucleotide-gated ion channels (Bastiani and Mendel, 2006) whereas G12 and G1 activates Rho and Rap small GTPases (Kozasa et al., 1998).

2.12.2 Biology of Heterotrimeric G proteins in *C. elegans*

The *C. elegans* genome encodes 21 G alpha, 2 ß and 2 gamma subunits. The alpha subunits have one homolog to each of the known mammalian G alpha family Gs Gi/o Gq and G12 represented by GSA-1, GOA-1, EGL-30 and GPA-12. The remaining of the 21 alpha subunits are most similar to Gi/o but are not sufficiently homologue to allow classification.

In *C. elegans* most G alpha proteins are believed to be involved in muscle activity and perception (Jansen et al., 1999). Nevertheless, several GPCRs and heterotrimeric G proteins were found to control cellular proliferation and differentiation. In our laboratory for example, the GPCR SRA-13 was identified to inhibit MAPK activation not only in the AWA and AWC chemosensory neurons and but also during vulval induction (Battu et al., 2003). Moreover, being involved in the orientation, positioning and morphology of the mitotic spindle in *C. elegans* and *Drosophila*, heterotrimeric G proteins were identified to be involved in asymmetric cell division controlling cell size and fate (Bellaiche and Gotta, 2005). The expression pattern of several G alpha proteins such as for example *gpa-15* that is expressed in the AC and the DTCs (Bastiani and Mendel, 2006) leads to the suggestion that

heterotrimeric G proteins are involved processes during development besides muscle activity and perception.

2.12.3 Contribution of Chemokines during Biological Processes

Chemokines are a large group of low molecular weight cytokines. Chemokines activate cells though cell surface seven trans-membranes, G-protein-coupled receptors (GPCRs) and are known to attract and activate different types of cells.
So far, 18 chemokine receptors have been identified, divided into four subgroups, as each receptor binds to one of the four chemokine subfamilies (CXC, CC, C and Cx3C) (Strieter et al., 1992).
Although the primary function of chemokines identifed was the attraction of leukocyte, there is clear evidence that chemokines are involved in tumor-related processes such as growth, angiogenesis and metastasis. Chemokines produced by tumour cells attract infiltrating leukocyte and promote proliferation. They can also affect the microenvironment by promoting vascularisation. Chemokines are known to stimulate specific receptors that alter the adhesive capacity of tumour cell and their migration and invasion into circulation and extravasation towards distant organs (Singh et al., 2007).
A very prominent chemokine for instance is CXCL8, identified to be involved in angiogenic activity through the up-regulation of MMP-2 and MMP-9 in tumour and endothelial cells (Strieter et al., 1992). Matrix metalloproteinases (MMPs) are a family of extracellular endopeptidases that degrade ECMs and other extracellular proteins (Buss et al., 2007). Up to date, it is unclear whether *C. elegans* has homologues of chemoreceptor genes (Fredriksson and Schioth, 2005; Zlotnik et al., 2006).

2.13 Aim of these Studies

AC attachment and invasion into the vulval tissue are two processes that have not been understood in detail jet. Some conserved molecular factors that are involved in the dissolving of the two basal laminae between the gonadal and the vulval tissues have been identified. As a result, the AC has access to the vulval cells and is able to invade. But, so far unidentified cues secreted from the vulval cells to guide the AC on its way during invasion are likely to exist. The objective of this thesis was to identify new additional genes that play a role in regulating the mechanism of AC attachment, dissolving the basal laminae and invasion and to possibly identify the signalling cues coming from the VPCs.

Therefore, I performed an EMS mutagenesis screen and further experiments described below to identify genes that are involved in this process. Further, I wanted to identify with the same screen genes that are involved in the anchorage of the vulva and the uterus inside the animal's body.

3 Results

3.1 Characterisation of AC Attachment

At the early L3 stage, the AC induces vulval development and later, during the mid L3 stage, it invades the vulval tissue.

During the L2 stage, before the invasion of the AC and the induction of vulval development, the gonadal and the vulval tissues are separated by two basal laminae. During this period, the position between the AC and P6.p changes constantly due to the movements of the animal. In contrast, at the time of induction, the AC cell is attached in a hat-like shape on the basolateral side just above P6.p. Nevertheless, the two basal laminae between the gonad and the VPCs are still intact and direct contact between the two tissues is established when the AC invades the vulval tissue between the two innermost 1° cells, the vulF cells (Sherwood et al., 2005).

The mechanism of induction has been well studied. It is mediated via LIN-3 EGF, which is secreted from the AC to bind to its receptor LET-23 EGFR that is located at the basolateral side of the vulval precursor cells (Aroian and Sternberg, 1991). In addition, other components of AC invasion that are involved in dissolving the two basal laminae such as FOS-1 c-FOS and EGL-43 EVI-1 have been identified (Hwang et al., 2007; Rimann and Hajnal, 2007).

How the AC reaches P6.p, thereby gaining the optimal position to invade the developing vulva remains to be investigated. The AC is may already be attached before the time of induction. On the other hand, attachment may be caused by an attractive signal that P6.p produces in response to its induction. In this case it remains to be investigated how closely attachment is co-regulated with invasion.

3.2 Studies of Attachment in Wild-type Animals

To gain a better understanding of the process of AC attachment, I first studied this process in wild-type animals. Therefore, we measured the different distances between the AC and the P6.p nucleus. The measurement was performed at three points during development of the animal: at early L2, mid L2 and at the early L3. 20 animals were analysed per stage. The distance between the nucleus of the AC and P6.p was measured in parallel to the ventral epidermis (see Graph 1).

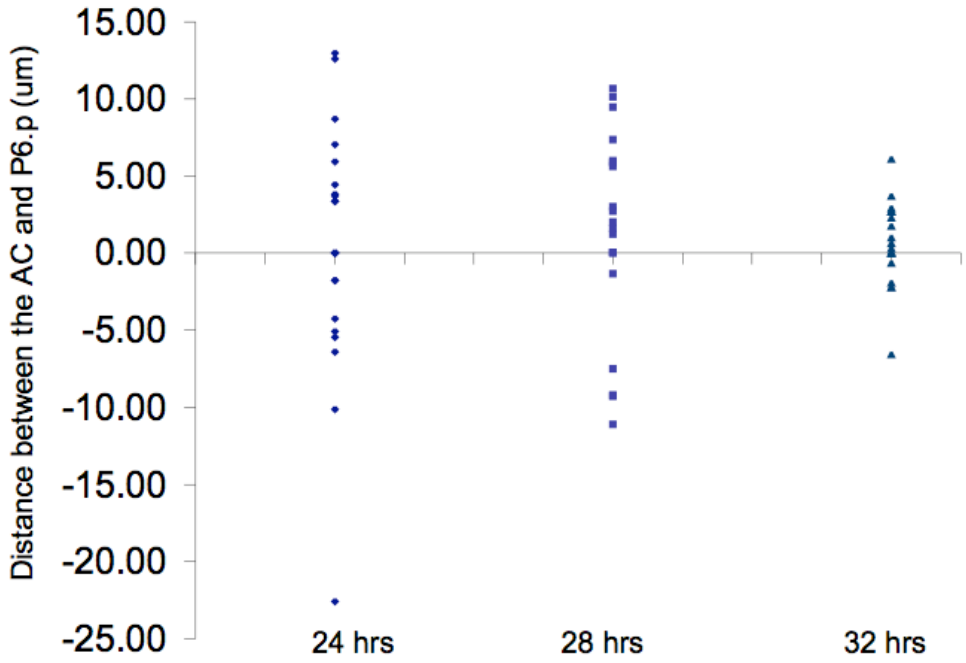

Graph 1 Time Course of AC positioning in wild-type animals. The time course depicts the AC position to P6.p. Early L2 stage corresponds to 24hrs, mid L2 stage corresponds to 28hrs and early L3 stage to 32hrs post L1. For every time point 20 animals were scored. Every data point corresponds to the distance between the nuclei of the AC and P6.p, respectively. P6.p was taken as reference point, while the position of the AC changes (positive distances are anterior from P6.p and negative distances are posterior from P6.p.

The AC was visualized with the reporter *lin-3::pat-3::gfp* (strain: *unc-119(e2498)*III*; zhEx87[lin-3::pat-3::gfp, unc-119(+)].*

This chimeric *lin-3* transgene in which the extracellular *egf* domain is fused with the *pat-3* integrin transmembrane can't be cleaved and therefore, remains at the membrane, nicely outlining the form of the AC from the L2 stage (Dutt et al., 2004).

During the early L2 stage, the distance between the AC and P6.p varied from 12.96µm to -22.6µm (AVG 5.6, 95%C.I. +/- 2.23), during mid-L2 stage, the distance varied between 10.67µm and -11.14µm (AVG 5.2, 95%C.I. +/- 1.73), and finally, at the time of induction, the distance varied between -6.08µm and -6.56µm (AVG 2, 95%C.I +/- 0.82) (see Graph 2).

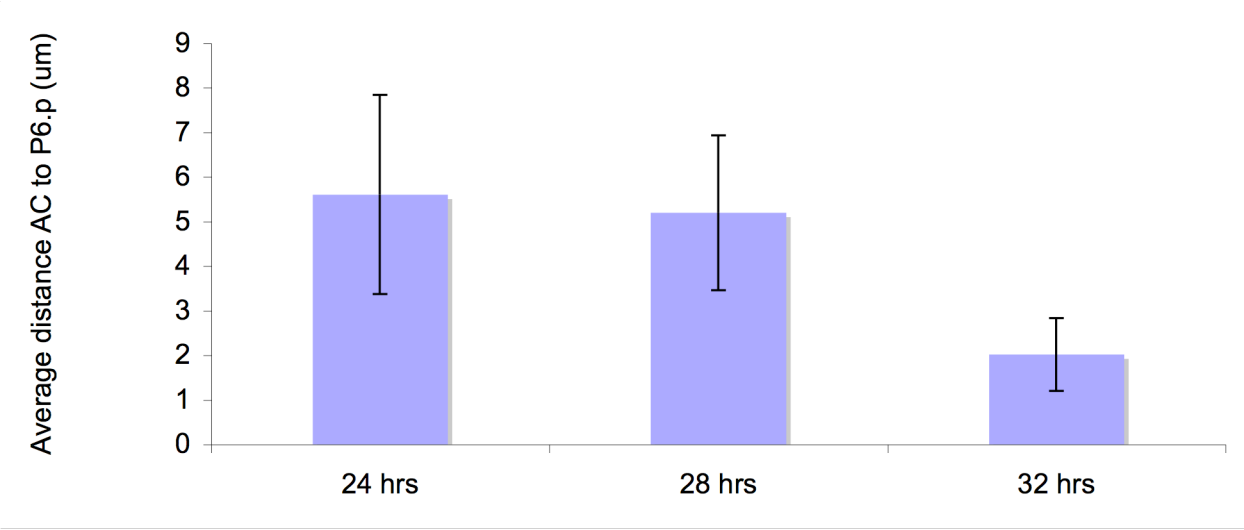

Graph 2. Average distance between the AC and P6.p nuclei at different developmental stages. At the early L2 stage (24 hrs), the average distance between AC and P6.p is 5.6 µm (C.I., 2.23), at mid L2 (28 hrs) it is 5.2 µm (C.I., 1.73) and at early L3 only 2.2 µm (C.I., 0.82). The C.I. diminishes with time, indicating that the liberty of relative movement of the two cells gets lower, as they get closer. In addition, it must be noted that the difference between the average distance of AC to P6.p in early L2 stage and mid L2 stage are not significant (overlapping C.Is), whereas the average distance at the early L3 stage is significantly smaller than at both previous measurements. Early L2 stage corresponds to 24hrs, mid L2 corresponds to 28hrs and early L3 32hrs post L1. Error bars represent the 95% confidence intervals (C.I.) of each measurement.

The results confirm that the distance between the AC and P6.p decreases between the mid L2 stage and the early L3 stage, leading to attachment. Between the early L2 and the mid L2 the changes are not significant (see Graph 2). Nevertheless, at the time of induction, the nuclei of the AC and the P6.p cell nuclei are in very close proximity (see Graph 1/2).

3.3 Different Mutant Backgrounds and their Impact on AC Attachment

To further analyse AC attachment, we studied this phenomenon in different mutant backgrounds. All experiments were performed as described for the wild-type background, but were performed only at the early L3 stage. First, we studied AC attachment in *lin-39(n1880)* loss-of-function mutants to test if adoption of vulval cell fate is a premise for AC attachment.

lin-39 is a Hox gene, which was found to be crucial for the specification of vulval precursor cells in the early L1 (Clark, 1993 #2). The AC was visualized with the extrachromosomal reporter *lin-3::pat-3::gfp* (strain: *lin-39(n1880); extrachromosomal array: zhEx168[lin-3::pat-3::gfp, lin-48::gfp].*) The results of these experiments show that the distance between the AC and P6.p cell remains high in *lin-39* loss-of-function mutants (see Graph 3/4). While the average distance between the AC and P6.p in wild-type animals is of 2µm, the distance in *lin-39(n1880)* is of 29µm at the early L3. From this result, we can conclude that VPC specification is crucial for the attachment of the AC to P6.p (see Graph 4).

Second, to test whether the loss of vulval induction leads to the loss of AC attachment, we tested AC attachment in mutant backgrounds that affect core components of vulval induction. Instead of using the LIN-3 reporter as described before, a transcriptional *cdh-3::cfp* reporter was used here. CDH-3 is an effector protein of AC invasion that is expressed in the AC from the time of induction onwards (Sherwood et al., 2005).

The *let-23* mutation chosen for the experiment mislocalises LET-23 to the apical compartment of the VPCs and causes a vulvaless (Vul) phenotype *(let-23(sy1)* (Aroian and Sternberg, 1991). The result indicates that the attachment of the AC is reduced in the *let-23* background. (see Graph 3/4) The average distance between the AC and P6.p is at 4.3µm in contrast to 2µm average distance in wild-type animals.

Similar experiments were performed in a *lin-3* deficient background. The chosen allele *lin-3(e1417)* has lost its function of EGF transcription solely in the AC (Hwang et al.; 2003). (see Graph 3/4). In a *lin-3(e1417)* background, the average distance increases to almost 8µm in the *lin-3(e1417)* mutant background at the time of induction.

Graph 3. Analysis of AC position in different mutant backgrounds: The distance between the AC and P6/P6.p is measured at 32 hrs post L1, an equal to the early L3 stage. Every data point corresponds to the distance between the nuclei of the AC and P6.p, respectively. P6.p was taken as reference point, while the position of the AC changes (positive distances are anterior from P6.p and negative distances are posterior from P6.p. The experiments were performed with the alleles *lin-39(n1880*), *let-23(sy1)* and *lin-3(e1417).* 20 animals per line were scored.

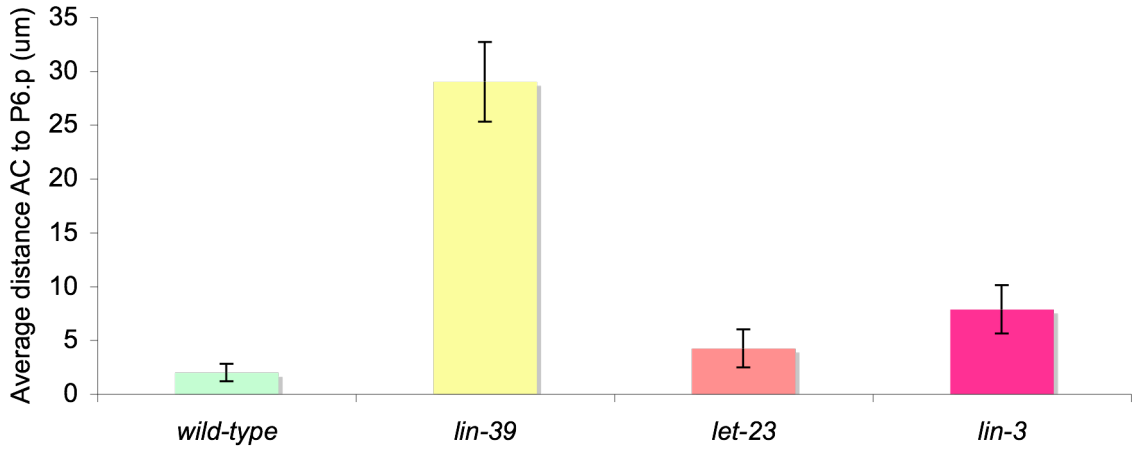

Graph 4. Average distance between the AC and P6/P6.p in different mutant backgrounds at the early L3. The average distance between the AC and P6.p in wild-type animals is 2 µm (C.I., 0.82). This distance increases to 29 µm (C.I., 3.72) in *lin-39(n1880)* mutant animals where P6 did not differentiate to adopt VPC fate. In mutants of the EGF signalling pathway (*let-23(sy1)* and *lin-3(e1714)*) the average distance between AC and P6.p increases two and fourfold respectively (p-value = 0.03 for let-23 and >0.001 for lin-3). Error bars represent the 95% confidence intervals measurement.

3.4 Targeted RNAi Screen for Genes Involved in AC Attachment and Invasion in a Sensitised Background

So far, the mechanism of AC invasion has not been elucidated in detail. While the basics of the mechanism that leads to the dissolving of the basal laminae between the two different tissues were identified recently, the attracting cues that guide the AC along its way remain to be identified.

During the mapping process of *zh70* (see 3.7), *gpa-15* emerged as a possible candidate. *gpa-15* encodes a member of the G protein alpha subunit family of heterotrimeric GTPases. Heterotrimeric GTPases mediate extracellular signals that are taken up by GPCRs, one of the largest groups of cell surface receptors. The *C. elegans* genome encodes 21 G alpha subunits that are believed to interact with a large group of the identified receptors, many of which have no identified functions so far. In addition to being expressed in a subset of neurons, *gpa-15* is expressed in the AC and in the DTCs (Bastiani and Mendel, 2006). DTCs are responsible for the guidance of the growing gonad arms. However, the role of GPA-15 in these tissues has not been investigated yet. It is notable that both aforementioned cells, the DTCs and the AC depend on guidance cues to become localised properly during development (Merz et al., 2001). Furthermore, it has been suggested that some factors that are involved in gonad guidance are also involved in attachment and invasion of the AC (unpublished results, Joshua W Ziel et al.; 2007, International Worm Meeting). We speculated that *gpa-15* might be involved in AC attachment or invasion due to the before mentioned findings. However, the loss-of-function mutant *gpa-15(pk447),* does not exhibit a Pvl phenotype. Nevertheless, redundancy of different pathways and genes is often observed during developmental processes. Therefore, we performed a synthetic RNAi screen in a *gpa-15* loss-of-function background to analyse the other identified G protein alpha subunits. Moreover, the screen was performed in a wild-type background.

In addition to *gpa-15*, we tested *srw-33* and *Y54E2A.1* two GPCRs, for their involvement in invasion and attachment, since both proteins are annotated on wormbase as exhibiting a Pvl phenotype. The genes of interest were individually knocked down by RNA interference. The experiments were repeated twice at a concentration of 4mM IPTG and once at a concentration of 6mM IPTG in both, an *rrf-3* background and in a *gpa-15* loss-of-function background. Six of the RNAi clones

were contaminated. The results from these clones were discarded (see Table 1). During the first step of the screening procedure, the corresponding Pvl phenotypes were identified. Subsequently, the animals were analysed at the eight-cell stage of vulval development with Normarski optics to investigate whether the Pvl phenotype resulted from an attachment or invasion defect.

Over all, no invasion or attachment phenotype was observed in any of the analysed animals.

Sequence name	Main name	RNAi clone	contaminated
T19C4.6	*gpa-1*	E12 151	
F38E1.5	*gpa-2*	A5 145	
E02C12.5	*gpa-3*	D10 147	
T07A9.7	*gpa-4*	F1 92	X
F53B1.7	*gpa-5*	A3 179	X
F48C11.1	*gpa-6*	G9 196	
R10H10.5	*gpa-7*	B3 110	
F56H9.3	*gpa-8*	G9 154	
F56H9.4	*gpa-9*	G10 154	
C55H1.2	*gpa-10*	B2 141	
C16A11.1	*gpa-11*	A4 42	
F18G5.3	*gpa-12*	F8 190	X
F18E2.5	*gpa-13*	A12 155	X
B0207.3	*gpa-14*	A12 8	
M04C7.1	*gpa-15*	H4 13	
Y95B8A.5	*gpa-16*	-	
C34D1.3	*odr-3*	B3 156	
C26C6.2	*goa-1*	H8 11	X
R06A10.2	*gsa-1*	G12 1	
M01D7.7	*egl-30*	A11 2	
Y54E2A.1	-	B7 64	X
T26H5.5	*srw-33*	G8 161	

Table 1. This list of the genes that were downregulated performing RNAi experiments to identify molecular factors involved in AC attachment or invasion.

3.5 Characterization and Mapping of the Mutant *pvl-6(ga81)*

3.5.1 The Phenotype of *pvl-6(ga81)*

The mutant *pvl-6(ga81)* was isolated in a mutagenesis screen by the Eisenmann laboratory (Eisenmann and Kim, 2000). *pvl-6(ga81)* mutants exhibit a Pvl phenotype. Furthermore, the interactions between the AC and P6.p are defective in these mutants. In accordance, it is described that the AC lacks the potential to invade the vulval tissue in *pvl-6(ga81)* mutants (Eisenmann and Kim, 2000). Moreover, at the time of invasion, the AC is not attached above P6.p in *pvl-6(ga81)* mutants. This suggests a function of *pvl-6(ga81)* in AC attachment. We were able to reproduce this finding (see Fig. 5).

Figure 5. *pvl-6(ga81)* displays an AC attachment defect. The Normarski image displays the vuval tissue of a *pvl-6(ga81)* hermaphrodite at the eight-cell stage. The AC has not invaded the vulval tissue. Anterior is to the left.

However, *pvl-6* had not been cloned so far and in accordance, its molecular function is not known. Before cloning the gene, I wanted to analyse the attachment and invasion defects of *pvl-6(ga81)* in more detail. Therefore, I crossed animals containing the AC marker *cdh-3::cfp* to *pvl-6(ga81)* mutants. In contrast to the original strain, these animals did not show a clear phenotype anymore. The cross was repeated several times, but the phenotype was always lost. Moreover, the original plates lost the phenotype over the different generations as well. David Eisenmann also observed a loss of the *pvl-6(ga81)* phenotype, which suggests that the reason might be a suppressor mutation.

3.5.2 FLP Mapping Results of *pvl-6(ga81)*

In the Eisenmann laboratory, *pvl-6(ga81)* was confined to a region between -20.00 and -5.25cM on chromosome V (Eisenmann and Kim, 2000). These results were reconfirmed in our laboratory performing FLP experiments. The crosses were

performed as depicted in figure 7. Interestingly, crossing Hawaii with *pvl-6* animals resulted in a loss of the Pvl phenotype. While the F2 cross-progeny from the cross between Hawaii and *pvl-6* still showed a relatively clear Pvl phenotype, the F3 progeny was not usable to confirm the homozygosity of *pvl-6*. Therefore, the results obtained by performing the FLP experiments are not reliable. Nevertheless, the region between ZH5-03a at -15.16cM and ZH5-06 at 3.39cM is represented in 8 out of 48 lysates by the Hawaii genome most possibly sorting this region out as the possible location of *pvl-6* (see Figure 8).

The FLP ZH05-13 at -18.57cM is represented six times with the Hawaii genome. ZH5-02a at -19.99cM, the last FLP on the left side of chromosome V was represented by five lysates with Hawaii coming from the right side and in addition one FLP from the left side, results that are rather contradictory. In conclusion, my results confirm the mapping results of the Eisenmann laboratory. Unfortunately, due to the instability of the phenotype we decided not to investigate the mutants *pvl-6(ga81)* further.

3.6 RAS/MPK Pathway Does not Act in the AC during AC Invasion

One of the functions of the FOS-1 c-FOS pathway is to regulate effector proteins that are secreted form the AC to dissolve the basal laminae between the vulval and the uterine tissue during AC invasion (Sherwood et al., 2005). Until now, nothing is known about the mechanism of FOS-1 activation.

Furthermore, the effector genes that have been identified so far, *zmp-1*, *cdh-3* and *him-4*, only exhibit a 25% penetrant invasion phenotype in triple mutants. This suggests that there must be more genes working in parallel to *zmp-1*, *cdh-3* and *him-4*, downstream of FOS-1 c-FOS. Optionally, these effectors could be activated by a pathway, which might act in parallel to the FOS-1 c-FOS pathway (Sherwood et al., 2005).

In conclusion, there should be more yet unidentified components expressed in the AC, downstream or in parallel of the FOS-1 c-Fos pathway that are involved in dissolving the basal laminae. Since it has previously been shown that components of the EGFR/RAS/MAPK pathway are expressed in the AC, I decided to study the impact of this pathway on AC invasion (Dent and Han, 1998).

For this purpose, I built the following strain: *gaIs47[lin-31-mpk-1(Siegfried et al.), lin-31-dmek(Siegfried et al.)]; unc-32(e189) mpk-1(ga117)/gc1* III. *mpk-1* encodes a protein kinase which acts in the vulval precursor cells to affect induction of vulval cell fates downstream of LET-60 RAS. The chosen allele, *mpk-1(ga117)* was shown to eliminate *mpk-1* activity in the whole animal (Lackner and Kim, 1998). Since *mpk-1* affects multiple phenotypic traits including sterility, the mutation was balanced using the inversion gc1. To study the impact of RAS/MAPK signalling loss-of-function solely in the AC and in order to maintain vulval induction, the pathway was rescued by expressing *mpk-1* under the promoter of *lin-31*. *lin-31* is a tissue-specific effector of RAS/MAPK signalling that is expressed in vulval precursor cells. The animals homozygous for *mpk-1(ga117)* were recognised through the cis-linked marker *unc-32(e189)* that leads to uncoordinated (Unc) movements and a sterile phenotype. I studied the Unc descendents of the balanced strain *gaIs47[lin-31-mpk-1(Siegfried et al.), lin-31-dmek(Siegfried et al.)]*; *unc-32(e189) mpk-1(ga117)* for defects in AC invasion.

Moreover, *mpk-1* and *mek-2* overexpression in the vulval cells leads to a multivulva (Muv) phenotype. Muv animals are defined by the ectopic induction of VPCs. Nervertheless, P5.p, P6.p and P7.p undergo wild-type morphogenesis, which means that AC invasion can be studied in these animals. To identify defects corresponding AC invasion in these animals, 25 adult hermaphrodites were studied under Normarski optics for a Pvl phenotype that was expected to result from an invasion defect. In addition, the animals were studied at the mid-L3 stage for invasion defects. None of the animals showed a defect in AC invasion. From these results, I concluded that RAS/MAPK signalling is not involved in AC invasion in tissues different from the VPCs and vulval cells.

The following pages are written in a format of a manuscript. Therefore, the text is sometimes a repetition of the described mechanisms in the introduction and the results of the thesis that are described after this manuscript in more detail.

3.7 Forward Genetic Screen Identifies Novel Genes Involved in the Development of the Egg-laying System of the *C. elegans* Hermaphrodite

3.7.1 Abstract

The egg-laying system of *C. elegans* is a popular model with which to study the molecular processes that control organ morphogenesis. It consists of the vulva that is connected to the uterus via a subset of specialised ventral uterine cells. The anchor cell serves as the key organizer during the establishment of the connection between the vulva, the uterus and the lateral hypodermis. The AC invades the vulval tissue, thereby building the first physical contact between the vulva and the uterus. We performed a forward genetic EMS mutagenesis screen for isolating genes regulating uterus development and AC invasion. Since mutations that cause sterility cannot be isolated with standart protocols, we performed a clonal screen to increase our coverage. We identified ten mutants; nine of them are sterile and one is fertile. We classified the mutants into three groups according to their phenotype. The class I consists of mutants with a defect in differentiation of the ventral uterine cells. The mutants of class II show a similar phenotype but in addition ectopic expression of the used AC reporter in the uterine cells. The class III consists of two mutants that both with an AC invasion defect, The two mutants with an AC invasion phenotype are new alleles of *fos-1* and *lin-28*. The linkage group of the eight remaining mutants was defined by FLP mapping. In addition, we defined the sub-chromosomal region of a set of mutants. The identification of *fos-1* and *lin-28* shows that this screen was powerful enough to isolate genes that are important for vulval anchoring and highlights the necessity to characterize the remaining mutants further.

3.7.2 Introduction

How cells grow, differentiate and finally undergo morphogenesis to eventually form an organ is a fundamental question that developmental biologists would like to answer on a molecular level. *C. elegans* is famous for its invariant somatic cell lineage, which makes the hermaphrodite of *C. elegans* amenable to study pattern

formation and morphogenesis. The model organ chosen in this study to examine cell communication during organogenesis is the egg-laying system of the hermaphrodite.
The development of the egg-laying system is genetically accessibly because the mutations involved in vulval development are often viable and the corresponding phenotypes are easily discernable under the microscope making it a practical model to study organogenesis.
The egg-laying system is built form two tissues, the vulval tissue and a part of the uterine tissue. The vulval and the uterine tissue differentiate from two different germ layers. While the vulval tissue is a specialised epidermal tissue, the uterine tissue derives form the mesoderm. Nevertheless, their development is tightly synchronised in space and time to ensure the egg-laying functionality and to anchor the vulva in the animal's body. The development involves bidirectional signaling between two tissues to synchronise their individual development, cell migration events, the proteolysis of extra-cellular matrix (ECM), cell invasion and tubulogenesis.
Interestingly, most of the mentioned developmental steps are organized or even directly performed by the anchor cell (AC), a cell that originates from the ventral uterine tissue.
During the L2 stage, the AC is born via lateral signalling mediated by LIN-12 NOTCH (Wilkinson et al., 1994). In consequence, at the early L3 stage, the AC induces vulval development via LIN-3 EGF (Aroian and Sternberg, 1991). The vulval cells start dividing to eventually build a vulva consisting of 22 cells. About four hours after vulval induction, the AC further induces six ventral uterine (VU) cells via LIN-12 NOTCH to adopt π cell fate (Newman et al., 1995). After one round of cell division four of the π cells are further induced to adopt uv1 cell fate via LIN-3 EGF signalling (Newman and Sternberg, 1996). The induction is regulated by the expression of LIN-3 EGF in the vulval cells most closely located to the ventral uterus. The uv1 mononucleate cells establish the connection between the uterus and the vulva. The remaining eight π cells undergo further differentiation to form the utse (uterine seam cell) syncytium (Newman et al., 1999). The utse forms the connection between the uterus and the lateral seam cells, thereby contributing to the maintenance to the egg-laying system in the animal's body. In addition, the AC contributes to the connection between the vulva and the uterus, by invading the vulval tissue during the mid L3. This invasion step is not elucidated in detail yet, but the dissolving of the two basal laminae

between the uterine and the vulval tissue is mediated via FOS-1 c-FOS signalling (Sherwood et al., 2005). After the AC has performed its duties for this connection, it fuses to the utse, thereby cleaning the way for the eggs and sperms that need to pass (Sapir et al., 2007).

In case this connection is not properly established, the vulva is not anchored properly in the animal's body but everts out of the animal.

This often leads to a protruding vulval phenotype (Pvl) that is very well visible under the dissecting microscope.

In order to isolate genes that have an impact on developmental processes such as AC attachment, AC invasion, or genes that are involved in the development of ventral uterine cells responsible to establish the connection between vulval and uterine tissue, we performed a forward genetic mutagenesis screen.

So far, classical mutagenesis screens were designed and performed in a fashion that allowed the identification of fertile mutants, while mutants that affect multiple phenotypic traits such as sterility were lost. In contrast, the screen performed in this study was designed in a clonal fashion. In accordance, after mutagenesis of the P0 animals, a certain amount of the first progeny (F1) was plated in a manner such that every F1 animal was isolated from the others on a single plate. The F2 generations of the single plates were used to study the phenotype of animals homozygous for the mutant allele but also to maintain the strain due to the heterozygous animals on the same plate. This allows the identification of genes that, in addition to the developmental effect of interest, lead to sterility or late lethality.

To identify mutants with an AC attachment, AC invasion phenotype or mutants leading to a lack of connection between the uterus and the vulval tissue, we screened for mutants exhibiting a Pvl phenotype. Furthermore, the mutant lines were rescreened for AC mislocalisation during different stages using the AC marker *cdh-3::cfp*. Performing this screen we isolated three groups of mutants based on their distinct phenotypes.

The first group displays an AC fusion defect during the L4 stage, supposedly due to the lack of properly differentiated uterine tissue. This phenotype showing the incompetence of the AC to fuse to the ventral uterine tissue was already observed in previously identified mutants of genes involved in the differentiation of the uterine tissue, the uv1 and utse cells.

The second group displays genes that in addition to an AC fusion defect as was described for the first group, exhibit ectopic expression of the AC reporter in the uterine tissue. This phenotype might derive from a misregulation of AC fate adoption and the ectopic expression of the reporter can be interpreted as differentiation of two ACs. The genes of this group might represent downstream factors of the LIN-12 NOTCH signalling pathway.

Finally, the third group comprises two mutants that both exhibit an invasion defect. The genes of the third group were both cloned. *lin-28*, a heterochronic gene leads to the premature induction of vulval development, thereby disturbing the timing between the uterine and the vulval development which is crucial for invasion. The second mutant represents an allele of *fos-1*. This gene is an important component during AC invasion, responsible for the disruption of the two basal laminae between the vulval and uterine tissue. The two identified genes show that the screen has the potential to systematically identify genes necessary for the uterus development.

3.7.3 Results

3.7.3.1 Rationale of the Clonal Forward Screen

In order to isolate genes that have an impact on developmental processes such AC attachment and AC invasion to the vulval tissue or factors that are directly involved in the development of ventral uterine cells responsible of establishing the connection between vulval and uterine tissue, we performed a forward genetic mutagenesis screen.

It is believed that mutants for genes involved in these developmental processes exhibit a protruding vulva phenotype (Pvl) due to the following reasons.

The AC is the key organiser of the development of the connection between the uterus and the vulva. To assure this connection, the AC has to attach and to invade the vulval tissue.

Furthermore, the AC coordinates the individual development of the vulva and the uterus, inducing cell fate adoption in both tissues, the uterine and the vulval tissue. In accordance, the induction of vulval development and π cell fate differentiation in the uterine tissue are performed by signals produced in the AC. It is important to note that the induced π cells differentiate further and not only form the two tissues that connect the vulva and the uterus, defined as uv1 cells but also the utse syncytium

that forms adherens junctions with the uterus and the seam cell, a specialised lateral hypodermis of the animal to anchor the egg-lying system in the animal's body.
The utse syncytium eventually fuses with the AC removing the bulky AC and making space for the eggs to be laid.
So far, most genes involved in the processes described here have been shown to display a Pvl phenotype. That the genes we are searching for will lead in a mutated form to a Pvl phenotype is further supported by the study of previously identified genes. For example, *egl-43 ev1-1*, a key actor during AC invasion displays a highly penetrant Pvl phenotype (Rimann and Hajnal, 2007). Another example is *egl-13*, a gene responsible for the maintenance of uterine π cell fate. *egl-13* deficient animals exhibit a Pvl phenotype.
So far, classical mutagenesis screens were designed and performed in a fashion that allowed the isolation of fertile mutants, while sterile or late lethal mutants due to pleiotrophic effects were lost. To identify mutants of a classical mutagenesis screen, the F1 animals of the mutagenised parents were grown on the same plates and the F2 progeny with the mutant phenotype of interest directly picked form those plates and maintained to produce further progeny.
In contrast, performing a clonal forward screen, as described here, allows the recovery of mutations of interest that in addition to the vulval and uterus phenotype also cause sterility (see Fig. 6).
Therefore, each F1 animal, hypothetically being heterozygous for a mutation of interest but exhibiting a wild-type phenotype was plated on a single plate.
In case the F2 generation revealed a phenotype of interest, the plate was isolated. From those plates heterozygous animals were used for the maintenance of the strain, and the phenotype of the homozygous, sterile, animals was further studied.

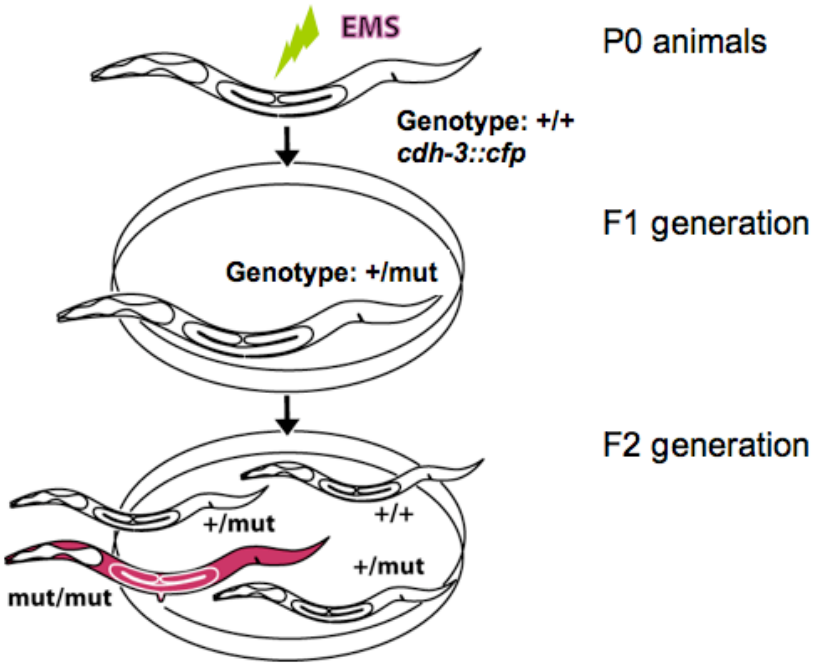

Figure 6. Schematic representation of the clonal forward mutagenesis screen. P0 animals at the L4 stage containing the *cdh::cfp* reporter to identify the AC were mutagenised with EMS. The F1 generation was cloned to independent plates and the F2 generation was screened for animals exhibiting a Pvl phenotype.

3.7.3.2 Screening procedure

The screening procedure was divided in two steps. First, we screened for a protruding vulva phenotype (Pvl). Second, the isolated lines were rescreened using an AC marker to study the cause of the Pvl phenotype.

In more detail, the plates carrying the cloned F1 progeny were analysed under the dissecting microscope for animals with an everted vulva. Generally, on plates carrying mutants with a 100% penetrant Pvl phenotype, one out of four animals was expected to exhibit such a phenotype, whereas among the F3 generation, the fraction of animals being homozygous for the mutation had already declined. Therefore, the worms were analysed as soon as the first animals of the F2 generation reached adulthood. We decided to choose only lines with a penetrance

higher than 30%, since lines below this threshold would be very laborious to map. Finally, the strains of interest were re-screened using Normarski optics. Mixed population of animals were analysed at different stages during development.

The mutants were studied from early L3 onwards, to examine whether they exhibit an AC displacement phenotype resulting from an attachment defect. Furthermore, the mutants were analysed at the four-to-eight-cell vulval stage during the mid L3 to identify animals that exhibit an invasion defect. Lastly, during the L4 stage, when the AC has fused to the utse tissue in wild-type animals, the lines were examined for defects in ventral uterine formation. In mutants that exhibit a defect in the development of this tissue, the AC has no differentiated tissue to fuse to.

To facilitate the screening procedure, we used a strain containing the an AC reporter *cdh-3::cfp* (Inoue et al., 2002). CDH-3 is a component of the AC invasion machinery that is expressed in the AC from the early L3 to the L4 stage, when the AC fuses to the utse cells (Rimann and Hajnal, 2007). It is important to note that at the time when we performed the screen the function of this gene was not known.

During EMS mutagenesis, several mutations can accumulate in the same mutagenised animal. To analyse a mutant phenotype of interest, it is of importance to introduce the original wild-type background into the mutant in order to get rid of phenotypically unrelated mutations. Every strain was out crossed once with the original wild-type strain before the first mapping step.

After the linkage group of the mutants was identified and the mutations were balanced, they were further out crossed at least twice, before further mapping procedures.

3.7.3.3 FLP Mapping to Identify the Linkage Group and Subchromosomal Region of the Mutation

Genetic mapping with DNA sequence polymorphisms is an efficient method to clone mutants. At the University of Zurich, a new approach for automated fragment length polymorphisms (FLP) mapping was established (Zipperlen et al., 2005). This improved method is very convenient, since 120 FLPs covering the whole genome between *C. elegans* Bristol, N2 and Hawaii, Cb4856 were identified and the corresponding PCR reactions were optimised.

To perform mapping experiments, the FLPs were used as explained hereafter. Bristol, which contains the mutation of interest and Hawaii were crossed together and

animals of the F2 generation that were homozygous for the mutation of interest were isolated due to their phenotypes (see Fig. 7). The cross was performed with Hawaii males containing *sur-5::cfp* in the form of an extra-chromosomal array to easily identify the F1 cross progeny (see Fig. 7).

To identify the chromosomal linkage group of the identified mutants, 16 lysates of individual F2 progeny were analysed by a defined set of 12 FLP reactions, two per chromosome, thus covering the whole genome.

Subsequently, a second round of FLP mapping was used to identify the subchromosomal region of the mutation. Usually, 48 individual single worm lysates were analysed with a defined set of eight FLP reactions covering the chromosome of interest.

Third, the experiment was repeated using additional FLP markers within the remaining region to further reduce the size of the region down and to reconfirm the results form the previously performed round. In theory, with this method, the region can be reduced to an interval of 3cM only.

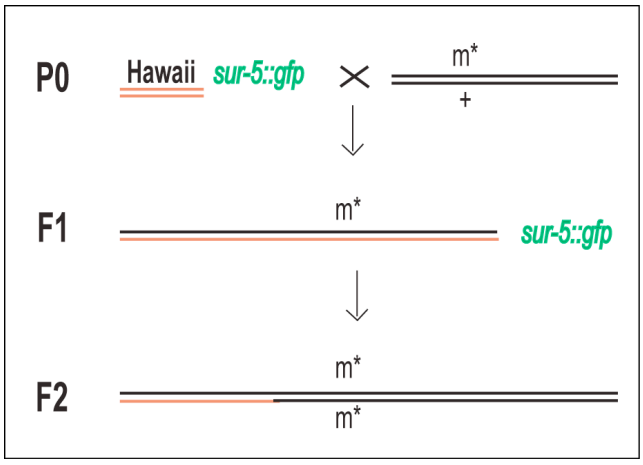

Figure 7. Schematic representation of the crossing procedure for the mapping experiments. Red defines the Hawaii genome; black represents Bristol genome; m* the mutation of interest in a Bristol background. The extrachromosomal array [*sur-5::gfp*] was used in the Hawaii strain to identify the cross progeny. The F2 progeny represents an informative animal due to a cross-over event in relative close vicinity to the mutation.

3.7.3.4 Overview of Isolated Mutants

The mutagenesis was performed within 10 sub-screens. All together, 5300 F1 clones were analised, among them 115 mutant strains exhibited a strong enough Pvl. Finally, we identified ten mutant strains with phenotypes of interest. Nine of them are sterile, whereas one is fertile (*zh70*). Based on their phenotypes, the mutants were grouped into three categories that are described below.

Group	Allele	LG	Subchromosomal Region (Zahn et al.)	Balancer	Comments
I	*zh68*	IV	-	*nT1[qIs51]*	candidate: *nhr-67*
	zh69	IV	-16.26-10.37	*nT1[qIs51]*	candidate: *nhr-67*
	zh76	IV	3.25-5.7	*nT1[qIs51]*	candidate: *nhr-67*
	zh74	II	1.09-3.45	*mIn1[dpy-10(e128)*mIs14]	*egl-43* ruled out
	zh75	II	-	*mIn1[dpy-10(e128)*mIs14]	
	zh77	?	-	-	
II	*zh72*	IV	-16.26-10.37	*nT1[qIs51]*	candidate: *lag-1*
	zh73	I	2.73-3.91	*hT2[bli-4(e937) let-?(q782) qIs48*	candidates: *sup-17* and *aph-1*
III	*zh70*	I	-	*hT2[bli-4(e937) let-?(q782) qIs48*	confirmed allele of *lin-28*
	zh71	V	-	*nT1[qIs51]*	confirmed allele of *fos-1*

Table 2. Overview of the mutants identified in the clonal forward mutagenesis screen.

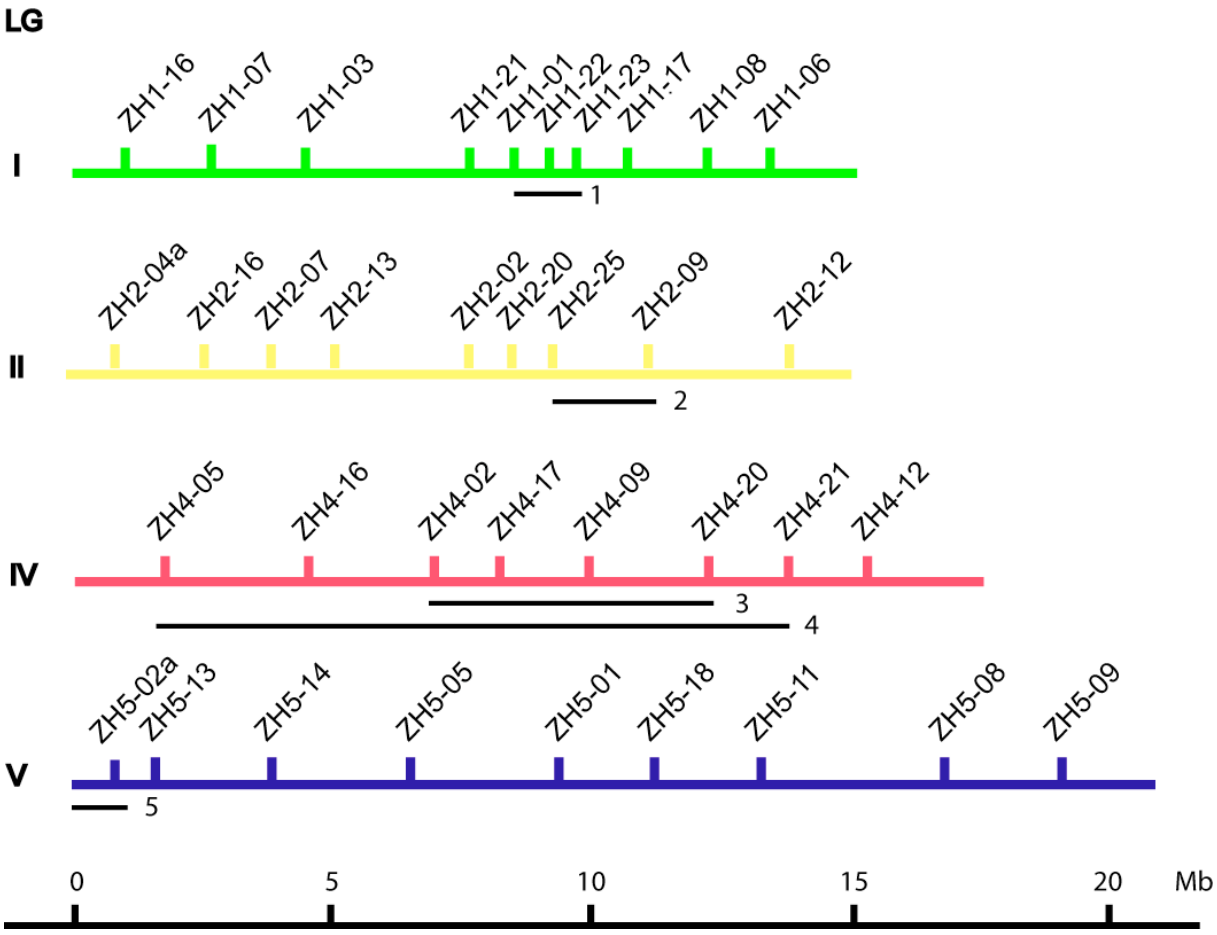

Figure 8. Schematic representation of the distribution of the FLPs used to perform mapping experiments of the mutants *zh69, zh70 (lin-28)* LGI, *zh71 (fos-1)* LGV, *zh74 and zh76.* 1 depicts the expected region of *zh73*, 2 the expected region of *zh74*, 3 the suggested region of *zh76* and 4 the suggested region of *zh69* and *zh72,* 5 the expected region of *pvl-6(ga81).*

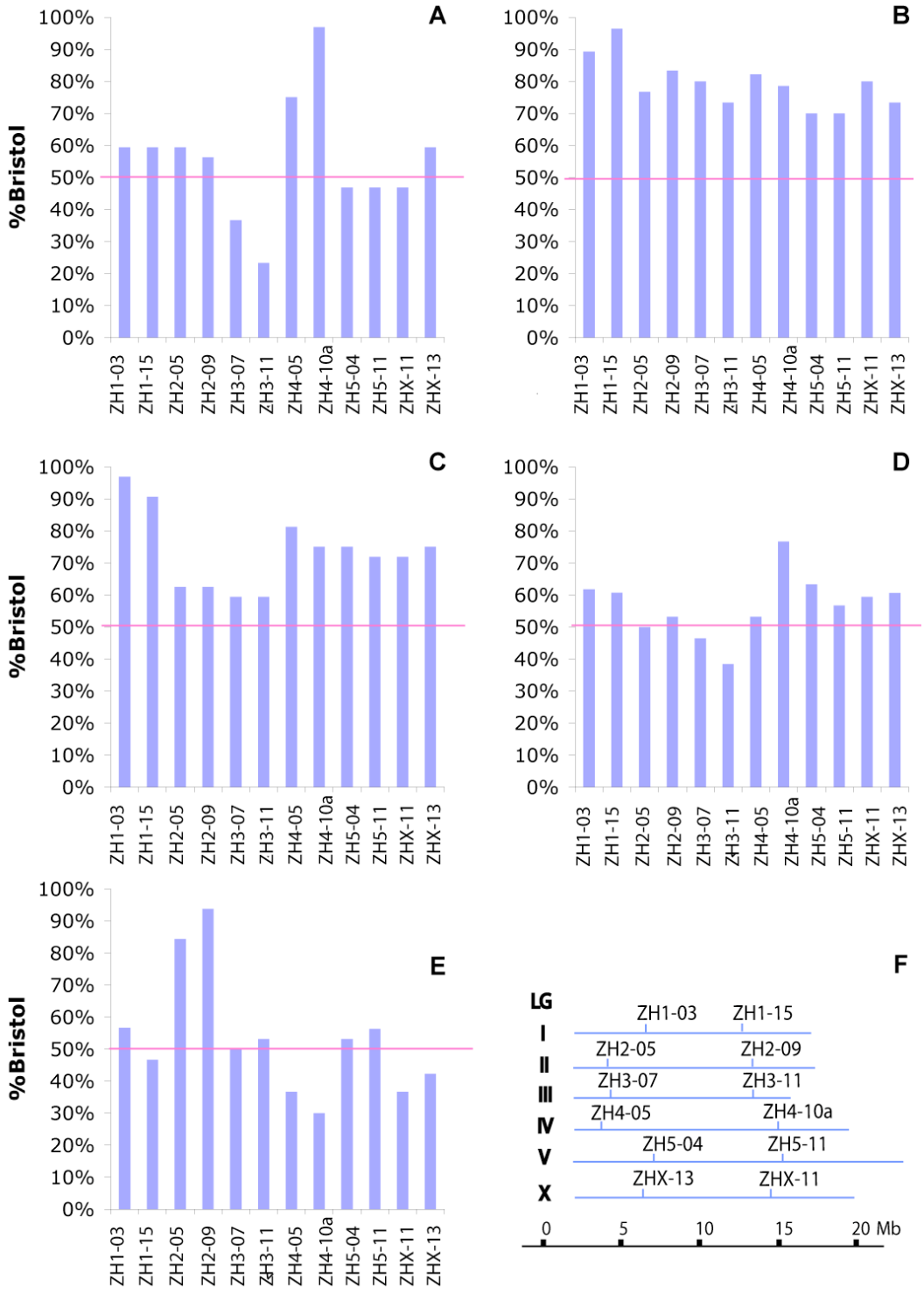

Figure 9. Schematic representation of the results to define the linkage group of the animals.
To identify the linkage group of the isolated mutants, 16 lysates of individual F2 progeny were analysed by a defined set of 12 FLP reactions, two per chromosome (F). The different graphs display the results obtained from the following mutants. (A) *zh72,* (B) *zh73,* (C) *zh77,* (D) *zh68,* (E) *zh75*.

3.7.3.5 Group I

In wild-type animals, the utse cell builds together with the AC a thin laminar process at the L4 stage. The utse syncytium is together with the uterine-vulval cells (uv1) responsible for the establishment of a connection between the vulva, the seam cells and the uterus. The utse and uv1 cells differentiated from π cells, specific descendants of the ventral uterine cells (Chang et al.; 1999, Newman et al.; 1996). Mutants that lead to a differentiation of this connection show a Pvl phenotype.

The first group consists of six mutants (*zh68, zh69, zh74, zh75, zh76, zh77*) (see Fig. 10). All mutants of this group are sterile. They were isolated due to their Pvl phenotype and due to their defect in AC fusion to the utse syncytium at the fourth larval stage (L4). Further analysing the mutants, no utse formation was observed in these mutants, but instead a thick layer of cells in the ventral uterus, dorsally from the vulva was observed. The mutations were analysed earlier during L3 larval stage to determine whether there is an additional developmental defect during the early interaction between the AC and the vulval tissue. Interestingly, *zh68* was the only allele that also showed an early defect in the interaction between the AC and the vulval tissue. Whether the origin of this phenotype is caused by a defect in AC attachment remains to be investigated. The early defects in AC to vulval tissue interactions observed in *zh68* mutants have very low penetrance and were observed only once.

From the phenotypes of the mutants of this group we suggest that these genes are possibly involved in the differentiation of the π cells, the uv1 cells and utse syncytium.

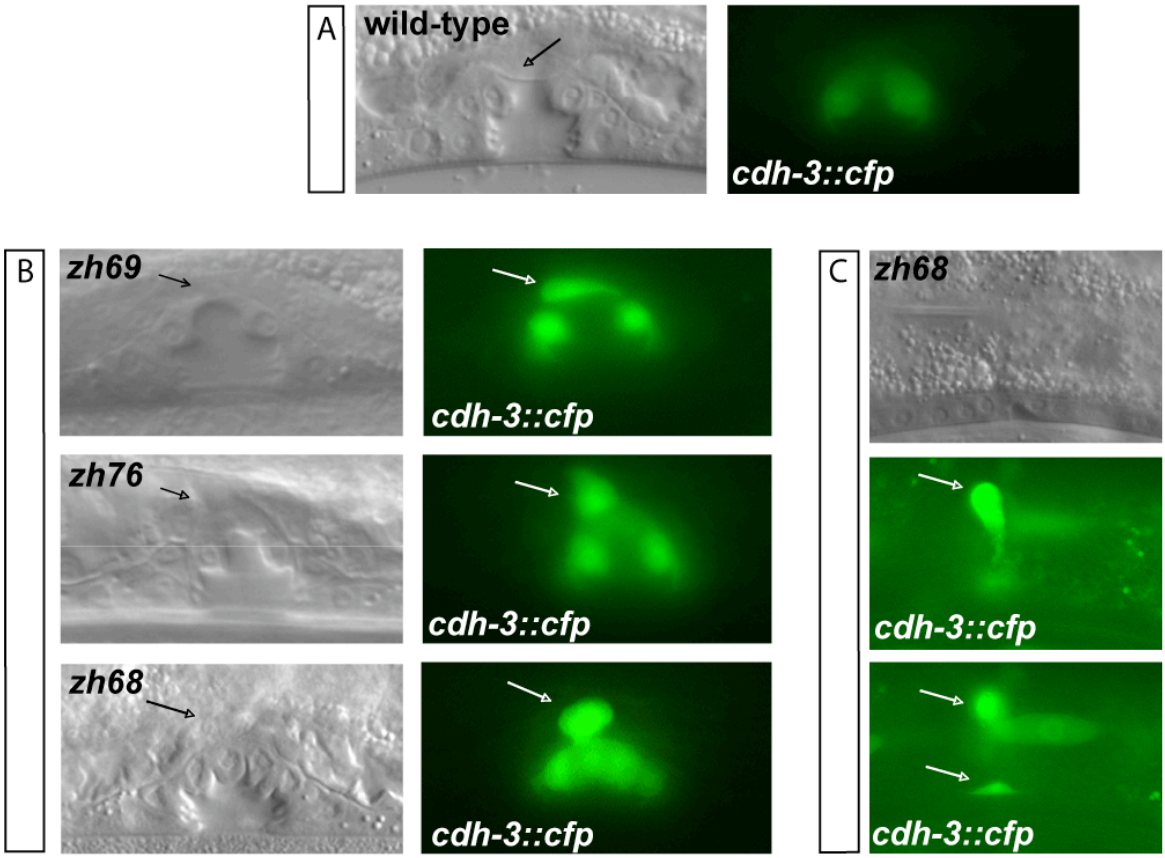

Figure 10. Mutants of Group I. These mutants exhibit a phenotype that becomes clearly visible during the L4 larval stage. It is suggested that the uterine tissue is not competent to fuse with the AC and therefore, the AC remains un-fused in these mutants. (A) The Normarski images show the vulva of a wild-type hermaphrodite in the L4 larval stage, (B) images of L4 stage of the mutants and (C) an eight-cell stage vulva of *zh68*. The depicted fluorescence is *cdh-3::cfp* expression (green). The arrows point at the utse in the wild-type image and at the un-fused AC in images that present the mutants. Anterior is to the left.

3.7.3.6 Mapping results of the Identified Mutants of Group I

Performing FLP mapping experiments with the FLPs displayed in Figure 9F, *zh68* showed linkage to chromosome IV. (see Fig. 9D/F). The high representation of Bristol genome (77%) for the FLP ZH4-10a suggests that the gene locates closest to this region defined by ZH4-10a. The mutation was balanced with the balancer *nT1[qIs51].*

zh69 showed linkage to chromosome IV, and therefore, was also balanced with the balancer *nT1[qIs51]*. Experiments form 96 lysates sized the suggested region of the mutation's location down to a region of ZH4-05 -16.26cM to ZH4-21 10.37cM (see Fig. 8 and Appendix).

zh76 showed the same linkage group as *zh68* and *zh69.* Performing mapping experiments with 96 lysates, the subchromosomal position of *zh76* was sized down to the region between the FLP ZH4-02 at 3.25cM and the FLP ZH4-20 at 5.7cM. The region is defined by two lysates for the FLP ZH4-02 and by one lysate for the FLP ZH4-20 (see Fig. 8).

zh74 showed linkage to chromosome II. Therefore, it was balanced with the balancer *mIn1[dpy-10(e128)*mIs14] II (Edgley and Riddle, 2001). Further FLP experiments obtained form 48 lysates sized the suggested region of the mutation's location down to a region between Zh2-25 at 1.09cM, and ZH2-09 at 3.45cM. The defined region is confined by ZH2-09 and ZH2-25 each by one lysate. It is important to note that the data has a lot of background noise.

zh75 was identified to be positioned on chromosome II, and was balanced with the balancer *mIn1[dpy-10(e128)*mIs14] (see Fig. 9E).

Finally, *zh77* was identified to be positioned on chromosome I (see Fig. 9C). Surprisingly, the balancer *hT2[bli-4(e937) let-?(q782)* did not balance the mutation, suggesting that the results obtained by *zh77* FLP mapping were wrong.

3.7.3.7 Group II

During the second larval stage, lateral inhibitory signalling by LIN-12 NOTCH between two developmentally equipotent ventral uterine cells causes one of them to adopt ventral uterine cell fate, while the other adopts AC fate. *lin-12* loss-of-function animals display two ACs (Wilkinson et al., 1994).

In addition to the phenotype that was described for group I mutants, the mutants of the second group II display ventral uterine cells that show ectopic expression of the *cdh-3::cfp* marker (*zh72, zh73*) (see Fig.11). The VU cells that exhibit ectopic expression are located in close vicinity to the AC. One explanation for the ectopic *cdh-3* expression in the ventral uterine cells of the mutants of this group would be their involvement in LIN-12 NOTCH signalling. As a result, the mutants described here might have 2 ACs. Moreover, it is known that the development of uv1 and utse cells involves LIN-12 NOTCH signalling. Therefore, the second defect highlights the interest of these mutants in relation to NOTCH signalling.

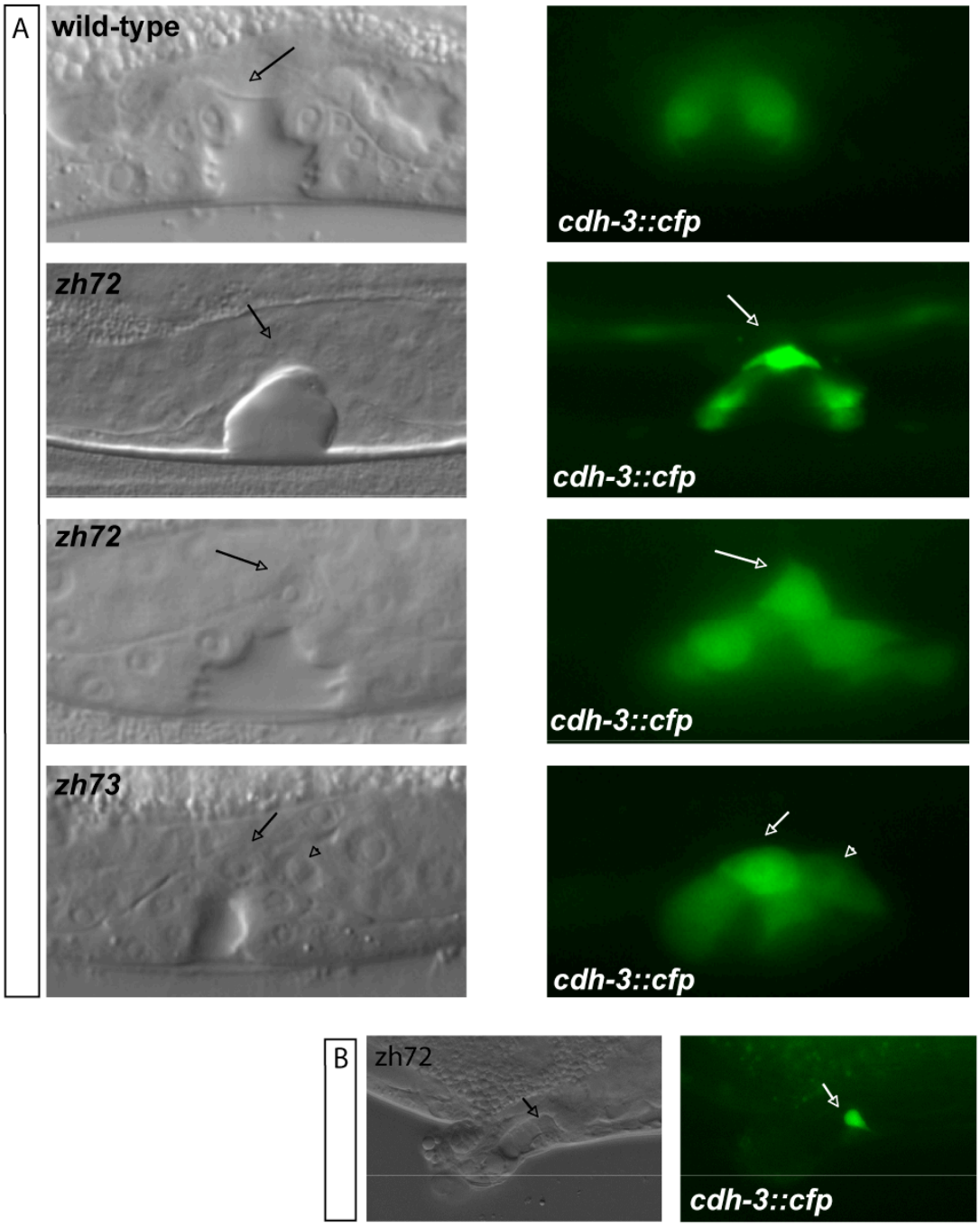

Figure 11. Mutants of Group II. These mutants exhibit a phenotype that becomes clearly visible during the L4 stage. In addition to the phenotype described for the group I, the mutants of group II exhibit ectopic *cdh-3::cfp* expression in the ventral uterine tissue. The Normarski images show the vulvae in the L4 larval stage (A) and an image of an adult hermaphrodite vulva that is everted (Pvl) (B). The depicted fluorescence is *cdh-3::cfp* expression (green). The arrows point the utse in the wild-type image and at the un-fused AC in images that present the mutants. The arrowhead points at the ectopic *cdh-3::cfp* expression. Anterior is to the left.

3.7.3.8 Mapping Results of the Identified Mutants of the Group II

Performing FLP mapping experiments, *zh72* was shown to map to chromosome IV. (see Fig. 9A). The mutation was balanced with the balancer *nT1[qIs51]*. The localisation of *zh72* was further sized down to a region between -16.26cM, (ZH4-5), and 10.37cM (ZH4-21) (see figure 8 and Appendix).

Performing FLP mapping experiments *zh73* was positioned on chromosome I (see Fig. 9B). Therefore, it was balanced with the balancer *hT2[bli-4(e937) let-?(q782) qIs48].*

Performing further FLP mapping experiments, analysing 48 lysates the region could be further sized down by excluding the region of ZH1-06 at 21.14cM and ZH1-08 at 13.12cM (each 2 lysates). Furthermore, one lysate was represented by Hawaii at the region of ZH1-23 at 3.91cM. From the other side, two lysates were represented by Hawaii genome at the region ZH1-03 and one of them covers the region of ZH1-01 at 2.79cM with Hawaii. In conclusion, *zh73* is might positioned within the region between 2.79cM and 3.91cM on chromosome I.

Within these region are two genes located that are involved in the LIN-12 NOTCH signalling. First, *sup-17* is located at 3.14cM on chromsome I. It encodes an ADAM protein, an integral membrane disintegrin and zinc-activated metalloproteinase, orthologous the vertebrate ADAM10 proteins. *sup-17* mediates LIN-12 receptor cleavage upon receptor binding. *sup-17* is not described to show an Pvl phenotype and animals defective for *sup-17* are described to only show two ACs together with an *adm-4* defect since *adm-4* acts redundantly together with *sup-17* (Jarriault and Greenwald, 2005). In addition in contrast to *zh73*, identified alleles of *sup-17* show a dumpy phenotype. From these mentioned findings we suggest that sup-17 can be ruled out as a canditate of *zh73*.

Second, *aph-1* is a component of the GLP-1/LIN-12 NOTCH pathway that is required maternally for embryonic viability. It also affects morphogenesis, egg-laying and germ line proliferation. In *aph-1(or28)* animals exhibit a recessive, fully penetrant egg-laying defect suggested to result from defects during π cell differentiation (Goutte et al., 2002). Nevertheless, the allele is maternally embryonic lethal. *aph-1(or28)* animals are not defective in the AC fate adoption (Lee et al.; 2005 International Worm Meeting). Thus, the ectopic expression of *cdh-3::cfp* speaks against the fact that *zh73* is allelic to *aph-1.* Nevertheless, *zh73* might be a weak allele of *aph-1* of due to defective π cell differentiation (Goutte et al., 2002).

3.7.3.9 Group III

The third group contains two mutants *zh70* and *zh71*. Both mutants display an AC invasion defect (see Fig. 12A and 13B/C/D)

3.7.3.10 *zh70* Represents a Novel Allele of *lin-28*

Through FLP mapping experiments, *zh70* was positioned on chromosome I. Further FLP mapping defined a region between 2.3cM (ZH1-21) and 3.73cM (ZH1-22). This region contains *lin-28* at the position 2.79cM (see suppl. information 3.9.6).

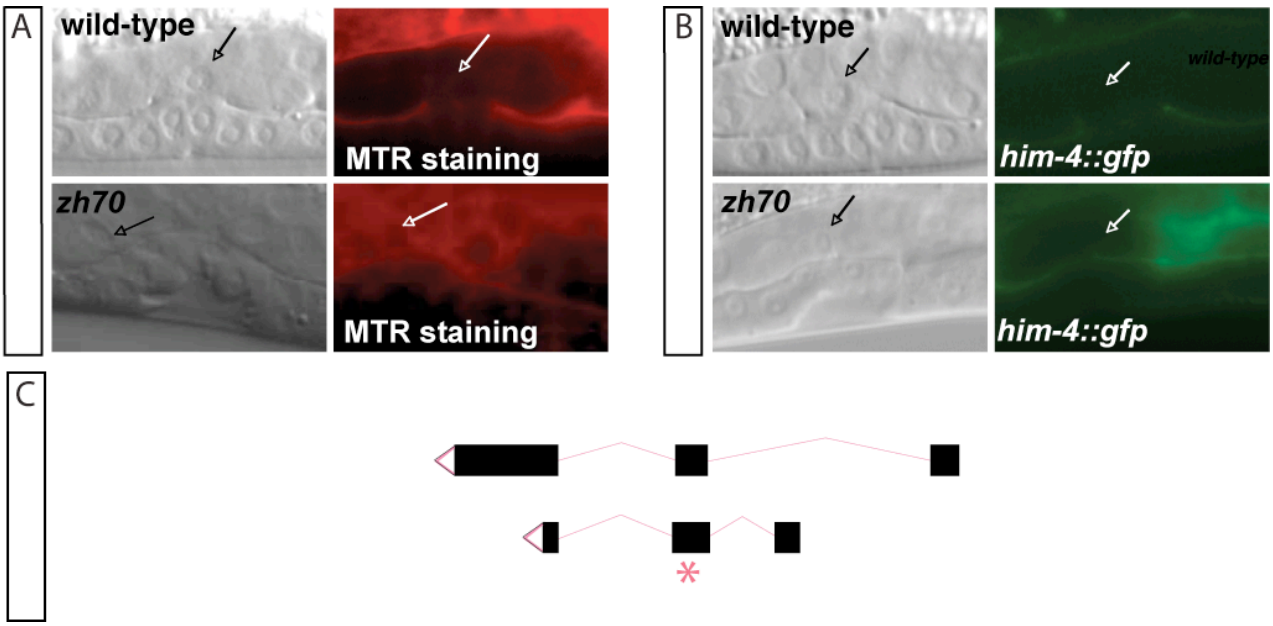

Figure 12*. lin-28 (zh70)* representing a mutant of the group III. The images A and B depict the loss of the disruption of the two basal laminae in *lin-28 (zh70)*. Upper panel depicts a wild-type vulva, lower panel a *lin-28 (zh70)* vulva. Anterior is to the left. (A) MitoTrsckerRed (MTR) staining outlines the basallaminae. (B) The basal laminae are outlined by *him-4::gfp*. (C) Schematic representation of *lin-28.* The asterix symbolises the T to A transition in the second exon, leading to a leucine to histidine exchange. The point mutation resides in the CSP (cold-shock-domain) of the gene, which is believed to be involved in binding to the target RNA.

lin-28 encodes a cytoplasmic protein that contains a cold shock domain and retroviral-type (CCHC) zinc finger motifs. In *C. elegans lin-28* is a gene of the heterochronic pathway. *lin-28* encodes a cytoplasmic mRNA-binding protein that binds to and enhances the translation of the mRNA (Polesskaya et al., 2007). Its

mutant shows a premature vulval induction in the L2 (Ambros and Horvitz, 1984). Due to the described timing defect of the animal, the invasion of the AC is delayed and all inductive signals are asynchronous, which leads to a strong Pvl phenotype.
The *lin-28* locus was sequenced and a T to A transition in the second exon was identified. The point mutation leads to a leucine to histidine exchange affecting both splice variants F02E9.2a (278T to A) and F02E9.2b (185 T to A) (see Fig. 13E). This amino acid change is positioned within the cold-shock domain of the protein that is believed to be involved in binding to the target RNA (Guo et al., 2006; Moss and Tang, 2003).

3.7.3.11 *zh71* Represents a Novel Allele of *fos-1*

Performing first FLP mapping experiments, *zh71* showed linkage to chromosome V. Further FLP results obtained form 48 lysates sized down the suggested region of the mutation's location between ZH5-13 at -18.57cM and ZH5-01 at 2.02cM (see suppl. Information 3.9.7). *fos-1 c-fos*, a gene identified to be a key component of AC invasion is located at -0.45cM, and was therefore sequenced and complemented (Sherwood et al., 2005). Both, sequencing and complementation experiments confirmed that *zh71* is an allele of *fos-1.*

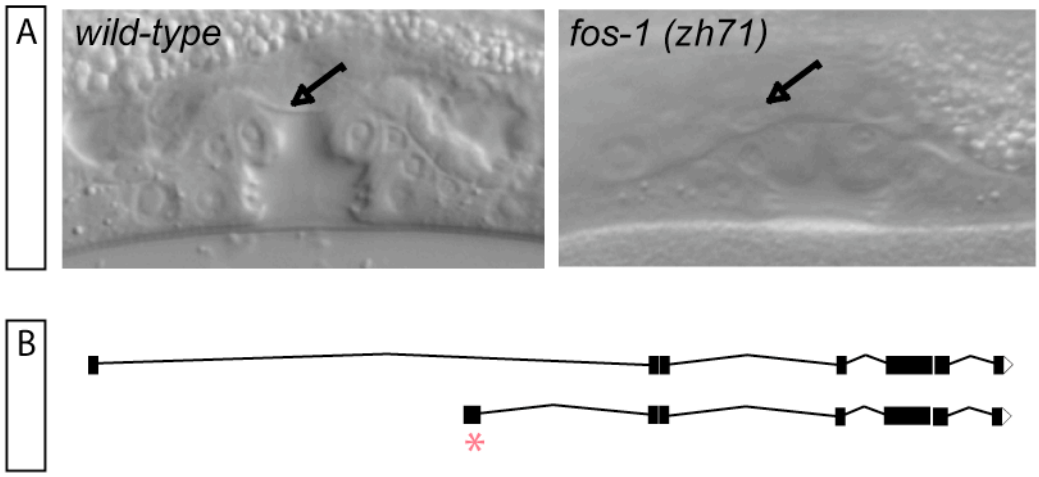

Figure 13. *fos-1(zh71)* representing a mutant of the group III.
The Normarski images depict the hermaphrodite wild-type vulva at the L4 larval stage and the vulva of *fos-1 (zh71)* at the L4 larval stage. (A) The arrows point the utse in the wild-type image and at the AC in images that present the mutants The basal laminae between the vulval tissue

and the uterine tissue is not dissolved. Anterior is to the left. (B) Schematic representation of *fos-1.* The asterix symbolises the T to C transition leading to a precocious stop codon in the *fos-1a* transcript

The *fos-1* exon region of the *zh71* mutant was sequenced and a T to C transition at the nucleotide 153 that leads to an early stop codon in the first exon of the transcript *fos-1a* was identified (see Fig.12B). The second transcript of *fos-1*, *fos-1b* is not affected by this mutation.

3.7.4 Discussion

In this paper, we describe a clonal EMS mutagenesis screen that we performed in order to identify genes involved in the communication between the AC, a cell with ventral uterine character and the vulval tissue. This communication results in the establishment of the connection between the uterus, the vulva and in addition the anchorage of the egg-lying system in the animal. From the screen, nine sterile mutants and one fertile were isolated. In contrast to usual mutagenesis screens, this screen was performed in a fashion that enabled us to maintain mutations that lead to sterility or late lethality (see Fig. 6). We classified the mutants that we obtained into three groups (see Table 2). These groups were defined with respect to their corresponding phenotypes as described above.

In wild-type animals, the AC fuses during the L4 larval stage to the utse syncytium. Thereby, the bulky AC is removed and a lumen through which the hermaphrodite will lay its eggs is created. The utse syncytium and four uv1 cells are crucial for the establishment of the connection between the uterine and vulval tissues. Both cell types differentiated from precursor cells, the π cells that derive from a subset of VU cells. LIN-12 NOTCH is the key factor of ventral uterine induction to π cell fate. Further several factors downstream form LIN-12 NOTCH were identified such as for example the EGL-13 a SOX domain transcription factor (Oommen and Newman, 2007). The mutants of these molecular factors show a Pvl phenotype because the vulva is not maintained within the animal due to a lack of anchorage of the vulva and the uterus in the body of the animal. A similar phenotype is observed in the mutants of group I (see Fig. 10). Group I contains mutants that exhibit an unfused AC in the L4 stage in addition to the a Pvl phenotype seen in adult animals.

The mutants of group II exhibit similar defects to that of group I, but in addition, group II mutants sometimes display ectopic *cdh-3* expression in the ventral uterine cells that are close to the AC (see Fig. 11). This is especially interesting since the ectopic *cdh-3* expression pattern might derive from a defect of AC/VU differentiation (Wilkinson et al., 1994). The AC is generated during the L2 larval stage. Its differentiation mediated via the LIN-12 NOTCH pathway through lateral inhibition. In accordance, in *lin-12* loss-of-function mutations, two ACs are generated instead of

one. The phenotype that we observed in group II mutants could reflect a similar malfunction of AC differentiation. Moreover, as mentioned above, LIN-12 NOTCH is a key component of one of the first differentiation steps that lead to the differentiation of π cells.

Due to these two observations, it is likely that group II mutants will reveal direct or indirect targets of NOTCH signalling.

Nevertheless, it is important to mention here that the reported ectopic expression of *cdh-3::cfp* in the ventral uterine cells is not penetrant and might derive from a background mutation that was created during the mutagenesis although the mutants were crossed out four times after their isolation.

Factors that are directly involved in AC fusion, such as *aff-1* were identified recently (Sapir et al., 2007). Nevertheless, these animals display a properly formed utse syncytium in contrast to the mutants of group I and II, which exhibit, in contrast to the fragile utse syncytium a solid layers of cells that block the connection between the uterus and the vulva. Further *aff-1* mutants are not noted to display a Pvl phenotype.

From these findings, we further suggest that the mutants of the group I and II are involved in the differentiation of the π cells, the utse syncytium of the uv1 cells rather then directly in the process of AC fusion.

Group III mutants exhibit a clear AC invasion phenotype. The mutants of this group display novel alleles of *lin-28* and *fos-1*.

The first group III mutant that we identified is the heterochronic gene *lin-28* (see Fig. 13). Mutations in *lin-28* lead to invasion defects due to errors in the developmental timing between the uterus and the vulva. In *lin-28* loss-of-function animals, the vulva is prematurely induced at the L2 stage. Unfortunately for these mutants, at the L2 stage, the AC has not yet developed to the point at which the AC can invade the vulval tissue. This results in an invasion and in a Pvl phenotype. In conclusion, we identified a new allele of *lin-28* that is indirectly involved in AC invasion due to the asynchronous developmental timing of vulval induction.

The second mutant of group III encodes for a novel allele of *fos-1* (see Fig. 12A). *fos-1 c-fos* is a key actor of AC invasion. So far, *fos-1 c-fos* is together with *egl-43 evi-1* the only factor that is directly involved in AC invasion with a strong penetrant phenotype (Rimann and Hajnal, 2007).

Since this screen led to the identification of *fos-1* and *lin-28,* we can conclude that the screen was adequately designed and powerful enough to identify genes that are

required for AC invasion. Furthermore, in addition of *fos-1 c-fos* and *lin-28,* we isolated a certain number of mutants that seem to be involved in the correct establishment and anchorage of the hermaphrodite's egg-laying system. Interestingly the phenotype of some of these mutants, group II mutants, hints at a possible function in LIN-12 signalling.

In conclusion, we isolated 8 yet uncharacterized mutants through a novel clonal screen that allowed us to isolate mutations affecting genes causing sterility. We now plan to characterize and clone these genes further, in order to identify new genes involved in the differentiation of π and/or utse cell fate. It will be of interest to identify genes that act downstream or in parallel to NOTCH LIN-12 during the differentiation of the cells involved in the establishment of the anchorage of the egg-laying system inside of the animal's body.

3.8 Outlook in Respect to the Manuscript

I suggest that the following experiments should be performed to analyse the mutants that were previously identified through the clonal screen in order improve the content of the manuscript.

1) Reconfirm the phenotypes of all the eight mutants with the *cdh-3::cfp* reporter.

2) Reconfirm the ectopic *cdh-3::cfp* in the mutants *zh72* and *zh73* and study the *cdh-3::cfp* expression during the early L3 larval stage. It might be of interest to study the relevance of this ectopic *cdh-3::cfp* expression with another AC marker.

2) *nhr-67* encodes a nuclear receptor that is orthologous to *Drosophila* and vertebrate *tailless* hormone receptors. *nhr-67* is located on Chrs IV at the position 4.92cM and has been suggested to have a role in uterine development (unpublished results, Bruce Wightmann, 2006, Development & Evolution Meeting).

In addition, downregulation of *nhr-67* by RNAi results in animals with a strong Pvl phenotype and an unfused AC at the L4 stage, a similar phenotype as the one observed in the mutants of *zh68*, *zh69* and *zh67*. I sequenced the exons of *nhr-67*. No mutation has been identified so far. However, a small region of the second exon of *nhr-67* remains to be sequenced of *zh69.* In addition, a small region at the beginning of exon seven of the mutants *zh68* and *zh76* has to be confirmed due to unclear sequencing results.

In conclusion, the open reading frame of *nhr-67* should be fully sequenced in *zh69*, *zh69* or *zh67* to test whether these mutants are allelic to *nhr-67* Complementationassays should also be performed.

3) To test whether *zh68*, *zh69* and *zh67,* all defined to be located on Chrs IV are allelic complementation assays should be performed.

4) To test whether *zh74* and *zh75* that are both situated chromosome II are allelic to each other, complementation experiments should be performed.

5) I suggest to analyse some of the group I mutants with transcriptional reporters of *lin-11, ida-1* and *egl-13*, since these genes are involved in the differentiation of the π cells (Cinar et al., 2003; Newman et al., 1999; Zahn et al., 2001).

6) Due to the mapping results and the phenotype of *zh72*, it remains to be investigated if *lag-1* is allelic to *zh72* (Christensen et al., 1996).

7) Due to the mapping results for *zh73*, the open reading frame of *sup-17* and *aph-1* should be sequenced to rule definitively out that *zh73* is an allele of *sup*-17 or *aph-1* (Goutte et al., 2002; Jarriault and Greenwald, 2005).

8) Analysis of the vulval development seems crucial to me to rule out whether the defect possibly originates in the vulval development or whether there is an additional vulval phenotype.

3.9 Supplementary Information on the Mapping Procedure not contained in the Manuscript

3.9.1 Candidate based Approach to Clone the Mutants of the Screen

With the FLP method the candidate region of a mutant can be confined to a minimal region of 3cM. To finally clone the gene, there are other available methods that in combination help to identify the mutation and the affected gene. For mutants that had been mapped to a small region, the chromosomal region defined by FLP mapping was analysed (www.wormbase.org). Genes that were annotated as exhibiting a Pvl phenotype when mutated or through RNAi were chosen to compile a list of candidate genes. Strong candidates that had been reported to exhibit a similar phenotype were subjected to complementation assays and sequencing experiments. The remaining hits were used to perform RNA interference experiments.

3.9.2 RNA Interference Experiments to Clone the Mutants

RNAi experiments were performed using a bacterial feeding method with two strains, the wild-type strain used for the screen containing the AC reporter *cdh-3::cfp* either in a wild-type background or in the RNAi hypersensitive strain *rrf-3 (pk1426)* loss-of-function background. The experiment was performed using the two different methods described in the methods in section. First, the RNAi plates with the different worms were screened for a Pvl phenotype and second, the plates were re-screened by gd optics and by observing *cdh-3::cfp* comparing their phenotypes with the phenotype of the corresponding mutation. I analysed 30 animals at the larval stage of interest for each candidate gene.

3.9.3 RNAi Experiments to Identify the Genetic Position of *zh68*, *zh69, zh76* and *zh72*

To identify candidate genes for *zh68*, *zh69, zh76* (group I) and *zh72* (group II), RNAi experiments were performed by me and in addition by Charlotte Chain under my supervision. Performing the experiments, 33 genes within the region -16.26 to 10.37cM on chromosome IV that were annotated as exhibiting a Pvl phenotype were downregulated (see Table 3). Furthermore, the experiment was performed in a *rrf-3*

background, containing the *cdh-3::cfp* AC marker to study the position of the AC from the mid L3 to L4 stage.

Sequence name	Main name	RNAi clone
E04A4.5	-	G12 97
Y24D9.4	*rpl-7A*	B3 97
F29B9.6	*Ubc-9*	F3 97
K08B4.1a	*lag-1*	D10 100
T22D1.10	*ruvb-2*	G1 101
C06G3.10	*cogc-2*	A3 102
C06G3.11a	*tin-9.1*	A4 102
C42D4.8	*rpc-1*	C10 102
C48A7.2	-	H3 102
C33H5.7	-	G10 103
F35H10.4	*vha-5*	H7 104
D2O96.8	-	B7 105
T26A8.4	-	C7 105
F08B4.5	-	G1 105
ZK1251.9	-	B8 108
F25H8.2	-	G3 108
F25H8.3	*gon-1*	G4 108
W01B6.9	*ndc-80*	B8 109
ZC168.3	-	G2 110
F36H1.2a	*tag-144*	D10 111
M7.1	*let-70*	E7 111
C08F8.1	*pfd-1*	G9 111
C08F8.8	*nhr-67*	H4 111
M04B2.1	*mep-1*	F5 113
F12F6.7	-	G2 112
K08E4.1	*spt-5*	F12 113
F28D1.7	*rps-23*	D10 114
F28D1.10	*gex-3*	E1 114
C25G4.6	-	F2 114

Sequence name	Main name	RNAi clone
T23F6.4	*rbd-1*	B4 115
C39E9.13	*rfc-3*	A2 116
C39E9.14a	*dli-1*	A3 116
Y62E10A.11	-	E7 116

Table 3. This table contains a list of genes that were downregulated by RNAi experiments to possibly phenocopy *zh76, zh68, zh69* and *zh72.*

This experiment was performed once by Charlotte Chain, and in contrast to the describtion given before, only five to ten animals per gene were examined. Charlotte observed phenotypes as described below. These experiments were only performed once and therefore should be repeated.

E04A4.5 is suggested to encode a mitochondrial import inner membrane translocase, subunit. RNAi against *E04A4.5* generated an AC attachment defect.

Secondly, *ZC168.3* downregulation shows an AC mislocalisation phenotype. *ZC168.3* encodes an origin recognition complex, subunit 5.

In addition, *C48A7.2*, is suggested to encode a Na+/Pi symporter. RNAi downregulation of this gene also showed an AC mislocalisation phenotype.

Thirdly, *rbd-1* downregulation resulted in a phenotype similar to *zh72* with ectopic *cdh-3* expression in cells that are close to the AC. *rbd-1* encodes an ortholog of *S. cerevisiae* MRD1. *rbd-1* may suppress tumor growth in the germline. RBD-1 is probably required for ribosome biogenesis (Bjork et al., 2002; Saijou et al., 2004).

Lastly, another candidate gene that we studied is *lag-1*. *lag-1* locates to chromosome IV at the position of 2.99cM. Its downregulation leads to an AC mislocalisation phenotype during the fourth larval stage. *lag-1* encodes a transcription factor orthologous to members of the CSL. LAG-1 functions as a downstream effector of LIN-12 Notch signalling. It is required for processes such as germline induction, AC/VU specification and secondary cell fate adoption during vulva development. *lag-1* is a transcriptional regulator of *lin-11* during π cell fate adoption and therefore an interesting candidate for *zh72* which shows ectopic *cdh-3::cfp* expression in the VU cells (Newman et al., 1999) and a potential defect in π cell differentiation.

To identify candidate genes for *zh76,* I performed RNAi experiments with 19 RNAi clones downregulating genes within the region between 3.25cM and 5.7cM on

chromosome IV (see Table 4). These genes were annotated to exhibit a Pvl phenotype in consequence of RNAi downregulation. The experiment was performed with wild-type worms containing the *cdh-3::cfp* marker to analyse the AC position from the mid-L3 to L4 stage. The procedure was repeated twice.

Surprisingly, in contrast to the previously described experiment, *nhr-67* downregulation showed a phenotype with an unfused AC in the L4 stage, similar to the previously described phenotype for *zh76*. Further, *spt-5* showed an invasion phenotype. The result is shown in Fig. 15 and the corresponding section.

Sequence name	Main name	RNAi clone
T26A8.4	-	C7 105
M04B2.1	*mep-1*	F5 112
ZC168.3	-	G2 110
F01G4.6	-	G8 111
F25H8.3	*gon-1*	G4 108
F01G4.2	*ard-1*	G4 111
K07F5.14	-	F2 108
F42G8.6	-	E3 104
F36H1.2	*tag-144*	D10 111
ZK809.4	*ent-1*	H12 112
F08B4.5	-	-
F25H8.2	-	G3 108
W01B6.9	*ndc-80*	B8 109
K08E4.1	***spt-5***	F12 113
F35H10.4	*vha-5*	H7 104
C08F8.8	***nhr-67***	H4 111
D2096.8	-	B7 105
C08F8.1	*pfd-1*	G9 111
ZK1251.9	-	B8 108
F12F6.7	-	G2 112
B0035.8	*his-48*	-

Table 4. This table contains a list of genes that were downregulated by RNAi experiments to possibly phenocopy *zh76*.

3.9.4 RNAi Experiments to Identify *zh74*

The 20 genes within the region from 1.09cM to 3.45cM on chromosome II that were annotated as exhibiting a Pvl phenotype were downregulated by RNA interference (see Table 5). The experiments were performed in a wild-type background that contained the *cdh-3::cfp* marker to analyse the AC position from the mid L3 to L4. Unfortunately, none of the candidate genes phenocopied *zh74.*

Sequence name	Main name	RNAi clone
ZK970.2	*clpp-1*	A5 56
ZK970.3	*mdt-22*	A5 56
R53.7	-	D8 55
R53.6	-	D7 55
D2013.7	*eif-3.F*	G2 53
R53.3	***egl-43***	D4 53
F59E10.1	*orc-2*	C3 57
C01G6.8	*cam-1*	F6 53
C08H9.2	-	B5 55
T23G7.1	*dpl-1*	D7 53
C09H10.2	*rpl-41*	-
C09H10.8	*glb-4*	-
C09H10.7	-	F7 57
Y53C12B.2	-	H2 54
R53.4	-	D5 55
R06F6.1	*cdl-1*	A11 57
F27E5.2	*pax-3*	G2 55
F59B10.1	*pqn-47*	E2 56
R166.4	*pro-1*	
T19E10.1b T19E10.1a	*ect-2*	A9 57

Table 5. The table contains a list of genes that were downregulated by RNAi experiments to possibly phenotcopy *zh74.*

3.9.5 Rescue Experiments with *egl-43*

It has been shown that *egl-43* plays a role in π cell induction during the development of the connection between the uterus and the vulva (Rimann and Hajnal, 2007).
Abrogated π cell induction leads to a Pvl phenotype and is suggested to lead to a unfused AC phenotype as seen in the mutants of group I. Therefore, we performed rescue experiments with an *egl-43* construct in *zh74* animals.
To perform this experiment, I used a construct built by Ivo Rimann. This construct rescues the invasion defect and the larval lethality of *egl-43* loss-of-function animals (Rimann and Hajnal, 2007). It contains a 6 kb region upstream of the *egl-43* start codon, the open reading frame and the entire 3'UTR region of *egl-43*.
I injected the construct and analysed the obtained lines for a rescued Pvl phenotype. Neither of the two analysed lines showed a rescue of the *zh74* mutant phenotype, suggesting that *zh74* is not allelic to *egl-43.*

3.9.6 Characterisation and Identification of *zh70,* a Novel Allele of *lin-28*

3.9.6.1 The two Basal Laminae are not Removed in *zh70* Animals

To determine if in *zh70* mutants the basal laminae are dissolved during the mid L3 stage, localisation of MitoTracker Red staining was performed in the *zh70* animals. MitoTracker Red dye was found to stain basement membranes in living animals. In wild-type animals, the basal laminae are always clearly removed at the eight-cell stage of the vulva. In contrast, *zh70* animals showed an intact structure at the eight-cell stage (see figure 13).

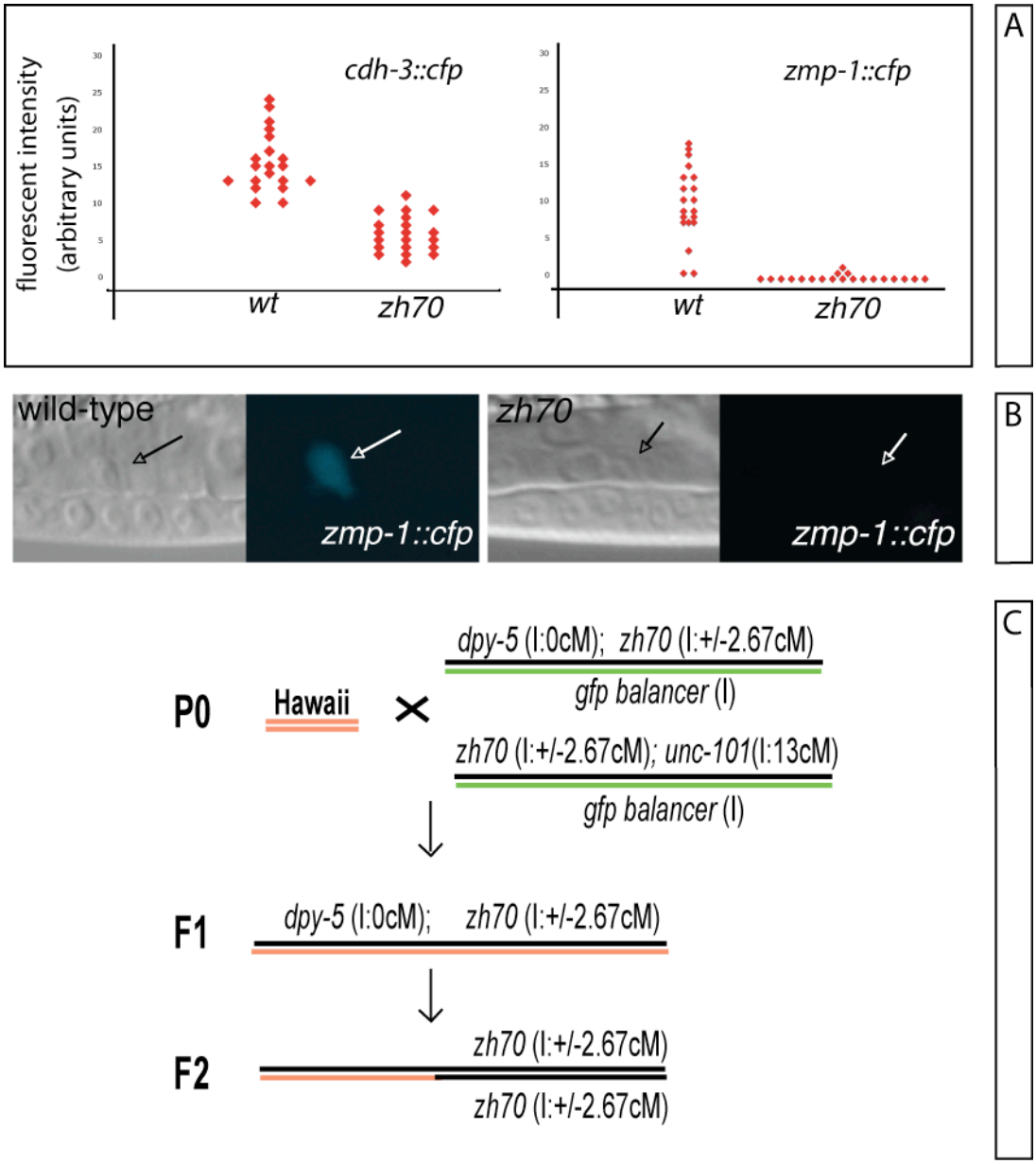

Figure 14. ***lin-28 (zh70)*** **represents a mutant of the group III. (A)** ***zmp-1::cfp*** **and** ***cdh-3::cfp*** **expression intensity in the AC at the four-cell-stage of vulval development in** ***lin-28(zh70)*** **mutants compared with the** ***zmp-1::cfp*** **and** ***cdh-3::cfp*** **expression in the AC at the four-cell stage of wild-type animals. (B) The images depict the vulva at the four-cell-stage of vulval development compared with wild-type of the mutant** ***lin-28(zh70).*** **(C) Schematic representation of the crossing procedure for the two factor mapping experiments. Red: Hawaii genome; black: Bristol genome; green: balancer; the F2 represents an informative worm due to a cross-over event in relative close vicinity to the mutation.**

3.9.6.2 Invasion Reporter Analysis of *zh70* Animals

The disruption of the basal laminae between the uterine tissue and the vulval tissue is regulated by FOS-1 and EGL-43. EGL-43 positively regulates the expression of the metalloproteinase *zmp-1*, the FAT-like proto-cadherin *cdh-3* and the hemicentin *him-4*. I wondered whether *zh70* might be involved in this pathway and performed reporter analysis for the three targets of FOS-1 signalling *cdh-3*, *him-4* and *zmp-1*.

The measurement was performed at the four-cell stage of vulval development. 20 *zh70* and 20 wild-type animals were recorded to measure the relative intensity of the *zmp-1::cfp* and the *cdh-3::cfp* reporters.

The results obtained by these expression studies show a clear decrease of the expression of the reporters in the AC at the four-cell stage of the vulva in *zh70* animals.

However, after I identified *zh70* as an allele of the heterochronic gene *lin-28*, I realised that the I was not observing a downregulation of reporter expression, but rather that at the L2 stage the gonad was not yet expressing the markers caused by *lin-28* loss-of-function.

3.9.6.3 FLP Mapping Results Define the Subchromosomal Region of *zh70*

Performing FLP mapping experiments, *zh70* was defined to be positioned on chromosome I, and was consequently balanced with the balancer *hT2[bli-4(e937) let-?(q782) qIs48].*

Performing further FLPs experiments, in total with 154 lysates, the region was sized down to a region between the FLP ZH1-21 at 2.3cM and ZH1-22 at 3.73cM (see methods, Table 7). The region was defined by two PCR reactions for ZH1-22 and one reaction for ZH1-21.

Lysates that were positive for ZH1-21 and ZH1-22 were analysed again together with new lysates with the FLP ZH1-01 at 2.79cM. This experiment did not confine the region further down.

In summary, five out of the 154 lysate confined the region to 2.3cM due to Hawaii genome at ZH1-21, while eight of the lysates confined the region to 3.73cM with ZH1-22 representing Hawaii genome at this site. These lysates were used for further analysis with polymorphisms between Hawaii and Bristol.

3.9.6.4 RNAi Experiments to Identify *zh70*

The genes within the region from 2.3 to 3.79cM on chromosome I defined by FLP mapping, that were also annotated as exhibiting a Pvl phenotype were individually knocked down by RNAi (see Table 6). Later during the mapping procedure when the region of was confined between 2.67 to 2.94cM, every single gene within this region, for which there was an available RNAi clone was knocked down. This later region included genes from *F08A10.1* to *R05D11.1* (list not shown).

Sequence name	Main name	RNAi clone
T01G9.4	*npp-2*	13 D2
T01G9.6	*kin-10*	13 D4
F16D3.4	-	13 E4
ZK858.1	-	15 B6
F20G4.3	*nmy-2*	12 F12
F43G9.1	-	14 A7
F43G9.12	-	14 B6
F32H2.1	*gei-11*	14 H2
C45G3.1	*aspm-1*	15 C9
T19A6.2	*ngp-1*	13 E9
C36B1.1	*cle-1*	
W10D5.3	*gei-17*	15 B5
C36B1.5	*prp-4*	14 D3
F25H5.4	*eft-2*	15 C5
Sequence name	Main name	RNAi clone
F52B5.6	*rpl-25.2*	13 D10
T01H8.5	*gon-2*	13 H11
C54G4.8	*cyc-1*	12 H7
ZK265.6	-	
K04G2.1	*iftb-1*	12 H9

Table 6. This table contains a list of genes with an annotated Pvl phenotype that were downregulated by RNAi experiments to possibly phenocopy *zh70.*

F43G9.1 knockdown showed a phenotype similar to *zh70* (see Fig. 15). The experiment with this clone was repeated and the phenotype confirmed. I sequenced the RNAi clone to confirm that it did target *F43G9.1*.

3.9.6.5 Sequencing Candidate Genes of *zh70*

There were several candidate genes that were sequenced to exclude whether they were allelic to *zh70*.

First, RNAi against *F43G9.1,* a suggested isocitrate dehydrogenase subunit at the position 3.00cM showed a strong invasion defect performing RNAi downregulation of the gene (see Fig. 15).

Second*, unc-120* encodes a member of the MADS-box family of transcription factors that is most closely related to Drosophila *blistered* and the vertebrate serum response factors (SRFs). The SRFs are transcriptional regulators of the signalling pathway positively regulating *c-fos* serum responsive element (SRE) (Zhang et al., 2008). Since invasion is regulated by FOS-1, the exon region of *F43G9.1* was sequenced in *zh70* animals.

None of the mentioned genes was proved to have a mutation in the genome of *zh70*, concluding that *F43G9.1, unc-120,* are not allelic to *zh70.*

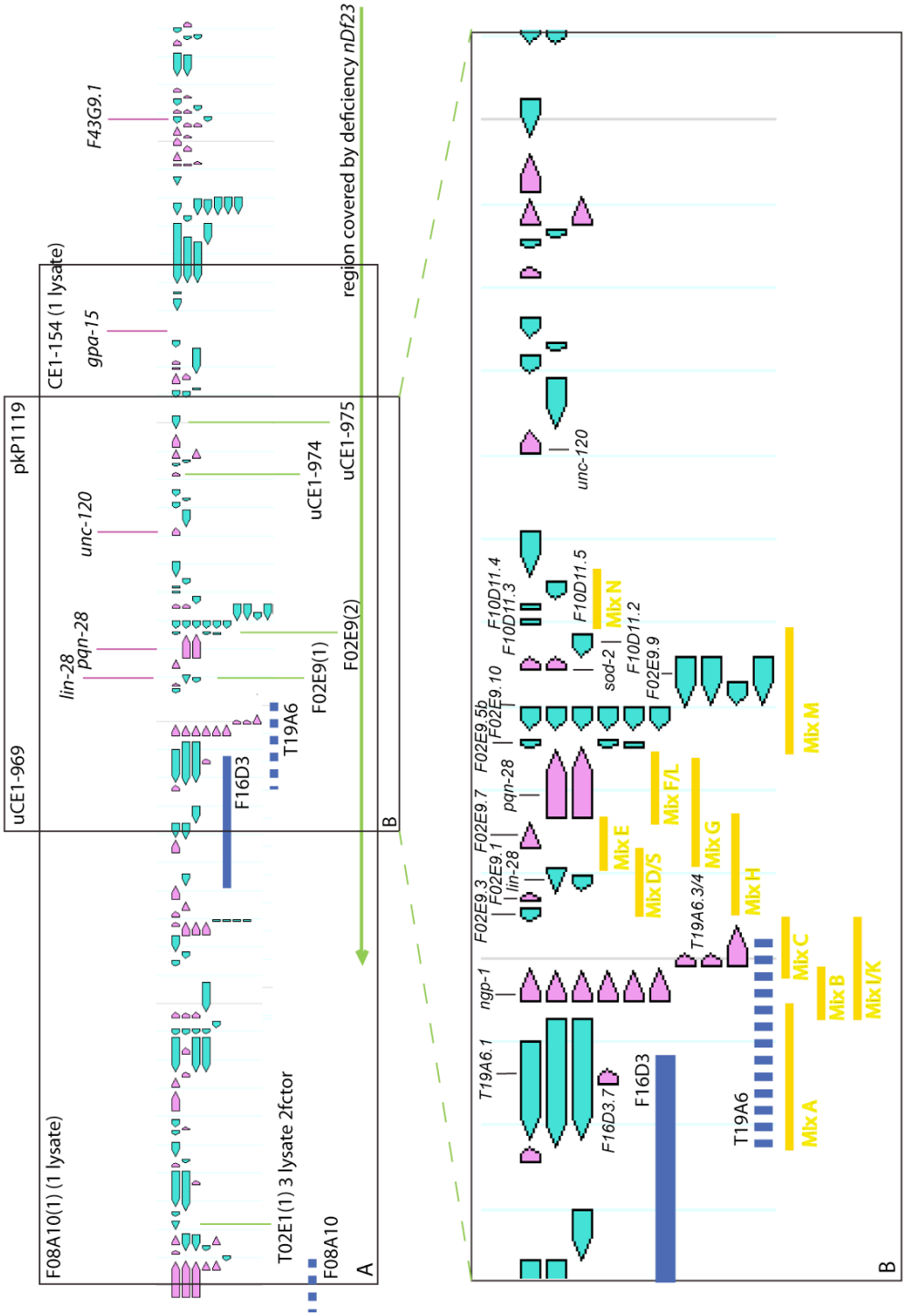

Figure 15. Schematic representation of the mapping procedure of *lin-28 (zh70).* (A) shows the region defined by FLP and manual mapping experiments confining the region (2.64 to 2.94cM) The labelled genes were sequenced during the mapping process. The deficiency *nDf23* is represented by a bold green line. (B) Two-factor mapping experiments confined the region down to a region between 2.768 and 2.88cM containing 34 remaining genes. The yellow bars represent the PCR mixes to perform rescue experiments. The dark blue bars represent cosmid to perform rescue experiments. The dark blue dashed line represents a cosmid that was verified with SNPs but has recombined.

3.9.6.6 Rescue Experiments with Candidate Genes of *zh70*

gpa-15 encodes a member of the G protein alpha subunit family of heterotrimeric GTPases. In addition of being expressed in a subset of neurons, *gpa-15* is expressed in the AC and in the DTCs (Bastiani and Mendel, 2006). Therefore, I amplified the open reading frame of *gpa-15* of wild-type animals to perform rescue experiments with *zh70* mutants. Briefly, the amplified *gpa-15* product was injected with the coinjection marker *sur-5::gfp*. We used *zh70/hT2[bli-4(e937) let-?(q782) qIs48]* animals for these rescue experiments because *zh70* shows a significantly reduced fecundity.

Lines with a stable extrachromosomal array were analysed as follows. Animals homozygous for *zh70*, thus without the GFP expression in the pharynx that originates from the balancer, were tested for a rescue of the Pvl phenotype. *zh70* animals exhibit a Pvl phenotype of about 95%. For every line, at least 25 animals were analysed for a rescue of the Pvl phenotype. In total, three lines were analysed, none of which showed a rescue of the Pvl phenotype. From these results I concluded that *gpa-15* is not allelic to *zh70*.

3.9.6.7 Further Mapping to Confine the Region of *zh70*

In order to confine the region where *zh70* was suggested be located further down, manual mapping experiments using nucleotide polymorphisms such as single nucleotide polymorphisms (SNPs) deletions or insertions covering the expected region were performed (Wicks et al., 2001). This method is similar to the FLP mapping method used before, but differs by the employment of polymorphisms that have to be confirmed before using and therefore, is not automated. The experiments were performed with the single worm lysates used for FLP mapping that were confining the region to 2.3 to 3.73cM.

The eight lysates confining the region to 3.73cM with ZH1-22 and the five confining the region to 2.3cM with ZH1-21 were tested with the following SNPs: (*F18C12[1]* at 2.48cM, *F08A10[1]* at 2.64cM, *T02E1[1]* at 2.69cM, *pkP1120* at 3.02cM, *CE1-154* at 2.94cM and *F10D11[1]* at 2.83cM, *pkP1119* at 2.88cM and *uCE1-969* at 2.76cM.

One of the eight lysates confined the region further down from ZH1-22 (3.73cM) to the SNP *pkP1120* (3.02cM). The same single worm lysate was tested for the Hawaii

genome using the SNP *CE1-154,* which confined the region further down to 2.94cM (see Fig. 14A).

The lysates confining the region with ZH1-21 were tested for their genomic origin within the remaining interval with the SNPs *F18C12[1] F08A10[1], T02E1[1].* One of the lysates was positive for Hawaii genome at the site of the SNP *F08A10[1],* confining the region further down to 2.64cM (see Fig. 14A). However, the SNPs used for analysis of the region within 2.64 to 2.94cM did not give further information of the location of *zh70*.

3.9.6.8 Cosmid Based Rescue Experiments to Clone *zh70*

Cosmids contain a specific, annotated region of the *C. elegans* genome. In this fashion, every region of the *C. elegans* genome was covered. Cosmids that span the genomic region from 2.64cM, 8198610Mb to 2.94cM, 8550709Mb were used to perform rescue experiments (see Table 12). *zh70* worms containing a cosmid that covers the mutated region in the form of an extrachromosomal array, should adopt a wild-type phenotype.

Before carrying the rescue experiments, the bacterial clones were purified controlled for size and content by restriction digestions. Unfortunately, most of the ordered cosmids had recombined before the purification or were very contaminated. Their size was too small and the restriction pattern was often not complete. For some cosmids a partially correct genomic region was verified by amplifying fragments of the cosmids using the SNP primers used before for the mapping experiment. These cosmids were used for rescue experiments despite of their incorrect size. The T19A6 and F08A10 were successfully tested by PCR analysis to contain the expected genomic region (SNPs T02E1[1] F08A10[1]).

The cosmid F16D3 could be successfully purified and its composition was confirmed by restriction digest (see Fig 14).

The cosmids T19A6 (region with the genes T19A6.1/2/3/4) and M04C7/T02H8/ R05D11 (region with the genes M04C7.1/3/4 and T01H85/1/2 and R05D11.1) were not injected since their size was much too small.

I injected mixes containing two to three cosmids (see table 13) and the coinjection marker *sur-5::gfp. zh70/hT2[bli-4(e937) let-?(q782) qIs48]* animals for these rescue experiments.

Lines with a stable extrachromosomal array were analysed as follows. Animals homozygous for *zh70*, with the extrachromosomal array containing *sur-5::gfp* and a cosmid mix were analysed for a rescue of the Pvl phenotype. *zh70* animals exhibit a Pvl phenotype penetrance of about 95%. For every line, at least 25 animals were analysed. For every injection mix, at least three lines were analysed.
None of the lines that I tested rescued the Pvl phenotype of *zh70* mutants. In conclusion, the genetic region covered by F16D3 is not likely to contain the mutation.

3.9.6.9 Two-factor Mapping to Identify *zh70*

Later, I performed two-factor mapping, in order to further reduce the region on chromosome I of candidates containing *zh70*. This method is based on classical mapping methods as those described before. But in contrast to the use of molecular markers such as FLPs or SNPs, the advantage of markers that are visible by eye under the dissecting microscope was used. Briefly, two visible markers for Bristol were chosen that are located as close as possible to the remaining region in which *zh70* was expected to be located. The chosen markers were mutations of *dpy-5* and *unc-101. dpy-5* is located at 0cM and *unc-101* is located at 13cM, together nicely framing the remaining region of *zh70*.
Building two strains, *zh70* was cis-linked to *dpy-5* (0cM) and to *unc-101*(13cM) respectively. The region was balanced the with the balancer *hT2[bli-4(e937) let-?(q782) qIs48]* (see Fig. 13F).
With these strains, I was able to identify recombination events between Bristol and Hawaii genome F2 cross-progeny between the markers and *zh70*, thereby avoiding the time required by the laborious sequencing of molecular markers.
By selecting worms with a Pvl phenotype that had lost the visible marker, 58 lines with recombination events between *dpy-5* and *zh70* were identified and further analysed with SNPs.
To analyse the 58 lines, the SNPs *UCE1-969* (2.76cM), *F10D11[1]* (2.83cM), *T02E1[1]* (2.69cM) and *pkP1120* (3.02cM) were used (see Fig. 14A/B and Table 8/9). *pkP1120* served as a control SNP outside of the region that was expected to identify Bristol genome. For three lysates of out of the 58 lysates, Hawaii genome was detected with *T02E1[1]* (2.69cM). Two of these lysates were identifed as having Hawaii genome at the sites of *UCE1-969* (2.76cM), thereby reducing the region to 2.76-2.92cM. These two lysates were further tested with the SNPs *F02E9[1]* 2.79cM

and *F02E9[2]* at 2.83cM. The genome of the two lysates was represented by Bristol, hence not confining the region further down.

The crossing procedure was repeated and another 38 lysates were analysed with *T02E1[1], F02E9[1], F02E9[2]* and *pkP1120*. Three were identified to represent Hawaii genome for *T02E1[1],* but Bristol genome for *F02E9[1], F02E9[2]* and *pkP1120*.

The three lysates which contained Hawaii genome for the SNP *T02E1[1]* were further identified to contain Hawaii genome at the site of the SNPs *uCE1-974* (2.85cM) , and *pKp1119* (2.88cM) but the region could not be reduced further.

Likewise, 144 lines with a cross over between *unc-101* and *zh70* were identified and further analysed with SNPs. The lysates were first of all analysed with *VF39H2L[2],* a FLP at 3.01cM. Three recombinants were identified by restriction digestion. The lysates were further tested for *uCE1-969* (2.768cM) and *pkP1119* (2.88cM). One of them gave a positive result for *uCE1-969*, which helped to scale the region down between 2.768 and 2.88cM, a region that contains 34 predicted genes (see Fig. 14B).

3.9.6.10 Deficiency Complementation Assays to Verify the Suggested Region of *zh70*

To confirm the results obtained by SNP mapping, complementation analyses with *zh70* using deficiencies were carried out. Deficiencies refer to relatively large deleted regions on chromosomes. The sizes of deficiencies vary from just a few cosmids to the loss of a large portion of the chromosome.

The idea behind this method, is to construct a heterozygous strain that bears the *zh70* mutation on one chromosome and a deficiency on the other. If the strain shows the phenotype of the mutation, this means that the mutation is situated in the region that is covered by the deficiency.

To confirm the region of expected *zh70* position, two deficiencies were tested for complementation. *nDf24* was annotated as covering the region between 1.8cM and 3.72cM of chromosome I, while *nDf23* was annotated as covering the region between 2.702cM and 3.647cM on chromosome I (see Table 14 and Fig. 14). Both deficiencies are homozygous lethal and therefore balanced (see methods). *zh70/+* males were crossed into strains containing either of the balanced deficiencies and the F1 progeny of the cross with *zh70* and the strain carrying *nDf23* was analysed for

cross progeny with a Pvl phenotype, suggesting that *zh70* locates to the expected region. Note, that the self-progeny of the deficiency strains did not result into a Pvl phenotype due to lethality. Males of the F1 progeny of three singled P0 animals suggested that the F1 animals contained cross progeny.
On the other hand, the F1 progeny of the cross between *zh70* and the strain carrying *nDf24* did not segregate animals exhibiting a Pvl. Nevertheless, the F2 progeny contained Pvl animals, suggesting that the crossing worked but the deficiency is not correctly annotated, was lost, or that *zh70* does not localise to the expected region. In summary, the complementation assay confirmed the region where *zh70* is situated to the region that is covered by *nDf23* and not *nDf24.*

3.9.6.11 PCR Fragments Based Rescue Experiments with *zh70* Mutants

Finally, PCR fragments spanning the remaining region were used to carry out rescue experiments. The open reading frames, together with their upstream sequences reaching the 3'UTR of the next gene were amplified. Some PCR products contained more than one gene and the corresponding upstream region. Operons were amplified at once. Genes that were too long to be amplified in one PCR reaction were amplified in two overlapping fragments. The two products were expected to recombine in the extra chromosomal array in the animal as a result of coinjecting the two fragments together (Mello et al., 1991).
A schematic representation of the PCR products tested is shown in figure 14. Different mixes of PCR fragments (see Table 16) were injected together with the coinjection marker *sur-5::gfp* For every line, at least 25 animals were analysed for a rescue of the Pvl phenotype under the dissecting microscope. As usual, for every injection mix, at least three lines were analysed for a rescue.
Finally, two mixes, one covering the region of *F02E9.1*, *lin-28* (*F02E9.2*) (mix S) and the other covering the region of *F02E9.1*, *lin-28* (*F02E9.2*) and *F02E9.7* (H) rescued the Pvl phenotype (81% and 98% rescue) (see Fig 14).

3.9.6.12 Sequencing *lin-28*

The *lin-28* locus was sequenced and a T to A transition in the second exon was identified. The point mutation leads to a leucine to histidine exchange (see Fig. 13E). The exons of both splice variants, *F02E9.2a* (278T to A) and *F02E9.2b* (185T to A) were affected.

This change is positioned within the cold-shock domain of the protein that is believed to be involved in binding to the target RNA (Guo et al., 2006).

3.9.7 Identification and Characterisation of *zh71,* a Novel Allele of *fos-1*

3.9.7.1 Complementation Assay of *fos-1* and *zh71*

fos-1 was tested to be allelic to *zh71* by performing complementation assays. *fos-1* and *zh71* are both sterile. Wild-type males were crossed into *fos-1/ nT1[qIs51]* animals. The non-green male progeny was crossed further into *zh71/+* animals. The P0 animals were singled out and the plates containing males and Pvls were analysed further. On three plates, the F1 generation contained males. The proportion of the hermaphrodites was analysed for a Pvl phenotype.

The F1 progeny was expected to be 25% Pvls in case of non-complementation and 75% wild-type phenotype. In case of complementation, no animals exhibiting a Pvl phenotype are expected. The three analysed plates showed twice 15% of animals exhibiting a Pvl and once 28% exhibiting a Pvl. The results suggest that *zh71* fails to complement *fos-1* and that *zh71* is allelic to *fos-1*.

Plate number	Phenotypes (N worms)	Percentage
Plate 1	wild-type (32)	
	Pvl animals (6)	
	males (18)	15%
Plate 2	wild-type (22)	
	Pvl animals(4)	
	males (45)	15%
Plate 3	wild-type (10)	
	Pvl animals (4)	
	males (17)	28%

3.9.7.2 Sequencing *zh71*

Due to the results obtained with the complementation assay, the coding region of *fos-1* gene in *zh71* animals was sequenced. A T to C transition at the nucleotide 153 leading to a premature stop codon in the first exon of *fos-1a* was identified (see Fig. 12B).

Taken together with the results of the complementation assay, *zh71* is now believed to be an allele of *fos-1*.

3.9.7.3 Invasion Candidates Identified Performing RNAi Experiments

While performing RNAi experiments to reveal the identity of the mutants identified during this screen, I observed some clones that exhibited an AC invasion deficient phenotype but that nevertheless, were found not to be allelic to any of the mutants.

Unfortunately, we could not follow these investigations due to a lack of time.

First, downregulation of the genes within the suggested region identified by FLP mapping of *zh76*, *spt-5* RNAi showed an clear and penetrant AC invasion phenotype (see Fig. 15 C).

spt-5 encodes a RNA polymerase II transcription elongation factor DSIF/SUPT5H/SPT5.

In addition, *F43G9.1*, the alpha subunit of the isocitrate dehydrogenase participating in the citric acid cycle in the mitochondria was identified to exhibit an invasion phenotype (see Fig. 15A/B).

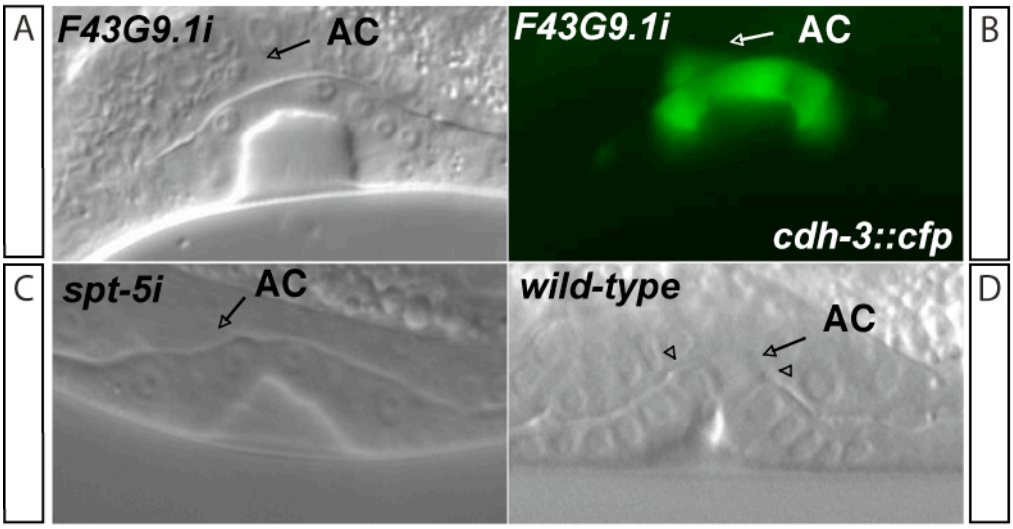

Figure 16. RNA interference experiments to down regulate candidate genes with an invasion defect (A) Normarski image of *F43G9.1* RNAi downregulation in a wild-type background at the L4 stage. (B) *cdh-3::cfp* fluorescence of the figure depicted in A (green). (C) Normarski image of *spt-5* RNAi downregulation in a wild-type background at the early L4 stage of a hermaphrodite vulva. (D) wild-type vulva of late-L3 hermaphrodite. The arrows point the at the ACs, arrowheads point at the basal laminae that are dissolved within the region between. Anterior is to the left.

4 General Discussion and Outlook

4.1 Characterisation of AC attachment

To induce vulval development and further, to invade the vulval tissue, the AC moves to a position dorsally in the gonad, in close proximity to the P6.p cell. While the mechanism of vulval induction is understood in detail, the mechanism behind AC attachment has not been understood yet. By performing time course experiments with wild-type worms, I could show that during the L2 stage, the AC and the future 1° cell approach each other, to finally find themselves attached to each other, at the early L3 stage.

From the early to the mid L2 stage, the average distance between the nuclei of the AC and the P6.p is not significantly reduced. However between the mid L2 and the early L3 stage, this distance shortens drastically, which leads to attachment. This suggests that AC attachment to the P6.p cell is not a gradual step that takes place during the whole L2 stage, but that in contrast, it takes place during a shorter period of time comprise between the mid L2 and the early L3 stage.

In addition, I wanted to know whether P6.p has to adopt a VPC cell fate to attain close contact with the AC*. lin-39* is a HOX gene that is required for to specify the mid-body region of the worm (Clark et al., 1993). In *lin-39* defective animals P3-P8 cells differentiate abnormally. In accordance, the VPCs are not specified and fuse to the hypodermal syncytium hyp7 (Shemer and Podbilewicz, 2002).

Hence, in order to test the hypothesis that proper VPC cell fate adoption by P6 is required for P6.p that the AC attaches to it, I performed experiments to study AC attachment, at the early L3, in *lin-39* loss-of-function animals. Interestingly, I found that the identity of the VPCs is essential for P6.p and the AC to approach each other (see Fig. 3/4).

In a wild-type background at the early L3 stage, the average distance between the nuclei of P6.p and AC was of 2µm, which I defined as attachment. In contrast, in a *lin-39* loss-of-function background, the AC did not attach to P6.p but instead, I observed an average distance of 29µm between the nuclei of those two cells. By studying the position of these two cell earlier in development, during the mid L2 stage, I found that in *lin-39* mutants P6.p and the AC are situated much further apart

than in wild-type animals (see Fig. 1 and 2). This suggests that the fusion of the P6.p cell to the hyp7 syncytium makes it impossible for the two cells to attach.

Besides studying AC attachment in animals with an improper cell fate specification of P6.p, I also studied the effect of mutations that result in a loss of vulval induction. Therefore, in parallel to *lin-39,* I also studied the effect of *let-23* and *lin-3* mutations on P6.p to AC attachment.
As it was mentioned earlier in the introduction, *let-23* and *lin*-3 carry the signal of vulval induction. Attachment of the AC to P6.p is clearly weakened but not abolished in *let-23* and *lin-3* mutants. We can interpret these results such that vulval induction is crucial for AC attachment and that the approaching movement between the AC and P6.p is regulated at least partly as a consequence of vulval induction.
However, it must be noted here that for this experiment I employed the *let-23* allele (*let-23(sy1)*). In mutant animals that carry this allele, LET-23 is mislocalised, but LET-23(sy1) is not completely inactive since, a small amount of LET-23 placed on the basal compartment of the cell can induce vulval induction. As a result in 23% of the cases the AC might be able to attach to P6.p in some animals. Therefore, mutants that have a complete loss of LET-23 receptor at the basolateral surface might show a stronger abrogation of AC attachment.
The above-mentioned cautionary note about the alleles that I employed for this experiment also applies for the results obtained in the *lin-3* background. *lin-3(e1417)* animals have an strongly reduced induction index, but nevertheless, some VPCs are still induced (Hwang and Sternberg, 2004). I suggest that these induced cells may have the capability to attract the AC, and to reach attachment.

Nevertheless, there could be an alternative explanation for the observed loss of AC attachment in *let-23* and *lin-3* deficient backgrounds. Synchronisation of the animals is often not fully precise. This leads to pictures of scored animals that are taken a bit after the possibly short moment of attachment. In accordance, these animals have developed further, after the hypothetical time of induction. In this case, the gonad keeps growing and the AC detaches form the vulval tissue despite its earlier attachment due to a missing invasion cue that normally follows vulval induction.

I observed that in Vul animals the AC often detaches during development and loses the established contact with the basal lamina of the gonad. This possibility would mask an AC attachment that occurs in an induction-independent way.

Nevertheless, the time course experiments performed with wild-type animals showed that the attachment between the AC and P6.p takes place very late, rather at the time of induction, which weakens the model of an attraction model that would be independent of induction.
After the induction of vulval development, the vulval cells start dividing and the AC invades the vulval tissue. Early steps of AC invasion become first visible under Normarski optics after induction, from the first division of the 1° cell onwards.
There might be already an early cue for invasion released from the 1°vulval cell that starts attracting the AC already at an earlier stage.
For instance, CDH-3, a gene involved in dissolving the basal laminae, is positively regulated by FOS-1 (Sherwood and Sternberg, 2003). The dissolution of the basal laminae underneath the AC is a crucial step of AC invasion (Rimann and Hajnal, 2007). *Cdh-3* belongs to a class of membrane proteins with prominent roles in cell adhesion (Pettitt et al., 1996). It is detected around the time of induction and therefore, it is tempting to suggest that due to its above-described function that *cdh-3* is involved in cell adhesion during AC attachment. This leads to the suggestion that attachment and invasion may be accomplished by one mechanism.

Nevertheless, I cannot rule out whether there is an early mechanism occurring before the induction time that would lead to the shortening of the distance between the AC and P6.p. Thus I can only speculate whether before the time of induction, P6.p or even all the three VPCs locate close to the symmetrical centre of the developing gonad during the early L2 stage. Wild-type localisation of the VPCs might happen in response to a signal that is not specifically released by the AC or P6.p but could be more broadly expressed throughout the developing gonad. The specification of VPC cell fate would make the cells competent to recognise this signal.

4.2 *pvl-6(ga81)* might Encode a Gene Involved in AC invasion

When I was studying the phenotype of *pvl-6(ga81)*, it showed a very clear invasion phenotype, just after I received the strain from CGC.

Interestingly, the phenotype was lost over a few generations and the phenotype was also lost when I crossed the mutants with different strains that contained reporters to study the phenotype or that were necessary for performing mapping experiments. The simplest explanation for this phenomenon would be the suppression of the phenotype by another mutation present in the *pvl-6* strain. In *C. elegans*, many different kinds of suppressors have been reported. They can be divided into intragenetic and extragenetic suppressors (Hodgkin, 2005).

The simplest scenario for an intragenetic suppressor mechanism is that of a reverton, in which a mutation is simply mutated back to wild-type (Novelli et al., 2004). Intragenetic reversion can also be achieved by means of exon skipping (Rogalski et al., 1995). Since the loss of my phenotype seems to occur gradually, I do not suggest this as a possible explanation.

The problem caused by an extragenetic suppression of a phenotype can usually be solved by crossing the mutants with a wild-type strain. In general, this should lead to the reappearance of the phenotype (Waterston, 1981).

In the case of *pvl-6(ga81)*, this did not occur. Nevertheless, if the suppressor mutation is located on the same chromosome, as long as close to *pvl-6*, this would make it very difficult to out-cross the suppressor in case the gene that corresponds to *pvl-6* is not known.

There could be multiple genetic traits affecting the phenotype. However, this explanation on its own does not explain the loss of the phenotype either. The phenotype loss might be due to subtle environmental changes that were overlooked.

Moreover, there are phenomena described in the literature that might reveal a mechanism responsible for the loss of the phenotype. In *A.thaliana* for example, it was shown that plants that are homozygous for a recessive mutation of *hothead* can inherit allele-specific DNA sequence information that was not present in the genome of their parents but present in previous generations (Lolle et al., 2005). It is postulated that such genetic restoration events are the result of a template-directed process that makes the use of an ancestral RNA-sequence cache. It is of interest that a second example of RNA mediated non-mendelian inheritance was also

described in the mouse. (Rassoulzadegan et al., 2006; Wagner et al., 2008). However, it has recently been found that *hothead* mutants have a marked tendency to outcross, in contrast to wild-type *A.thaliana,* which is mostly self-fertilising. In the same report, it is stated that isolated *hothead* plants have mendelian inheritance (Peng et al., 2006).

4.3 RAS/MAPK Signalling Does Not Act in the AC to Make the AC Competent to Invade

Since *let-60* expression was observed in the AC, I wanted to know whether it is involved in AC invasion acting in the AC (Dent and Han, 1998). The loss of this pathway in the AC and in the surrounding tissue with the exception of the vulval tissue did not lead to an invasion phenotype. From these experiments, I could rule out the possibility that the RAS/MAPK signalling pathway is involved in AC attachment and invasion in tissues other than the VPCs and the vulval cells. It must be noted that in order to prove or disprove a direct role for this signalling pathway in the VPCs and in the vulval cells after 1° cell fate induction, in regard to AC attachment and invasion, an inducible system that would allow to separate temporally the initial role of the RAS/MAPK pathway in inducing 1° cell fate from its putative role in the secretion of the attractive cue would be required. Moreover, the time that separates these two events might be too short for an inducible system to act.

4.4 Forward Genetic Screen for AC Attachment and Invasion Mutants

During my thesis, I performed a clonal EMS mutagenesis screen with the goal of identifying genes involved in the communication between the AC and the vulval tissue. This communication results in the establishment of the connection between the uterus and the vulva. I isolated nine sterile mutants and one that was fertile, from this screen. Subsequently, I classified the mutants that I obtained into three groups. These groups were defined in respect to their phenotypes.

4.5 Mutant Groups

4.5.1 Group I

The mutants of this group exhibit a Pvl phenotype. Furthermore, no utse formation was observed in these mutants but instead a thick layer of cells in the ventral uterus, situated dorsally from the vulva was observed.

Therfore, the AC fusion to the utse at the fourth larval stage (L4) is missing in these mutants. In wild-type animals, the utse cell builds a thin laminar process together with the AC, at the L4 stage. The utse syncytium, together with the uterine-vulval cells (uv1), is responsible for the establishment of a connection between the vulva, the seam cells and the uterus. The utse and uv1 cells differentiate from π cells, specified descendents of ventral uterine cells (Chang et al.; 1999, Newman et al.; 1996).

Preliminary analysis of the phenotype of the mutants of group I suggested that these genes could be possibly involved in the differentiation of the π cells, or be involved in the later utse cells differentiating together with the uv1 cells from the π cells.

The mutations were analysed earlier during the L3 larval stage to determine whether there is an additional developmental defect during the early interaction between the AC and the vulval tissue. Interestingly, *zh68* was the only allele that also showed an early defect in the interaction between the AC and the vulval tissue. Whether the origin of this phenotype originates from a defect of AC attachment remains to be investigated. The early defects in AC to vulval tissue interactions observed in *zh68* mutants have a very low penetrance and were observed only once.

The genes that cause a direct AC fusion defect that have been identified so far in other studies, such as for example those that are observed in *aff-1* defective animals show a normal utse differentiation (Sapir et al., 2007).

In contrast, the mutants of group I never had an utse syncytium and therefore, I suggest that they are not directly defective for the capacity of the AC to fuse together with the utse syncytium.

It should be noted once more, that *nhr-67* might be a candidate gene of interest for the mutants *zh68*, *zh69* and *zh76*. *nhr-67* exhibits a phenotype similar to the mutants *zh68*, *zh69* and *zh76* and encodes a nuclear receptor that is orthologous to the *Drosophila* and vertebrate *tailless* hormone receptors. *nhr-67* is located on Chrs IV at the position 4.92cM, and it has been suggested that it might have a role in uterine

development (unpublished results, Bruce Wightmann, 2006, Development & Evolution Meeting).

4.5.2 Group II

In addition to the phenotype that was described for group I mutants, the mutants of the second group display ventral uterine cells showing ectopic expression of the *cdh-3::cfp* marker (Fig.11). The VU cells that exhibit this ectopic expression are located in close vicinity to the AC.

One explanation for the ectopic *cdh-3* expression in the ventral uterine cells of the mutants of this group would be a misregulation during AC fate adoption. As a result, the mutants described here could have 2 ACs. In wild-type animals, during the second larval stage, lateral inhibitory signalling by LIN-12 NOTCH between two developmentally equipotent ventral uterine cells causes one of them to adopt ventral uterine cell fate, while the other adopts AC fate (Wilkinson et al., 1994). *lin-12* loss-of-function animals display two ACs and show an abnormally everted vulva (Pvl) (Wilkinson et al., 1994).

Moreover, it is known that the differentiation of π cells is induced via LIN-12 NOTCH signalling (Newman et al., 1995). Therefore, the second defect highlights the interest of these mutants in relation to NOTCH signalling.

Alternatively, genes leading to multiple AC's due to defects in the early-stage asymmetric division of somatic gonadal cells along the proximal-distal axes, such as *sys-1* to *sys-3* and *gon-14* to *gon-16*, have been identified (Siegfried et al., 2004).

The *gon* and *sys* mutant hermaphrodites, in contrast to those defective in LIN-12 signalling, have a loss or decreased number of distal tip cells (DTCs) owing to the loss of gonad symmetry (Siegfried et al., 2004). It remains to be investigated whether the number of DTCs in the mutants of the group II is changed, but the fact that the AC in these mutants are not clustered as seen in the mutants identified in the screen and described in LIN-12 candidates makes the participation of the mutants in establishment of gonad symmetry unlikely.

During the mapping procedure, I identified two regions in which the mutants of group II could be positioned.

zh72 could be positioned within the region comprised between -16.26 and 10.37cM on chromosome IV. Besides *nhr-67,* that was discussed previously as an interesting candidate gene for the mutants of group I and that has to be mentioned here also, *lag-1* could be an attractive candidate for being allelic to *zh72. lag-1* is a downsteam effector of the LIN-12 NOTCH pathway that binds to consensus CSL binding sites around target genes of LIN-12 NOTCH signalling (Christensen et al., 1996).

I performed RNAi experiments, and observed that the downregulation of *lag-1* phenocopies the phenotype of *zh72*. Nevertheless, *lag-1* is embryonic lethal, which suggests that for *zh72* to be allelic to *lag-1,* a weak allele would have been identified. In conclusion, *lag-1* is a candidate gene that should be analysed if further mapping of this mutant is pursued.

zh73 could be situated within the region between 2.73 and 3.91cM on chromsosome I. I suggest *sup-17* and *aph-1* as candidate genes for *zh73,* since both genes are located within the suggested region for *zh73*.

On one hand, *sup-17* encodes an ADAM protein, an integral membrane disintegrin and zinc-activated metalloproteinase. *sup-17* mediates LIN-12 receptor cleavage upon receptor binding. Nevertheless, *sup-17* is not described as showing a Pvl phenotype and animals defective for *sup-17* only show two ACs together with an *adm-4* defect, since *adm-4* acts redundantly together with *sup-17* (Jarriault and Greenwald, 2005).

On the other hand, *aph-1* is a component of the GLP-1/LIN-12 NOTCH pathway that is required maternally for embryonic viability. It also affects, egg laying and germ line proliferation (Francis et al., 2002). *aph-1(or28)* animals exhibit a recessive, fully penetrant egg-laying defect that is suggested to result from errors during π cell differentiation. Yet, this allele is maternally embryonic lethal. In contrast, *aph-1(or28)* animals are not defective in AC fate adoption (Lee et al.; 2005 International Worm Meeting). Thus, the ectopic expression of *cdh-3::cfp* speaks against the fact that *zh73* is allelic to *aph-1* Nevertheless, *zh73* might be a weak allele of *aph-1* that causes defective π cell differentiation (Goutte et al., 2002).

In conclusion, the ectopic expression in the ventral uterine cells of the two mutants needs to be examined further in order to draw conclusions about its origin. While performing RNAi experiments, a surprisingly high number of knocked down genes led to ectopic expression of *cdh-3* in the ventral uterine cells. This leads me to suggest that it might rather be the reporter construct that is susceptible to ectopic

expression. Furthermore, it is important to mention here, that the phenotype of ectopic expression in *zh72* and *zh73* is very low.

In the following paragraphs, I propose experiments, which might be of interest to be performed, in addition to the experiments that are proposed after the manuscript. These experiments would clarify which of the identified mutants be analysed and mapped further.

First, I strongly suggest analysing the development of the vulva in these mutants in detail, since many of the so far identified genes are involved, in parallel, in vulval cell fate specification. This may help to identify candidate genes within the regions and cloning the genes to the mutants would be simplified.

Second, *cdh-3* expression in the AC in the mutants of groups II and I were not downregulated in the AC. The capability of the AC to attach and invade the vulval tissue suggests a properly differentiated AC in the mutants of group I. The expression of other *zmp-1* and *lag-2* in the AC could be analysed to further confirm proper AC fate adoption.

Lastly, I suggest to study group I and II mutants with transcriptional reporters of *lin-29* and *lag-2, lin-11, ida-1* and *egl-13* in order to confirm the suggested defect in π cell or utse differentiation as well as to study the position of the mutated gene within the pathway during differentiation (Cinar et al., 2003; Newman et al., 1999; Zahn et al., 2001).

4.5.3 Group III

Group III mutants exhibit an AC invasion phenotype. In wild-type animals, the AC invades the vulval tissue during the mid L3 stage, thereby establishing the connection between the uterus and the vulva such that the egg can later be laid (Sherwood et al., 2005). I identified the mutants of this group as being novel allele of *lin-28* and *fos-1*.

The first group III mutant that I identified is the heterochronic gene *lin-28*. Mutations in *lin-28* lead to invasion defects due to errors in the developmental timing between the uterus and the vulva (Ambros and Horvitz, 1984; Morita and Han, 2006). In *lin-28* loss-of-function animals, the vulva is prematurely induced at the L2 stage. In these mutants at the L2 stage the AC has not yet developed to the point at which the AC

can invade the vulval tissue. This results in a Pvl phenotype and in an invasion defective phenotype. In conclusion, I identified a new allele of *lin-28* that is indirectly involved in AC invasion due to the asynchronous developmental timing of vulval induction.

The second mutant of group III encodes for a novel allele of *fos-1. fos-1 c-fos* is a key actor of AC invasion. *fos-1 c-fos* is together with *egl-43 evi-1* one of the only two factors involved in AC invasion with a strong penetrant phenotype that have been identified so far (Rimann and Hajnal, 2007).

4.6 Rationale of the Screen

In general, large-scale screening for loss-of-function mutants is a potent tool to identify genes that give new insight in developmental biology. In order to conduct such a screen properly, it is desirable to estimate the degree of saturation of the screen. This gives an answer to the question of the possible target genes that have been identified. I screened 5300 F1 clones for the desired phenotype.

Screening 5000 F1 clones equals 10'000 haploid genomes. It is assumed that with the EMS concentration of 50mM that was employed for this screen, approximately 2'000 haploid genomes would have to be screened in order to observe a null mutation in every gene (Jorgensen and Mango, 2002). Thus, the screen that I described in this thesis should have covered the genome five times. On the other hand, there are scientists that suggest that a screen is saturated if the same gene is isolated several times. Ivo Riman performed an EMS mutagenesis screen to identify LIN-12 NOTCH signalling targets in our laboratory. During the screening procedure, he isolated a surprisingly high number of mutants that affected the same gene (personal communications with Ivo Rimann) .

In contrast, *fos-1* and *lin-28* were only identified once during my screening procedure. Nevertheless, there are three mutants showing a similar phenotype that were mapped to the same region on chromosome IV and two that locate to chromosome II. These mutants were not complemented so far, not ruling out the possibility that the alleles could represent the same gene.

Surprisingly, only two mutants exhibiting an AC attachment or invasion were identified. There are several points that need to be discussed in order to explain this.

First of all, the so far identified, most downstream, factors that are involved in degrading the basal laminae during invasion of the AC are *cdh-3*, *him-4* and *zmp-1*. The triple mutant of *zmp-1*, *cdh-3* and *him-4* shows an invasion defect of only 25% (Sherwood et al., 2005). Therefore, because of their very low penetrant phenotype, these mutants would hardly be identified in a mutagenesis screen. For instance, if a mutant that has a penetrance of 25% regarding only homozygous animals, in a clonal screen the phenotype would be less then 6% on the plate. Moreover, even if such a low penetrant mutant were identified, the mapping procedure that would follow would be extremely difficult.

Second, by performing a clonal screen, sterile mutations can be maintained but nevertheless, mutations that lead to early lethality during development are lost.

This might be a reason why no other invasion mutants were identified with this screen. There are known factors such as the transcription factor *egl-43* that cause an early larval arrest in addition to an invasion phenotype (Rimann and Hajnal, 2007). Transcription factors such as EGL-43 EVI-1 are usually involved in many different steps during development (Garriga et al., 1993; Hwang et al., 2007).

Third, our screen is based on the hypothesis that lack of attachment and invasion leads to a Pvl phenotype. The so far identified components of AC invasion in other laboratories all exhibited a Pvl phenotype, thus confirming this hypothesis (personal communication with students of the Sherwood laboratory, L.A. meeting 2007). Examples comprise, for example, *unc-6* Netrin and *unc-40* DCC. Null mutations of these genes result in penetrant AC invasion defects (Joshua W Ziel et al, L.A. meeting 2007). Nonetheless, the Pvl phenotype is moderately penetrant and surprisingly, it is not mentioned on the wormbase pages of the corresponding genes.

Furthermore, *fos-1* and *egl-43* display a penetrant phenotype. Besides their impact on AC invasion, these genes are also involved in the induction of π cell fate (Hwang et al., 2007; Rimann and Hajnal, 2007).

Since mutations affecting genes that are involved only in π cell and utse differentiation such as for example *egl-13* Sox also lead to a Pvl phenotype; the Pvl phenotype of *fos-1* and *egl-43* mutants could result from both defects rather than only from an invasion defect. This leads to the question of whether genes that are involved only in invasion might be overlooked during the screening procedure due to a low penetrant phenotype.

When I designed this screen, I wanted to isolate genes involved in AC attachment and invasion. Nevertheless, I also became interested into the phenotype of unfused ACs during the fourth larval stage, which I observed in mutants of groups II and I.
Mutants of the first group are likely to be genes of the regulatory network that controls the development of the cell types that establish the connection of the vulva and the uterus.
I can now question whether the design of this screen was appropriate to identify genes involved in the establishment of the connection between the uterus and the vulva. There are several points that might answer this question.
First, *egl-13* is known to be involved in the uterus-vulva connection being a component during π cell fate adoption and utse differentiation (Cinar et al., 2003). *egl-13* exhibits a protruding vulva, that results most probably from the defects in the differentiation of π cells and of the utse. Surprisingly, loss-of-function animals of *egl-38* a regulator of uv1 development do not exhibit a Pvl phenotype despite the fact that the uv1 cells connect the vulval cells and the utse cells, as is described in literature.
However, *egl-38* is also a regulator of vulF differentiation. Hence, it can be speculated that defects of vulF differentiation lead rather to an Egl phenotype due to a morphogenetic defect of the vulF cells that in this case would be epistatic to a Pvl phenotype caused by the uv1 defect. Unfortunately, *egl-38* mutants would be lost with the framework of this screen.
Moreover, genes involved in the process of π cell and utse differentiation so far, are often involved in addition in vulval development. For example, *lin-11* defective animals exhibit a Vul phenotype due to defects in vulva differentiation and would also be lost in this screen despite the fact that it is a key component during π cell differentiation.
Nevertheless, with this screen there is the possibility to identify specific alleles of such mutants as that are only involved in the connection of the vulva and the uterus but that do not affect other tissues. Thus, an allele that only leads to a defect in π cell and not to defects of vulval development because it has for example a mutation within the enhancer region that leads to changes of tissue expression would be isolated with such a screen.
In conclusion, this screen led to the identification of new alleles of *fos-1* and *lin-28*. Hence, this confirms that the screen was adequately designed and powerful enough

to identify genes that are required for AC invasion. Furthermore, I isolated eight mutants that seem to be involved in the correct establishment of the hermaphrodite's egg-laying system. The mutants of group II are of particular interest, since, as it was described in the preceding paragraphs, their phenotype hints to a possible function in the LIN-12 signalling pathway. Thus I suggest, as a follow-up to this work, to study the relation between the mutants of group II and LIN-12 more in detail.

5 Material and Methods

5.1 Strains and General Methods

For maintaining and manipulating, *C. elegans* standard methods were used (Brenner, 1974). Unless otherwise mentioned, the variety Bristol, strain N2 was used as the wild-type reference strain. The experiments were performed at 20° C. For the mapping experiments, Hawaii (*CB4856*) was use.

5.2 Genes and Alleles used in this Project

LG I

gpa-15[pk447] I

*nDf24/unc-13(e1091) lin-11(n566)*I

*nDf23/unc-13(e1091) lin-11(n566)*I

LG II

*let-23(sy1)*II*, syIs52[cdh-3::cfp, unc-119(+)]* X; *unc-119*(?)

*let-23(sy1)*II

rrf-3[pk1426] II; *syIs52[cdh-3p::cfp], unc-119[+] X*

rrf-3[pk1426] II

LG III

*lin-39(n1880)*III

*lin-39(n1880)*III*; zhEx168[lin-3::pat-3::gfp, lin-48::gfp]*

*unc-119(e2498)*III*; zhEx87[lin-3::pat-3::gfp, unc-119(+)]*

gaIs47[lin-31-mpk-1(Siegfried et al.)] , lin-31-dmek(Siegfried et al.)] (LG?); *unc-32(e189) mpk-1(ga117)/gc1* III

unc-32(e189) mpk-1(ga117)/gc1 III

LG IV

*lin-3(e1417)*IV

*lin-3(e1417)*IV*, syIs52[cdh-3::cfp, unc-119(+)]* X; *unc-119*(?)

syIs76*[zmp-1::pes-10::cfp,unc-119(+)]*IV (Inoue et al., 2002)

LG V

fos-1(ar105/nT1[qIs51] V (Sherwood, 2005 #100)

pvl-6[ga81] V

LG X

syIs52[cdh-3::cfp, unc-119(+)] X; *unc-119* (III) (Inoue et al., 2002)

In order to simplify the handling of the strains containing the mutations of interest that cause sterility, the following balancers for the specific chromosomes were used:
+/mIn1[dpy-10(e128) mIs14] II (Edgley and Riddle, 2001)
+/hT2[bli-4(e937) let-?(q782) qIs48] I;III (Edgley et al., 2006)
+/nT1[qIs51] IV;V (Koh et al., 2004)

5.3 Transgenic Arrays

Ex[-6-egl-43L, sur-5::gfp]
Ex[sur-5::cfp]
zhEx168[lin-3::pat-3::gfp, lin-48::gfp]

5.4 EMS Mutagenesis for the Clonal Screen

Caution:
EMS (ethyl methane sulfonate) is carcinogenic and has to be handled with extreme care only under the fume hood, wearing gloves. It is effectively hydrolised and inactivated by strong alkali. All contaminated glassware must be soaked in 1M NaOH for at least 24hrs.

Day1: Mutagenesis
Plates with worms of mixed stage *(syIs52[cdh-3p::CFP], unc-119[+]X)* were washed from the plates with M9 and collected in a 13ml Falcon tube. The volume was reduced to 2ml by settling the worms and taking off of the supernatant.
2µl of EMS solution mixed was dissolved in 2ml M9 (50mM final concentration) and the solution was added to the Falcon tube with the worms. The tube was carefully sealed with Parafilm. The suspension was incubated for 4 hrs on a tilt shaker at room temperature. Next, the worms were washed with M9 3 times by filling the tube with M9 and centrifugation of the worms to take off the EMS containing supernatant with a pipette. Then, the worms were suspended in 1ml M9 and the suspension was distributed to 7 agar plates with bacteria and the worms were kept at least 12hrs (overnight).
Day 2: Isolation of P0 animals that will produce mutagenised F1 progeny

100 adult animals were picked form the plates and distributed on 10 fresh agar plates containing bacteria (10 adults per plate).

Day4/5: Cloning of the F1 progeny

200-500 F1 animals were singled out to separate plates

Day7-11: Screening F2 animals

The plates were screened for animals of the F2 generation exhibiting a protruding vulva (Pvl) under the dissecting microscope.

The animals from plates exhibiting animals with a Pvl phenotype were then rescreend with Normarski optics and the *cdh-3::cfp* expression was analised for mutant lines with a displaced or unfused AC during the L3 an L4 stage. The screen by Normarski optics was carried out often with F3 animals dependent on the amount of Pvl containing plates that were identified before. In case of overgrowth, 20 animals from positive plates were singled out again on new plates to maintain the mutation leading to sterility.

The strains of interest were frozen, the original plate was kept and 20 animals were singled out to maintain the mutants.

On **day 9/10**, a new round of EMS mutagenesis was set up.

5.5 Worm lysates

Worms were lysed using the following protocol. Worms, one to ten per tube were picked and placed into PCR tubes containing 10µl 1x lysis buffer (see below). The tubes were then subjected to liquid nitrogen and incubated in a thermocycler (PCR machine):

Lysis Program on a thermocycler:

Step	Duration	Temperature
1	60mins	60°C
2	15mins	95C°

5.6 FLP mapping

An automated high-throughput genotyping method based on fragment length polymorphisms (FLPs) established at the University of Zurich by Peder Zipperlen was

used to define the linkage group of the mutation and the sub-chromosomal position of the mutation of interest identified (Zipperlen et al., 2005).

To identify the linkage group of the mutants, Hawaii animals containing a extrachromosomal array with *sur-5::gfp* were crossed into the strains potentially heterozygous for the mutations. The *sur-5::gfp* array was used to identify the F1 cross progeny. F2 cross progeny that showed the phenotype was selected. To obtain the genomic DNA of the worms, single worms were lysed. The lysates were diluted with dH_2O in a volume of 100µl and the lysates were used for FLP and later for SNP mapping. To identify the subchromosomal region of the mutations, the mutants were crossed with Hawaii in a balanced version, simplifying the crossing procedure.

FLP name:	Chrs:	Variation:	Genetic position (Zahn et al.):	Genomic position (Mb):
ZH5-03a	5	*snp_F41B5[5]*	15.16	2239674
ZH5-06	5	*snp_D2023[10]*	3.39	11827565
ZH05-13	5	*pkP5101*	18.57	1551233
ZH5-02a	5	*snp_C05E4[5]*	19.99	749491
ZH4-10a	4	*snp_K08D8[2]*	6.51	12912461
ZH4-5	4	snp_Y41D4[3]	16.26	1704245
ZH4-21	4	*snp_C08F11[4]*	10.37	13629492
ZH4-02	4	*snp_T22D1[1]*	3.25	6926773
ZH4-20	4	*snp_M18[1]*	5.7	12104780
Zh2-25	2	*snp_T23G7[2]*	1.09	9183067
ZH2-09	2	*snp_B0491[2]*	3.45	11359423
ZH1-06	1	*snp_Y87G2*)	21.14	13512378
ZH1-08	1	*snp_F56H6[4]*	13.12	12289459
ZH1-23	1	*snp_F26E4[4]*	3.91	9791574
ZH1-01	1	*snp_F02E9[1]*	2.79	8408841
ZH1-21	1	*snp_F27D4[1]*	2.3	7707664
ZH1-22	1	*snp_F14B4[1]*	3.73	9279918
ZH1-01	1	*snp_F02E9[1]*	2.79	8408841

Table 7. The table contains list of FLP that confined the region of the mutant

5.7 Manual mapping

Once the sub-chromosomal position of the *zh70* was defined by FLP mapping, additional polymorphisms were used to narrow down the candidate region. Identified polymorphisms between Hawaii, *CB4856* and Bristol, *N2* were found on the polymorphism database at the Washington University in St. Louis (Wicks et al., 2001) and the wormbase (www.wormbase.org) The polymorphisms were analysed by PCR (polymerase chain reaction) amplification of the region of the selected SNP and the PCR product was sequenced or subjected to a restriction digest dependent on the nature of the polymorphism. The templates used for the PCR derived from the single worm lysates left form the FLP mapping or from additional recombinants. The PCR reaction mixture was analysed after the PCR reaction on a 0.8% agarose gel for correct fragment length and the amount of product obtained.

PCR program for polymorphism analysis:

Step	Duration	Temperature
1	2mins	94°C
2	1min	94°C
3	40s	see list
4	40s	72°C
5	30x step 2-4	
6	4mins	72°C
7	forever	12°C

variation	Primers	Primer Fwd (5' to 3')	Primer Rev (5' to 3')	PCR length (nt)
pkP1121	(Hengartner lab)	-	-	837
pkP1120	(Hengartner lab)	GGAATTATATTTGGAAGT	CAAACATAGCTGTCTGTA	510
F18C12[1]	OSV13/14	GAATCACCGCCAACATGAGA	CCAGTGTCCCGATAGAAAAC	839
T01G9[1]	OSV15/16	TATTCCGAGACTCCCATCTCC	ATCATTTCGGAGCTTCTGACC	787
T02E1[1]	OSV32/33	ATACTAACCTATCTAAAGTCCC	CAAACCATGCTCATTACCTCC	834
F10D11[1]	OSV34/35	TTGTATCTCACTGTTTGTGCC	AAATATTGGACCTTTTGAATCCC	802
CE1-154	OSV44/45	CGCGATGATGATGGTGAAGC	CTAATGGAACTCCTGGACCG	975
F30F8[1]	OSV38/39	CGGAAAGGTTGGTGCAACCACC	GTATCCCTTCTTAGCAGAGG	841
F08A10[1]	OSV40/41	TTAATGGGAATATCCCTGCCG	CAATTCTAGATCCTGTTCTTCC	876
F10D11[1]	OSV42/43	CTGACAGACATTCCTGCTCC	CAACTCAAGTGCTGCTCAACC	786
uCE1-977	OSV46/47	CACTTTATCTACTTCCTAGACG	TGGAAATTATGACGAGTTTCCG	896
pkP1119	OSV49/48	CTCCATTTTGGAACTCCCAG	TCAAATTTGGCACGTCATCAG	335
T02E1[1]	OSV51/50	TCATTACCTCCATCTTGTAGG	TCTCCCAAGCACATCTTTGC	720
uCE1-969	OSV60/61	AGAAAGCAAGTTGAGCGATGG	CAGTGTTACTTGCAGCGGAGC	971
F02E9[1]	OSV62/63	TATCATCGTCAGATGTAGTCG	TCACCGGTGAAGATCTATTCG	1069
F02E9[2]	OSV64/65	ACGTTATCGTGATCTGACACG	CACCTAATATGACGTCAGTCG	935
VF39H2L[2]	OSV72/73	CGTACCTATAAACAGATTCTCC	AATTTCAGGCTCCACTTTATGC	782
uCE1-974	OSV77/78	ATGTCACAACCGACTTTGACG	TACACGTTGTTGCCGTGAGC	859
uCE1-975	OSV79/80	GTGTTGAAATGGGCGACAGTG	CTAGTTAAGGGTCAGAGGAACG	597

Table 8: The table contains polymorphism used for mapping of *zh70,* its primer name and the sequence of the primers.

Assay	genetic position (Zahn et al.)	Gene	Polymorphism	annealing Temp (°C)
pkP1121	3.56	*mef-2*	A/G	60
pkP1120	3.02	*K07A12.2*	G/A	60
F18C12[1]	2.48	*F18C12.1*	A/-	60
T01G9[1]	2.7	*T01G9.2*	G/C	63
T02E1[1]	2.69	*T02E1.2*	A/C	58
F10D11[1]	2.83	*F10D11.2*	-/GAG	63
CE1-154	2.94	*gon-2*	T/C	63
F30F8[1]	2.37	*F30F8.1*	G/A	did not work
F08A10[1]	2.64	*F08A10.1d*	-/T	59
F10D11[1]	2.83	*F10D11.2*	-/GAG	63
uCE1-977	2.94	*M04C7.4*	C/T	60
pkP1119	2.88	*K02B12.3*	T/C	60
T02E1[1]	2.69	*T02E1.2*	A/C	58
uCE1-969	2.76	*rsd-6*	A/T	58
F02E9[1]	2.79	*F02E9.2b*	-/ATA	60
F02E9[2]	2.83	*F02E9.5b.1*	T/G	60
VF39H2L[2]	3.01	*sig-7*	A/-	62
uCE1-974	2.85	*D1081.5*	T/C	60
uCE1-975	2.86	*D1081.8*	T/-	did not work

Table 9: The table contains polymorphism used for mapping of *zh70,* genetic position, the gene in which the polymorphism is posited, the polymorphism and the used annealing temperatures.

5.7.1 Restriction Digest of PCR for Polymorphism Analysis

The PCR products of the SNPs containing restriction sites were digested during 4hours or overnight at 37°C in a reaction volume of 10 µl.

The digested fragments were loaded and analysed on a 0.8% agarose gel by comparing them with the cleaved control N2 and CB4856 products.

Variation:	Primers:	Enzyme:	Resulting bands (reference strain/polymorphic strain):
VF39H2L[2]	OSV72/73	*DraI*	354 and 227/782
pkP1119	OSV49/48	*EcoRI*	335/225 and 110

Table 10: The table contains polymorphism used for mapping of *zh70* that are analysed by digestion.

5.7.2 Sequencing the Polymorphisms

In order to sequence the PCR products, they were purified with the Quiagen QIA quick PCR Purification Kit.

5.8 RNAi Experiments

5.8.1 Feeding of RNAi Clones

The JA feeding library is based on bacterial *E.coli* strains HT115 (DE3), that produce dsRNA against specific mRNAs of *C. elegans* upon induction by IPTG (Kamath et al., 2003). The transcription of this sequence is under the control of two T7 promoters flanking the insert specific for *C. elegans*. Induction by IPTG (Isopropyl ß-D-1-thiogalactopyranoside) on worm plates leads to the transcription of the *C. elegans* specific sequence.

5.8.2 Sequencing of the RNAi Clones

The clones were grown overnight in a volume of a volume of 4ml in 2x TY media containing 50µg/ml ampicillin. Further, the plasmid was purified with the QIAGEN Plasmid kit. The obtained DNA was further sequenced with the primer L4 440.

Primer name:	Primer sequence:
L4 440	AGGAGGCAACCTGGCTT

Table 11: Table contains the sequence of the primer to sequence RNAi clones.

5.8.3 Preparation of RNAi Plates and Bacteria

RNAi producing bacteria from the frozen JA RNAi library were picked and grown overnight on double selective plates at 37°C (ampicillin=50µg/ml, tetracycline=12.5µg/ml). For feeding the worms, a liquid culture of the bacteria was grown. The liquid culture was grown for eight hours or overnight in a volume of 4ml in 2x TY media containing 50µg/ml ampicillin. The RNAi plates used are NGM plates (Nematode growth medium) with additional 50µg/ml ampicillin and IPTG at a concentration of 6mM. After pouring these plates they were seeded with the RNAi liquid culture. One day after, the worms were placed on the plates. The experiments were performed at room temperature.

5.8.4 RNAi Experiments

To perform RNAi experiments, the worms were treated in two different ways. Either, five adult worms were placed directly on the RNAi plates or the adult worms were bleached before with bleach solution to synchronised them. The bleached worms were placed on NGM plates lacking bacterial food and incubated overnight. After an incubation time of at least 13hrs (overnight) the synchronised worms were placed on the RNAi plates. In case the F0 generation was analysed, about 40 animals were placed on a plate, in case the F1 generation was analysed, five worms were placed on a plate. In case RNAi feeding leads to sterility of the worms, the F0 generation was analysed. Dependent on the experiment, the worms were then once reached the stage of interest analysed with Normarski optics.

5.9 Generation of Transgenic Lines

The PCR products were injected as followed using overlapping fragments that undergo homologous recombination (Mello et al., 1991).
The concentration of 5-10ng/µl of the different PCR products together with the coinjection marker *psur-5::gfp* of a concentration of 30-50ng/µl and the plasmid pBS-KS- to reach the concentration of 200ng/µl lead to the generation of stable lines containing extrachromosomal arrays.

5.10 Cosmid Rescue

Briefly, the cosmids were selected on plates containing either Kanamycin or Ampicillin (see list of cosmids). The plates were incubated overnight at 37°C and single colonies were picked and grown in selective media overnight again in a volume of 10ml. 3 times 1.5ml was centrifuged in the same Eppendorf tube at room temperature during 1min. The recovery pellet of the two Eppendorf tubes was pooled and used to purify the cosmids with the Qiagen Purification Kit using P1/P2/N3. In addition, 1/10 of the volume of 3M NaAc (ph=5.2) and 1 times the volume Isopropanol was added. The tube was centrifuged for 15mins full speed at 4°C. The supernatant was discared and the pellet was dissolved in 10µl H_20.
The likewise obtained cosmid was then tested for the expected DNA fragment by a restriction digest (see table). To select a convenient enzyme, the DNA Strider was 1.4f6 was used. The restriction digest was performed according to the suggestions of the manufacturer (Roche and Biolabs).
The cosmids were injected in mixes first at a concentration of 10 ng/µl, then at a concentration of 5 ng/µl in case no stable lines could be identified working with the higher concentration. *sur-5::gfp* (30ng/µl) was used as coinjection marker and the mixes were filled op to a concentration of 180-200ng/µl per mix with empty bluescript vector.

Name:	Resistance:	Restriction digest:
F08A10	Kanamycin	*Eco* RI
T02E1	Kanamycin	*Xba* I/*Bcl* I
ZK265	Kanamycin	*Eco* RI/ *Xba* I
T01G9	Kanamycin	*Eco* RI
F52B5	Kanamycin	*Bam* HI
C34B7	Ampicillin	*Xba* I
F16D3	Kanamycin	*Xba* I
T19A6	Kanamycin	*Pst* I
F02E9	Kanamycin	*Hind* III
F10D11	Kanamycin	*Xba* I/*Bam* HI
D1081	Ampicillin	*Bam* HI
K02B12	Kanamycin	*Pvu* I
M04C7	Ampicillin	*Eco* RI
T01H8	Kanamycin	*Eco* RI
R05D11	Ampicillin	no digest control

Table 12: The table contains list of cosmids to perform rescue experiments of *zh70*

Mix number:	Cosmids:	Covered region (Mb):
1	F08A10	I: 8196052…8208733
2	T02E1, ZK265, T01G9	I:8210664….8296905
3	T01G9, F52B5, C34B7	I:9274005…..8341701
4	C34B7, F16D3	I:8330544…8386666
5	F02E9, F10D11	I:8405948..8445442
6	D1081, K02B12	I:8464627…..8529375

Table 13: The table contains list of the cosmid mixes and the covered region to perform rescue experiments of *zh70.*

5.11 Deficiencies to Perform Complementation Assays with *zh70*

strain	genotype	suggested region
MT2181	*nDf24/unc-13(e1091) lin-11(n566)*I	1.8-3.72cM
MT2180	*nDf23/unc-13(e1091) lin-11(n566)*I	2.702-3.647cM

Table 14: The table contains the deficiencies used for mapping of *zh70*

The deficiencies are lethal. Heterozygotes animals of both strains exhibit a wild-type phenotype, segregating heterozygous wild-type phenotype animals, dead eggs homozygous for the mutation, and vulva less uncoordinated animals, homozygous for the balancer, that are small, kinky, paralyzed and vulvaless. The animals homozygous for the deficiency do not exhibit a Pvl phenotype.

5.12 PCR Rescue to Identify *zh70*

Long PCR fragments up to 12kb were generated using the La TaKaRa Polymerase Kit. An extension time of 1min/kb was used.

PCR program for PCR rescue fragments:

Step	Duration	Temperature
1	2mins	94°C
2	1min	94°C
3	40s	58°C
4	see fragment length	72°C
5	30x step 2-4	
6	4mins	72°C
7	-	12°C

Oligo name	Primer Fwd (5' to 3')	Primer Rev (5' to 3')	PCR product (nt)	Reaction No
OSV81/82	ATTCATGAGTAAGAAAGGGGG	GGATGGCACCGATAGATACG	6000	1
OSV83/84	TCTTATGGAGTTGCTCTTGG	TAATTTCAGTGGGAGGATCG	5920	2
OSV85/86	GAATTGACTTCCGAAGTGGC	TTCACCGGTCCATAATCTGG	6730	3
OSV87/88	ACAAGTGGAAAGCAGTGTGG	TTCTTCCTAACCTTCGCATGC	6330	4
OSV89/90	AGAAAAGACGAAAGGTCAAGC	GTTGATGTTGAAGCAATGTGC	6250	5
OSV91/92	CTACTCGGTATTGCATATGC	ACTACATTCAAGAGCGATCG	5390	6
OSV93/94	CCTGAGAGTGCAATTTGAGG	AAGTGATGACGAGCTACTGC	5500	7
OSV95/96	ATCGGTTATTCCCATCATTCC	ATTGATCTCCTCCATTGTTGC	6110	8
OSV97/98	ACATCGACACGATCAACTGC	GATCAGAACCAGATGTTCCC	5030	9
OSV99/100	GCAATTTGCCCTTGATCTACC	CCAAAGATTCATCACTGACGG	5340	10
OSV123/124	ACAATTATCAGCTATCGTGCC	AGAATAGCTTGGAGAGCAGC	8350	11
OSV125/127	CAAATCCCAACTGAAGCTCG	GCTGAAGAAGTGCTACGTGG	7500	12
OSV129/128	ACATAGTTCGCAGCAGATGG	TGAACATGGACTTCACATTGC	7400	13
OSV130/131	CGACTAACCATTTCGACTTGC	CATCGGTTCACCACAACTACC	9500	14
OSV87/90	ACAAGTGGAAAGCAGTGTGG	GTTGATGTTGAAGCAATGTGC	11960	15
OSV97/100	ACATCGACACGATCAACTGC	CCAAAGATTCATCACTGACGG	9550	16
OSV91/94	CTACTCGGTATTGCATATGC	AAGTGATGACGAGCTACTGC	9570	17

Table 15: The table contains primers, the sequence of the primers and the length of the product used to perform rescue experiments of *zh70.*

5.13 PCR Fragment Injection to Identify *zh70*

The reporter *sur-5::gfp* (40ng/µl) was used as coinjection marker and injected together with the cosmids mix (5-10ng/µl each cosmid).

Reaction No	containing genes	injection mix	injection mix
1/2/3	*T19A6.1* *F16D3.7*	A	
4	*T19A6.2 (ngp-1)*	B	I
5	*T19A6.3/4*	C	
6/7	*F02E9.1/2/3* *(lin-28)*	D	
8	*F02E9.7*	E	G
9/10	*F02E9.4 (pqn-28)*	F	
11/12	*Operon* *CEOP1476*	M	
13	*F10D11.3/4/5*	N	
14	*D1081.4*		
15/3	*T19A6.2 (ngp-1)* *T19A6.3/4*	K	
16/8	*F02E9.4 (pqn-28)* (one reaction)	L	
17/5	*F02E9.1/2/3* *(lin-28)* (one reaction)	S (rescue)	
17/5/8	*F02E9.1/2/3* *(lin-28)* (one reaction) *F02E9.7*	H (rescue)	

Table 16: The table contains list of the PCR mixes and its containing genes to perform rescue experiments of *zh70.*

5.14 MitoTracker Red Staining

The mitotracker Red staining was adapted form (Sherwood et al., 2005). Worms were incubated for 2hours at room temperature in 10µM solution of MitoTracker Red CMXRos (Moleculer probes) in M9. The initial volume was diluted 5 times by addition of M9 and pipetted on NGM plates with food. Animals were allowed to recover for 1h at room temperature.

5.15 Microscopy of *C. elegans*

For observation under Normarski optics, the animals of the indicated stages were mounted on 4% agarose pads. Fluorescent images were aquired on a Leica DMRA wide field microscope equipped with a cooled CCD camera (Hamamatsu ORCA-ER) controlled by openlab 3.0 software package (Improvision) For quantification of GFP intensity, in the AC, all *gfp* images were acquired with the same microscopy and the same software settings. The mean intensity of *gfp* expression in the nucleus of the AC was measured by using the measurement tool in the Openlab 3.0 software package (Improvision). Each measurement was standardised to the background intensity in the same picture.

5.16 Sequencing the Candidate Genes of *zh70*

Candidate genes within the region suggested by FLP mapping and RNAi results suggested several candidate genes that might be allelic to *zh70*. The used primers to sequence and amplify the genes are listed below.

5.16.1 *F43G9.1*

Oligo name	Sequence (5' to 3')	PCR product No
OSV17	AGGGTTCAGAATGCTTGGCAAG	1
OSV18	GATCTGTGTCCTTTTCCAATTG	
OSV19	CAGCTTGCTCGCGGCAGATG	2
OSV20	CTTTCGATTTCACTTCTATGTG	
OSV21	AAAGTGTTTTAGTGTCTAACAGCC	-

Table 17

5.16.2 *unc-120*

Oligo name	Sequence (5' to 3')	PCR product No
OSV66	GAATCAATTAACCATCTACCG	1
OSV67	AACCTGCCGCAACTAAATAGG	
OSV68	ACTTTCCTCTATGGCGATGC	2
OSV69	AACCAAAGTCGTACACACACC	
OSV70	GGAAGAATGGTATTACCTATGC	
OSV71	CAGATGTTGACAAGATCGTGG	

Table 18

5.16.3 *lin-28*

Oligo name	Sequence (5' to 3')	PCR product No
OSV132	ATTTCATCATCGGAAGTTCAG	PCR product No 1
OSV133	CGAATCGTCACTGGAAATTCG	

OSV134	TACCTAAATACTTTGAGAGTGG	PCR product No 2
OSV136	CGATTCTCGACCTTGTATCC	
OSV135	CAGGATATGTTGTCAATGCGC	to sequence PCR No 2

Table 19

5.17 Rescue Experiments with *zh70*

The exon regions of some candidate genes were amplified to perform rescue experiments. The reporter *sur-5::gfp* (40ng/µl) was used as coinjection marker and injected together with the PCR fragment mixes (5-10ng/µl each cosmid).

5.17.1 *gpa-15* Rescue Construct and Sequencing Primers

Oligo name	Sequence (5' to 3')	PCR product No
OSV54	GATGTATCGCCTCTCAACACC	1
OSV59	TTCGCTGTCACATATGTGGC	
OSV58	CAATGAGCATAACCACAGTCG	2
OSV55	TAAACATATGATGGCATGCGCC	
OSV56	CGTCCCTGGTTATTATAGTTCC	3 nested primers
OSV57	AATTAGCGTGTGATTGTCACCG	

Table 20

5.17.2 Primers to confirm the deletion of *unc-120(tm1973)*

Oligo name	Sequence (5' to 3')
OSV74	AAAGTTACCATACCAATACTGG
OSV75	TTCAGAACATGACCGAAGCC
OSV76	CTTCCCGAAGGATATTTGAGG

Table 21

5.18 Equipment

PCR machines:

-BioRad MyCycler

-MJ Research Inc., PTC-100

Table centrifuges:

-Eppendorf Centrifuge 5810 (for 15ml Falcon tubes)

-Eppendorf Centrifuge 5415D (for 1.5ml Eppendorf tubes)

Sequencing machine:

-ABI Prism BigDye Terminator

Spectrometer:

-NanoDrop ND-1000

Microscopes:

-Leica DMRA (high resolution Normarski and fluorescent microscope)

-Leica DMIRB (high resolution microscope used for injections)

- dissecting microscope !!!!!

Camera:

-Hamamatsu ORCA-ER (Normarski and fluorescent pictures)

Software:

-Improvision, Openlab 3.1 (acquisition of microscopy pictures)

-Adobe Systems Inc., Adobe Illustrator, Adobe Photoshop

-Gene Codes Corporation, Sequencer (analysis of DNA sequences, PCR primer design)

- CEA France, DNA Strider 1.4f6 (analysis of DNA sequences, PCR primer design, DNA restriction fragment digests)

5.19 Solutions and Chemicals

LB Medium

Sodium chloride 10g

Bactotryptone 10g

Bacto Yeast Extract 5g

H_20 1L
Autoclaved

Bleach solution
2.3ml dH_20
2ml 4M KOH
0.7 NaHypochlorit

EMS solution:
2ml M9
20µl EMS (Sigma M0880-10G)

1x Lysis buffer
50mM KCl
10mM Tris (ph=8.2)
2.5mM $MgCl_2$
0.45% NP-400
45% Tween-200
0.01% Gelatine
200g/ml Proteinase K

M9
3g KH_2PO_4
6g Na_2HPO_4
5g NaCl
1ml 1M $MgSO_4$
1L H_2O

6 References 1

Ambros, V., 1999. Cell cycle-dependent sequencing of cell fate decisions in Caenorhabditis elegans vulva precursor cells. Development. 126, 1947-56.

Ambros, V., Horvitz, H. R., 1984. Heterochronic mutants of the nematode Caenorhabditis elegans. Science. 226, 409-16.

Araki, Y., et al., 2003. Novel cadherin-related membrane proteins, Alcadeins, enhance the X11-like protein-mediated stabilization of amyloid beta-protein precursor metabolism. J Biol Chem. 278, 49448-58.

Aroian, R. V., Sternberg, P. W., 1991. Multiple functions of let-23, a Caenorhabditis elegans receptor tyrosine kinase gene required for vulval induction. Genetics. 128, 251-67.

Bargmann, C. I., et al., 1993. Odorant-selective genes and neurons mediate olfaction in C. elegans. Cell. 74, 515-27.

Bargmann, C. I., Horvitz, H. R., 1991. Chemosensory neurons with overlapping functions direct chemotaxis to multiple chemicals in C. elegans. Neuron. 7, 729-42.

Bargmann, C. I., Kaplan, J. M., 1998. Signal transduction in the Caenorhabditis elegans nervous system. Annu Rev Neurosci. 21, 279-308.

Bastiani, C., Mendel, J., 2006. Heterotrimeric G proteins in C. elegans. WormBook. 1-25.

Battu, G., et al., 2003. The C. elegans G-protein-coupled receptor SRA-13 inhibits RAS/MAPK signalling during olfaction and vulval development. Development. 130, 2567-77.

Beitel, G. J., et al., 1990. Caenorhabditis elegans ras gene let-60 acts as a switch in the pathway of vulval induction. Nature. 348, 503-9.

Beitel, G. J., et al., 1995. The Caenorhabditis elegans gene lin-1 encodes an ETS-domain protein and defines a branch of the vulval induction pathway. Genes Dev. 9, 3149-62.

Bellaiche, Y., Gotta, M., 2005. Heterotrimeric G proteins and regulation of size asymmetry during cell division. Curr Opin Cell Biol. 17, 658-63.

Berset, T., et al., 2001. Notch inhibition of RAS signaling through MAP kinase phosphatase LIP-1 during C. elegans vulval development. Science. 291, 1055-8.

Bettinger, J. C., et al., 1996. Stage-specific accumulation of the terminal differentiation factor LIN-29 during Caenorhabditis elegans development. Development. 122, 2517-27.

Bjork, P., et al., 2002. A novel conserved RNA-binding domain protein, RBD-1, is essential for ribosome biogenesis. Mol Biol Cell. 13, 3683-95.

Brenner, S., 1974. The genetics of Caenorhabditis elegans. Genetics. 77, 71-94.

Brockie, P. J., et al., 2001a. Differential expression of glutamate receptor subunits in the nervous system of Caenorhabditis elegans and their regulation by the homeodomain protein UNC-42. J Neurosci. 21, 1510-22.

Brockie, P. J., et al., 2001b. The C. elegans glutamate receptor subunit NMR-1 is required for slow NMDA-activated currents that regulate reversal frequency during locomotion. Neuron. 31, 617-30.

Broday, L., et al., 2004. The small ubiquitin-like modifier (SUMO) is required for gonadal and uterine-vulval morphogenesis in Caenorhabditis elegans. Genes Dev. 18, 2380-91.

Buss, A., et al., 2007. Matrix metalloproteinases and their inhibitors in human traumatic spinal cord injury. BMC Neurol. 7, 17.

Chang, C., et al., 2000. Caenorhabditis elegans SOS-1 is necessary for multiple RAS-mediated developmental signals. Embo J. 19, 3283-94.

Chang, C., et al., 1999. Reciprocal EGF signaling back to the uterus from the induced C. elegans vulva coordinates morphogenesis of epithelia. Curr Biol. 9, 237-46.

Chao, M. Y., et al., 2004. Feeding status and serotonin rapidly and reversibly modulate a Caenorhabditis elegans chemosensory circuit. Proc Natl Acad Sci U S A. 101, 15512-7.

Chen, N., Greenwald, I., 2004. The lateral signal for LIN-12/Notch in C. elegans vulval development comprises redundant secreted and transmembrane DSL proteins. Dev Cell. 6, 183-92.

Chinenov, Y., Kerppola, T. K., 2001. Close encounters of many kinds: Fos-Jun interactions that mediate transcription regulatory specificity. Oncogene. 20, 2438-52.

Choi, J., et al., 2006. N-ethylmaleimide sensitive factor is required for fusion of the C. elegans uterine anchor cell. Dev Biol. 297, 87-102.

Christensen, S., et al., 1996. lag-1, a gene required for lin-12 and glp-1 signaling in Caenorhabditis elegans, is homologous to human CBF1 and Drosophila Su(H). Development. 122, 1373-83.

Cinar, H. N., et al., 2003. The EGL-13 SOX domain transcription factor affects the uterine pi cell lineages in Caenorhabditis elegans. Genetics. 165, 1623-8.

Clark, S. G., et al., 1993. Control of cell fates in the central body region of C. elegans by the homeobox gene lin-39. Cell. 74, 43-55.

Cooke, S. F., Bliss, T. V., 2006. Plasticity in the human central nervous system. Brain. 129, 1659-73.

Dent, J. A., Han, M., 1998. Post-embryonic expression pattern of C. elegans let-60 ras reporter constructs. Mech Dev. 72, 179-82.

Dutt, A., et al., 2004. EGF signal propagation during C. elegans vulval development mediated by ROM-1 rhomboid. PLoS Biol. 2, e334.

Edgley, M. L., et al., 2006. Genetic balancers. WormBook. 1-32.

Edgley, M. L., Riddle, D. L., 2001. LG II balancer chromosomes in Caenorhabditis elegans: mT1(II;III) and the mIn1 set of dominantly and recessively marked inversions. Mol Genet Genomics. 266, 385-95.

Eisenmann, D. M., Kim, S. K., 2000. Protruding vulva mutants identify novel loci and Wnt signaling factors that function during Caenorhabditis elegans vulva development. Genetics. 156, 1097-116.

Euling, S., Ambros, V., 1996. Heterochronic genes control cell cycle progress and developmental competence of C. elegans vulva precursor cells. Cell. 84, 667-76.

Francis, R., et al., 2002. aph-1 and pen-2 are required for Notch pathway signaling, gamma-secretase cleavage of betaAPP, and presenilin protein accumulation. Dev Cell. 3, 85-97.

Fredriksson, R., Schioth, H. B., 2005. The repertoire of G-protein-coupled receptors in fully sequenced genomes. Mol Pharmacol. 67, 1414-25.

Garriga, G., et al., 1993. Migrations of the Caenorhabditis elegans HSNs are regulated by egl-43, a gene encoding two zinc finger proteins. Genes Dev. 7, 2097-109.

Glodowski, D. R., et al., 2005. Distinct LIN-10 domains are required for its neuronal function, its epithelial function, and its synaptic localization. Mol Biol Cell. 16, 1417-26.

Goutte, C., et al., 2002. APH-1 is a multipass membrane protein essential for the Notch signaling pathway in Caenorhabditis elegans embryos. Proc Natl Acad Sci U S A. 99, 775-9.

Greenwald, I., Seydoux, G., 1990. Analysis of gain-of-function mutations of the lin-12 gene of Caenorhabditis elegans. Nature. 346, 197-9.

Guo, Y., et al., 2006. Identification and characterization of lin-28 homolog B (LIN28B) in human hepatocellular carcinoma. Gene. 384, 51-61.

Hamm, H. E., 1998. The many faces of G protein signaling. J Biol Chem. 273, 669-72.

Han, M., et al., 1993. C. elegans lin-45 raf gene participates in let-60 ras-stimulated vulval differentiation. Nature. 363, 133-40.

Han, M., Sternberg, P. W., 1990. let-60, a gene that specifies cell fates during C. elegans vulval induction, encodes a ras protein. Cell. 63, 921-31.

Hanna-Rose, W., Han, M., 1999. COG-2, a sox domain protein necessary for establishing a functional vulval-uterine connection in Caenorhabditis elegans. Development. 126, 169-79.

Hill, R. J., Sternberg, P. W., 1992. The gene lin-3 encodes an inductive signal for vulval development in C. elegans. Nature. 358, 470-6.

Hills, T., et al., 2004. Dopamine and glutamate control area-restricted search behavior in Caenorhabditis elegans. J Neurosci. 24, 1217-25.

Hintsch, G., et al., 2002. The calsyntenins--a family of postsynaptic membrane proteins with distinct neuronal expression patterns. Mol Cell Neurosci. 21, 393-409.

Hirsh, D., et al., 1976. Development of the reproductive system of Caenorhabditis elegans. Dev Biol. 49, 200-19.

Hodgkin, J., 2005. Genetic suppression. WormBook. 1-13.

Hopper, N. A., et al., 2000. ARK-1 inhibits EGFR signaling in C. elegans. Mol Cell. 6, 65-75.

Huang, L., Hanna-Rose, W., 2006. EGF signaling overcomes a uterine cell death associated with temporal mis-coordination of organogenesis within the C. elegans egg-laying apparatus. Dev Biol. 300, 599-611.

Huang, Y., et al., 2005. S-nitrosylation of N-ethylmaleimide sensitive factor mediates surface expression of AMPA receptors. Neuron. 46, 533-40.

Hwang, B. J., et al., 2007. C. elegans EVI1 proto-oncogene, EGL-43, is necessary for Notch-mediated cell fate specification and regulates cell invasion. Development. 134, 669-79.

Hwang, B. J., Sternberg, P. W., 2004. A cell-specific enhancer that specifies lin-3 expression in the C. elegans anchor cell for vulval development. Development. 131, 143-51.

Ikeda, D. D., et al., 2008. CASY-1, an ortholog of calsyntenins/alcadeins, is essential for learning in Caenorhabditis elegans. Proc Natl Acad Sci U S A. 105, 5260-5.

Inoue, T., et al., 2002. Gene expression markers for Caenorhabditis elegans vulval cells. Mech Dev. 119 Suppl 1, S203-9.

Jansen, G., et al., 1999. The complete family of genes encoding G proteins of Caenorhabditis elegans. Nat Genet. 21, 414-9.

Jarriault, S., Greenwald, I., 2005. Evidence for functional redundancy between C. elegans ADAM proteins SUP-17/Kuzbanian and ADM-4/TACE. Dev Biol. 287, 1-10.

Jorgensen, E. M., Mango, S. E., 2002. The art and design of genetic screens: caenorhabditis elegans. Nat Rev Genet. 3, 356-69.

Kaech, S. M., et al., 1998. The LIN-2/LIN-7/LIN-10 complex mediates basolateral membrane localization of the C. elegans EGF receptor LET-23 in vulval epithelial cells. Cell. 94, 761-71.

Kamath, R. S., et al., 2003. Systematic functional analysis of the Caenorhabditis elegans genome using RNAi. Nature. 421, 231-7.

Karp, X., Greenwald, I., 2003. Post-transcriptional regulation of the E/Daughterless ortholog HLH-2, negative feedback, and birth order bias during the AC/VU decision in C. elegans. Genes Dev. 17, 3100-11.

Kim, E., Sheng, M., 2004. PDZ domain proteins of synapses. Nat Rev Neurosci. 5, 771-81.

Kimble, J., 1981. Alterations in cell lineage following laser ablation of cells in the somatic gonad of Caenorhabditis elegans. Dev Biol. 87, 286-300.

Kimble, J., Hirsh, D., 1979. The postembryonic cell lineages of the hermaphrodite and male gonads in Caenorhabditis elegans. Dev Biol. 70, 396-417.

Kimble, J. E., White, J. G., 1981. On the control of germ cell development in Caenorhabditis elegans. Dev Biol. 81, 208-19.

Koh, K., et al., 2004. The nT1 translocation separates vulval regulatory elements from the egl-18 and elt-6 GATA factor genes. Dev Biol. 267, 252-63.

Konecna, A., et al., 2006. Calsyntenin-1 docks vesicular cargo to kinesin-1. Mol Biol Cell. 17, 3651-63.

Kozasa, T., et al., 1998. p115 RhoGEF, a GTPase activating protein for Galpha12 and Galpha13. Science. 280, 2109-11.

Kramer, J. M., 1994. Genetic analysis of extracellular matrix in C. elegans. Annu Rev Genet. 28, 95-116.

Kramer, J. M., 2005. Basement membranes. WormBook. 1-15.

Lackner, M. R., Kim, S. K., 1998. Genetic analysis of the Caenorhabditis elegans MAP kinase gene mpk-1. Genetics. 150, 103-17.

Lackner, M. R., et al., 1994. A MAP kinase homolog, mpk-1, is involved in ras-mediated induction of vulval cell fates in Caenorhabditis elegans. Genes Dev. 8, 160-73.

Lamb, R. F., et al., 1997. AP-1-mediated invasion requires increased expression of the hyaluronan receptor CD44. Mol Cell Biol. 17, 963-76.

Li, C., Chalfie, M., 1990. Organogenesis in C. elegans: positioning of neurons and muscles in the egg-laying system. Neuron. 4, 681-95.

Lolle, S. J., et al., 2005. Genome-wide non-mendelian inheritance of extra-genomic information in Arabidopsis. Nature. 434, 505-9.

Maricq, A. V., et al., 1995. Mechanosensory signalling in C. elegans mediated by the GLR-1 glutamate receptor. Nature. 378, 78-81.

Massie, M. R., et al., 2003. Exposure to the metabolic inhibitor sodium azide induces stress protein expression and thermotolerance in the nematode Caenorhabditis elegans. Cell Stress Chaperones. 8, 1-7.

Melkman, T., Sengupta, P., 2004. The worm's sense of smell. Development of functional diversity in the chemosensory system of Caenorhabditis elegans. Dev Biol. 265, 302-19.

Mello, C. C., et al., 1991. Efficient gene transfer in C.elegans: extrachromosomal maintenance and integration of transforming sequences. Embo J. 10, 3959-70.

Merz, D. C., et al., 2001. Multiple signaling mechanisms of the UNC-6/netrin receptors UNC-5 and UNC-40/DCC in vivo. Genetics. 158, 1071-80.

Miller, L. M., et al., 1993. lin-31, a Caenorhabditis elegans HNF-3/fork head transcription factor homolog, specifies three alternative cell fates in vulval development. Genes Dev. 7, 933-47.

Mohler, W. A., et al., 2002. The type I membrane protein EFF-1 is essential for developmental cell fusion. Dev Cell. 2, 355-62.

Mohri, A., et al., 2005. Genetic control of temperature preference in the nematode Caenorhabditis elegans. Genetics. 169, 1437-50.

Morita, K., Han, M., 2006. Multiple mechanisms are involved in regulating the expression of the developmental timing regulator lin-28 in Caenorhabditis elegans. Embo J. 25, 5794-804.

Moss, E. G., Tang, L., 2003. Conservation of the heterochronic regulator Lin-28, its developmental expression and microRNA complementary sites. Dev Biol. 258, 432-42.

Muller, S., et al., 2004. SUMO: a regulator of gene expression and genome integrity. Oncogene. 23, 1998-2008.

Nelms, B. L., Hanna-Rose, W., 2006. C. elegans HIM-8 functions outside of meiosis to antagonize EGL-13 Sox protein function. Dev Biol. 293, 392-402.

Newman, A. P., et al., 1999. The lin-11 LIM domain transcription factor is necessary for morphogenesis of C. elegans uterine cells. Development. 126, 5319-26.

Newman, A. P., et al., 2000. The Caenorhabditis elegans heterochronic gene lin-29 coordinates the vulval-uterine-epidermal connections. Curr Biol. 10, 1479-88.

Newman, A. P., Sternberg, P. W., 1996. Coordinated morphogenesis of epithelia during development of the Caenorhabditis elegans uterine-vulval connection. Proc Natl Acad Sci U S A. 93, 9329-33.

Newman, A. P., et al., 1995. The Caenorhabditis elegans lin-12 gene mediates induction of ventral uterine specialization by the anchor cell. Development. 121, 263-71.

Newman, A. P., et al., 1996. Morphogenesis of the C. elegans hermaphrodite uterus. Development. 122, 3617-26.

Novelli, J., et al., 2004. Gene interactions in Caenorhabditis elegans define DPY-31 as a candidate procollagen C-proteinase and SQT-3/ROL-4 as its predicted major target. Genetics. 168, 1259-73.

Nuttley, W. M., et al., 2002. Serotonin mediates food-odor associative learning in the nematode Caenorhabditiselegans. Proc Natl Acad Sci U S A. 99, 12449-54.

Nuttley, W. M., et al., 2001. Regulation of distinct attractive and aversive mechanisms mediating benzaldehyde chemotaxis in Caenorhabditis elegans. Learn Mem. 8, 170-81.

O'Shea, E. K., et al., 1992. Mechanism of specificity in the Fos-Jun oncoprotein heterodimer. Cell. 68, 699-708.

Oommen, K. S., Newman, A. P., 2007. Co-regulation by Notch and Fos is required for cell fate specification of intermediate precursors during C. elegans uterine development. Development. 134, 3999-4009.

Ozanne, B. W., et al., 2006. Invasion is a genetic program regulated by transcription factors. Curr Opin Genet Dev. 16, 65-70.

Palmer, R. E., et al., 2002. Caenorhabditis elegans cog-1 locus encodes GTX/Nkx6.1 homeodomain proteins and regulates multiple aspects of reproductive system development. Dev Biol. 252, 202-13.

Papassotiropoulos, A., et al., 2006. Common Kibra alleles are associated with human memory performance. Science. 314, 475-8.

Peng, P., et al., 2006. Plant genetics: increased outcrossing in hothead mutants. Nature. 443, E8; discussion E8-9.

Perkins, L. A., et al., 1986. Mutant sensory cilia in the nematode Caenorhabditis elegans. Dev Biol. 117, 456-87.

Perner, J., Ruffman, T., 1995. Episodic memory and autonoetic consciousness: developmental evidence and a theory of childhood amnesia. J Exp Child Psychol. 59, 516-48.

Pettitt, J., et al., 1996. cdh-3, a gene encoding a member of the cadherin superfamily, functions in epithelial cell morphogenesis in Caenorhabditis elegans. Development. 122, 4149-57.

Polesskaya, A., et al., 2007. Lin-28 binds IGF-2 mRNA and participates in skeletal myogenesis by increasing translation efficiency. Genes Dev. 21, 1125-38.

Rajakumar, V., Chamberlin, H. M., 2007. The Pax2/5/8 gene egl-38 coordinates organogenesis of the C. elegans egg-laying system. Dev Biol. 301, 240-53.

Rassoulzadegan, M., et al., 2006. RNA-mediated non-mendelian inheritance of an epigenetic change in the mouse. Nature. 441, 469-74.

Rimann, I., Hajnal, A., 2007. Regulation of anchor cell invasion and uterine cell fates by the egl-43 Evi-1 proto-oncogene in Caenorhabditis elegans. Dev Biol. 308, 187-95.

Rogalski, T. M., et al., 1995. Mutations in the unc-52 gene responsible for body wall muscle defects in adult Caenorhabditis elegans are located in alternatively spliced exons. Genetics. 139, 159-69.

Rongo, C., et al., 1998. LIN-10 is a shared component of the polarized protein localization pathways in neurons and epithelia. Cell. 94, 751-9.

Rose, J. K., et al., 2003. GLR-1, a non-NMDA glutamate receptor homolog, is critical for long-term memory in Caenorhabditis elegans. J Neurosci. 23, 9595-9.

Rose, J. K., Rankin, C. H., 2001. Analyses of habituation in Caenorhabditis elegans. Learn Mem. 8, 63-9.

Saijou, E., et al., 2004. RBD-1, a nucleolar RNA-binding protein, is essential for Caenorhabditis elegans early development through 18S ribosomal RNA processing. Nucleic Acids Res. 32, 1028-36.

Sapir, A., et al., 2007. AFF-1, a FOS-1-regulated fusogen, mediates fusion of the anchor cell in C. elegans. Dev Cell. 12, 683-98.

Schafer, W. R., 2005. Egg-laying. WormBook. 1-7.

Sengupta, P., et al., 1996. odr-10 encodes a seven transmembrane domain olfactory receptor required for responses to the odorant diacetyl. Cell. 84, 899-909.

Seydoux, G., Greenwald, I., 1989. Cell autonomy of lin-12 function in a cell fate decision in C. elegans. Cell. 57, 1237-45.

Sharma-Kishore, R., et al., 1999. Formation of the vulva in Caenorhabditis elegans: a paradigm for organogenesis. Development. 126, 691-9.

Shemer, G., Podbilewicz, B., 2002. LIN-39/Hox triggers cell division and represses EFF-1/fusogen-dependent vulval cell fusion. Genes Dev. 16, 3136-41.

Sheng, M., Sala, C., 2001. PDZ domains and the organization of supramolecular complexes. Annu Rev Neurosci. 24, 1-29.

Sherwood, D. R., et al., 2005. FOS-1 promotes basement-membrane removal during anchor-cell invasion in C. elegans. Cell. 121, 951-62.

Sherwood, D. R., Sternberg, P. W., 2003. Anchor cell invasion into the vulval epithelium in C. elegans. Dev Cell. 5, 21-31.

Siegfried, K. R., et al., 2004. The sys-1 and sys-3 genes cooperate with Wnt signaling to establish the proximal-distal axis of the Caenorhabditis elegans gonad. Genetics. 166, 171-86.

Singh, S., et al., 2007. Chemokines in tumor angiogenesis and metastasis. Cancer Metastasis Rev. 26, 453-67.

Sollner, T., et al., 1993. A protein assembly-disassembly pathway in vitro that may correspond to sequential steps of synaptic vesicle docking, activation, and fusion. Cell. 75, 409-18.

Sommer, R. J., et al., 1994. The evolution of cell lineage in nematodes. Dev Suppl. 85-95.

Strieter, R. M., et al., 1992. Interleukin-8. A corneal factor that induces neovascularization. Am J Pathol. 141, 1279-84.

Struhl, G., Adachi, A., 2000. Requirements for presenilin-dependent cleavage of notch and other transmembrane proteins. Mol Cell. 6, 625-36.

Tan, P. B., et al., 1998. MAP kinase signaling specificity mediated by the LIN-1 Ets/LIN-31 WH transcription factor complex during C. elegans vulval induction. Cell. 93, 569-80.

Tulving, E., 1987. Multiple memory systems and consciousness. Hum Neurobiol. 6, 67-80.

Vogel, B. E., Hedgecock, E. M., 2001. Hemicentin, a conserved extracellular member of the immunoglobulin superfamily, organizes epithelial and other cell attachments into oriented line-shaped junctions. Development. 128, 883-94.

Wada, K., et al., 1998. Cloning of three Caenorhabditis elegans genes potentially encoding novel matrix metalloproteinases. Gene. 211, 57-62.

Wagner, K. D., et al., 2008. RNA induction and inheritance of epigenetic cardiac hypertrophy in the mouse. Dev Cell. 14, 962-9.

Waterston, R. H., 1981. A second informational suppressor, SUP-7 X, in Caenorhabditis elegans. Genetics. 97, 307-25.

White, J. G., et al., 1976. The structure of the ventral nerve cord of Caenorhabditis elegans. Philos Trans R Soc Lond B Biol Sci. 275, 327-48.

Whitfield, C. W., et al., 1999. Basolateral localization of the Caenorhabditis elegans epidermal growth factor receptor in epithelial cells by the PDZ protein LIN-10. Mol Biol Cell. 10, 2087-100.

Wicks, S. R., et al., 2001. Rapid gene mapping in Caenorhabditis elegans using a high density polymorphism map. Nat Genet. 28, 160-4.

Wilkinson, H. A., et al., 1994. Reciprocal changes in expression of the receptor lin-12 and its ligand lag-2 prior to commitment in a C. elegans cell fate decision. Cell. 79, 1187-98.

Wilkinson, H. A., Greenwald, I., 1995. Spatial and temporal patterns of lin-12 expression during C. elegans hermaphrodite development. Genetics. 141, 513-26.

Wu, Y., et al., 1995. MEK-2, a Caenorhabditis elegans MAP kinase kinase, functions in Ras-mediated vulval induction and other developmental events. Genes Dev. 9, 742-55.

Yamaguchi, H., et al., 2005. Cell migration in tumors. Curr Opin Cell Biol. 17, 559-64.

Yoo, A. S., et al., 2004. Crosstalk between the EGFR and LIN-12/Notch pathways in C. elegans vulval development. Science. 303, 663-6.

Zahn, T. R., et al., 2001. IDA-1, a Caenorhabditis elegans homolog of the diabetic autoantigens IA-2 and phogrin, is expressed in peptidergic neurons in the worm. J Comp Neurol. 429, 127-43.

Zentall, T. R., et al., 2001. Episodic-like memory in pigeons. Psychon Bull Rev. 8, 685-90.

Zhang, H. M., et al., 2008. Mitogen-induced recruitment of ERK and MSK to SRE promoter complexes by ternary complex factor Elk-1. Nucleic Acids Res. 36, 2594-607.

Zipperlen, P., et al., 2005. A universal method for automated gene mapping. Genome Biol. 6, R19.

Zlotnik, A., et al., 2006. The chemokine and chemokine receptor superfamilies and their molecular evolution. Genome Biol. 7, 243.

Part II

1 Introduction

1.1 Memory and Learning

Memory is the ability of higher organisms to store and retain information and to recall it later (Tulving, 1987). Scientists have defined different kinds of memory. First of all, short-term memory allows retrieving information that was memorised during a period of up to one minute. The manageable capacity of information that can be memorised within this time is for obvious reasons very limited. In contrast, long-time memory can store much larger quantities of information, and the period during which the information can be memorised can even take a life span.

Long-time memory is composed of two different categories, procedural and declarative memory (Tulving, 1987). Procedural memory stores skills and procedures such as for example “knowing how to ride a bicycle”. It is also known as implicit or unconscious memory. Declarative memory is divided into semantic and episodic memory. Semantic memory stores abstract and theoretical information such as “knowing the name of Serge’s dog”. On the other hand, episodic memory is defined by the ability to memorise information that is linked to context related information, such as for example times, places and emotions (Tulving, 1987 #15). In literature, episodic memory is defined as a trait that depends on consciousness, and is therefore not found in nematodes (Perner and Ruffman, 1995). For this reason, the term “episodic-like memory” was defined (Zentall et al., 2001).

Another term that is closely linked to memory is learning. Learning relies on the acquisition of different types of knowledge supported by perceived information. It is defined as the process that produces memorised knowledge.

There are different types of learning. Habituation for instance, is an example of non-associative learning that is the result of a progressive diminution of behavioural responses to a defined stimulus. In conclusion, habituation is the moment at which responding ceases since the stimulus is neither rewarding nor harmful.

Another type of learning is associative learning. As the word already gives away, this type of learning principle is based on the assumption that stimuli and experiences reinforce one another and can be linked to enhance the learning process. In accordance, associative learning is limited to learning that occurs through conditioning.

Memory performance and the basis of learning are phenomena that are not profoundly understood so far, even less on a molecular level.
Nevertheless, modern research has identified two mechanisms that are believed to underlie learning and memory at the cellular level. Long-term potentiation is defined as an increase in the strength of the connections between a set of neurons that results from stimulation (Cooke and Bliss, 2006). Neurons communicate via synapses, and because memory is believed to be stored by the different localisation of specific proteins within these synapses, long-term-potentiation (LTP) and its opposing process, long term depression (LTD) are widely considered to be the major cellular mechanisms that underlie memory formation (Cooke and Bliss, 2006).

1.2 Memory Studies in Worms

It is now widely accepted that *C. elegans* has evolved mechanisms that can be defined as memory performance (Ikeda et al., 2008; Mohri et al., 2005; Nuttley et al., 2001; Rose et al., 2003; Rose and Rankin, 2001). This leads to the striking advantage that genes that have been suggested to be involved in memory in humans can be tested functionally by experimental manipulation, during memory performance tests in nematodes.
In accordance, to test conserved candidate genes that are supposed to be involved in memory and learning, several methods were established over the past years. For example, long- and short-time memory, can be studied by exposing the worms to a specific stimulus, such as tapping the plate they inhabit. (Rose and Rankin, 2001). Using this method, habituation capabilities are tested.
In our laboratory, we studied the relevance of certain candidate genes by performing associative memory assays using olfactory and thermosensory starvation conditioning assays (Ikeda et al., 2008; Mohri et al., 2005; Nuttley et al., 2002; Nuttley et al., 2001).
We performed experiments based on olfactory starvation conditioning. The worms were tested for their ability to link a positive stimulus such as an odorant with a negative stimulus such as starvation, thereby reversing the attraction to the odorant.
The type of performance tested here is defined as associative learning.

1.3 CLSTN an Identified Molecular Factor of Memory

Performing a genome-wide screen in humans based on a new high-density genotyping approach based on more than 500'000 single-nucleotide polymorphisms (SNPs) and performing a verbal memory task, candidate genes involved in human episodic memory were identified (Papassotiropoulos et al., 2006). To confirm the relevance of genes that were suggested to be involved in memory, we tested some candidates in the worm.

Previously, in this manner, CLSTN2 (encoding calsyntenin 2) was tested in our laboratory (Papassotiropoulos, 2006 #1, Hörndli; unpublished results). Furthermore the causal relationship between *calsyntenin* (the homologue of CLSTN2) function and memory was demonstrated by performing an associative learning assay (Nuttley, 2002 #30; Nuttley, 2001 #29).

CLSTN2 has been identified as a novel postsynaptic protein that is involved in the modulation of synaptic transmission (Hintsch et al., 2002). It is a type I transmembrane protein with two extra cellular calcium-binding caderin domains and two intracellular kinesin-light chain binding domains (Hintsch et al., 2002; Konecna et al., 2006). These domains are conserved in all three calsyntenin familiy members of vertebrates and the ortholog of invertebrates. Sequence alignment of members of the three vertebrate Calsyntenin members with the invertebrates calsyntenin have shown that the only *C. elegans* homolog CASY-1 is most closely related to CLSTN2. In *C. elegans, Casy-1* is expressed in the interneurons of the nerve ring and in the ventral cord motorneurons, whereas *Casy-1* is widely expressed in the nervous system of higher organisms

1.4 Glutamate Receptors and Memory

Glutamate receptors are a class of heteromeric ligand-gated ion channels that mediate the majority of the excitatory neurotransmission in the vertebrate central nervous system (CNS).

These transmembrane proteins can be classified on the basis of their pharmacological specificities by joining the N-methyl-D-aspartate (NMDA) or the non-NMDA class. In *C. elegans*, 10 putative ionotropic GluR subunits are known (Brockie et al., 2001a; Brockie et al., 2001b). GLR-1 to GLR-8 are members of the non-NMDA class.

The most intensively studied subunit in *C. elegans* is GLR-1. GLR-1 was identified as playing a role in many processes such as foraging behaviour (Hills et al., 2004), backing response (Maricq et al., 1995) avoidance of octanol (Chao et al., 2004) and long-term memory in habituation, examined performing tapping experiments (Rose et al., 2003). Surprisingly, *glr-1* deficient animals showed no defect in short-time memory for habituation but only in long-time habituation (Rose et al., 2003).

In addition, it has further been suggested that GLR-1 may be involved in associative memory in *C. elegans*, by performing associative memory assays with *glr-1* deficient animals (Hörndli, unpublished results).

One possible explanation for the similarity of the associative memory phenotypes of *glr-1* and *casy-1* defective worms is the involvement of CASY-1 in the regulation of synaptic function, localisation, or transport of glutamate receptors.

This is supported by the results obtained when expressing high levels of GLR-1 in *casy-1* deficient animals. The *casy-1* behavioural phenotype could be rescued by overexpression of *glr-1,* suggesting that the overexpression overcomes the mislocalisation of GLR-1 caused by the loss of CASY-1. (Hörndli, unpublished results).

Studies in vertebrates and *C. elegans* suggest that PDZ domain proteins such as *lin-10* are involved in proper localisation and stabilisation of ionotropic glutamate receptors like GLR-1 at the postsynaptic density (Kim and Sheng, 2004; Sheng and Sala, 2001)Rongo, 1998 #57).

CLSTN1 and CLSTN2 form a complex with the MINT2/X-11-like neuronal adaptor protein at the plasma membrane of neurons (Araki et al., 2003). The *C. elegans* ortholog of Mint2 is encoded by *lin-10* a PDZ and PTB domain protein (Kaech et al., 1998). Loss of function of *lin-10* causes a defect in the clustering of the glutamate receptor subunit GLR-1 at the synapses of ventral cord motorneurons and apical mislocalisation of the EGF receptor LET-23 in the vulval precursor cells (VPCs) (Kaech et al., 1998; Rongo et al., 1998). Mutations in the carboxyl-terminal PDZ domains prevent LIN-10 from regulating GLR-1 localisation in neurons. LIN-10 mutations defective in GLR-1 localisation lead to a diffusely distributed GLR-1 localization unlike the punctate GLR-1 distribution that is normally observed in wild-type animals. The vertebrate ortholog Mint2 can assume the function of LIN-10 for neuronal GLR-1 localisation (Glodowski et al., 2005). Like *glr-1* mutant animals, *lin-10* mutant animals are defective for the nose touch response. However, so far no

phenotypes other than the defective nose touch response have been described for the neuronal activity of LIN-10 in the literature (Rongo et al., 1998).

1.5 Olfaction

During evolution, *C. elegans* has developed a potent olfactory system in order to track down food, to distinguish for example, between high quality or low quality bacteria, to avoid noxious conditions and to mate (Bargmann et al., 1993; Bargmann and Horvitz, 1991). In addition, through unfortunate encounters, *C. elegans* can learn to associate the smell of low quality bacteria with their toxicity in order to avoid them in the future (Ikeda et al., 2008).

The sensory system of *C. elegans* comprises two groups of neurons, the amphid and the phasmid neurons, both built for sensing water soluble and volatile chemicals (Melkman and Sengupta, 2004).

The phasmid neurons are found in the tail of the animal, whereas the amphid neurons are localised in the pharynx of the animal. The dendrites of these neurons innervate the tip of the nose of the animal and their axons form connections with other neurons in the pharynx, thus making a part of the nerve ring (Bargmann and Kaplan, 1998). In general, chemosensory neurons build bilaterally symmetric pairs in which the left and right members of each class are structurally similar.

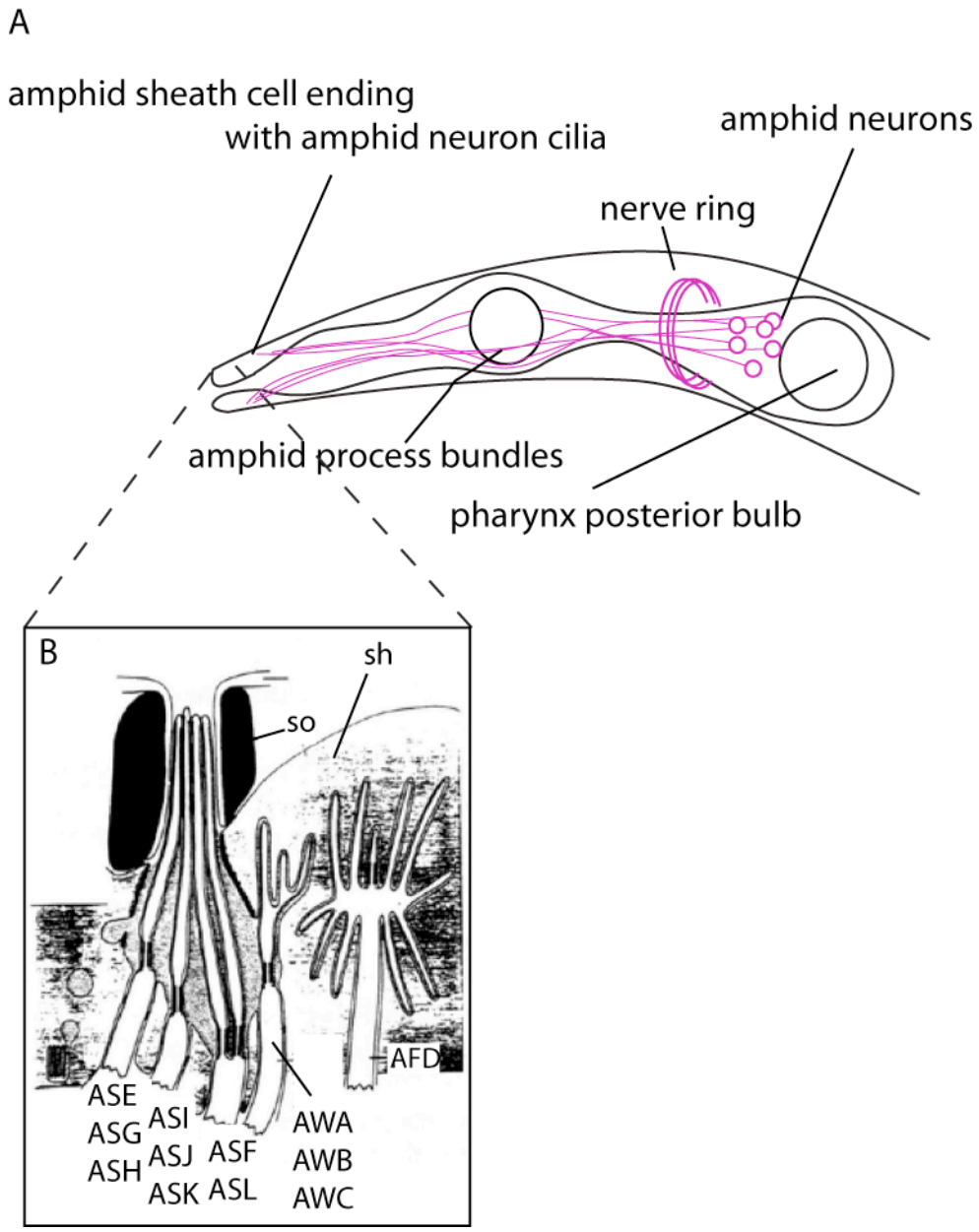

Figure 1. Schematic representation of the amphid chemosensation system (A) Disposition of the amphid chemosensory neurons. Anterior is to the left. (B) Detailed structure of the amphid sensory opening showing the socket (so), sheath (sh), and ciliated nerve endings. AWA, AWB, AWC, and AFD endings are buried in the sheath and not exposed through the amphid pore (adapted from Perkins et al (1986). Anterior is up.

The amphid neurons sense a variety of different cues. There are 12 classes of amphid neurons, some of which are mentioned below (Perkins et al., 1986). While the ASE, ASG, ASH, ASI neurons sense water soluble cues (gustatory), the AWA the AWB and the AWC neurons sense volatile cues (olfactory). Finally, the AFD neurons sense temperature changes (see Fig.1).

In accordance, volatile attractants such as isoamylalcohol, diacetyl, benzaldehyde and trimethylthiazole are sensed by AWA and AWC neurons. This also shows that AWA an AWC neurons share a partially overlapping function in sensing diacetyl and isoamylalcohol (Bargmann et al., 1993). Furthermore, the AWB neurons are involved in sensing volatile repellents as octanol and nonanol and the ASE in responding to attractive salts (Bargmann, 1991 #66).

Besides sensing volatile repellents, the ASH neuron pair responds to mechanical stimuli and high osmolarity. Finally, the ADL neurons respond to both volatile and water soluble chemicals. Moreover, the chemosensory neurons connected to four pairs of interneurons and five pairs of motorneurons (C.Bargmann, unpublished).

Odorant receptors are responsible for the recognition of chemicals. Usually, odorant receptors are G-protein coupled receptors (GPCRs). The *C. elegans* genome encodes more than 1000 GPCRs. About 500 of them are predicted to encode chemosensory receptors. For example, *odr-10,* mutant animals have a specific defect in chemotaxis to diacetyl, a volatile chemical that attracts the worm. ODR-10 is expressed in the AWA neurons (Sengupta et al., 1996).

1.6 Aim of these Studies

The aforementioned results that were obtained in our laboratory, suggest stronlgy that CASY-1 could be involved in trafficking or in localisation of the glutamate receptor subunit GLR-1. It is suggested that GLR-1 localises to the postsynaptic densities by a receptor localisation scaffolding complex that includes LIN-10. Moreover, preliminary studies performed in our laboratory also suggested that *lin-10* deficient animals show a reduced ability to memorise in an associative manner.
Therefore, we wondered whether the scaffolding protein complex of LIN-10, LIN-2, and LIN-7 that are known to localise LET-23 EGFR basolaterally in vulval precursor cells are equally involved in GLR-1 localisation (Kaech et al., 1998). By performing chemoattractive dependent associative learning experiments in *C. elegans* with mutants of the genes mentioned above, we wanted to gain insight of their putative role in associative memory.

2 Results

2.1 Chemotactic Starving Conditioning in *C. elegans* - General Remarks

In these studies we analysed the effect on associative learning of GLR-1 and the candidate proteins LIN-10, LIN-2 and LIN-7. From preliminary results obtained in our laboratory, we hypothesized that these proteins could build a complex that would localise GLR-1 to the postsynaptic density of neurons, thereby contributing to associative memory in *C. elegans*.

Therefore, we tested the ability of worms from *lin-10*, *lin-7* and *lin-2* defective backgrounds to reverse their attraction to an odorant after associating this odorant with a negative stimulus such as starvation thus performing an assay for chemotactic starvation (Nuttley et al., 2002).

In accordance, the worms were starved for two hours on plates containing no food but a source of the odorant diacetyl in a pure form at the cover (see Fig. 2). After washing the animals to liberate the animals from traces of diacetyl, we tested for their ability to associate the negative experience of starvation with the odorant.

Thus, about 100 to 150 worms were transferred to a central line on an empty plate containing a diacetyl source (0.1%) at the border of the plate and an ethanol source (used to dissolve the diacetyl) opposite of the diacetyl source. Both sources also contained traces of sodium azide, a metabolic inhibitor used to anesthetise the worms (Massie et al., 2003).

After one hour, the different plates containing previously conditioned or unconditioned worms were compared corresponding their distribution on the plates and the worms were counted and the chemotactic and learning index were calculated (see methods).

While the unconditioned wild-type worms were very keen on diacetyl and therefore straightly crawled to the diacetyl source, the conditioned animals had lost their interest in the chemical due to their ability to link the negative stimulus of starvation with diacetyl, an aptitude that is defined as associative learning. However, animals containing a mutation that cancelled associative learning would not be able to associate the two stimuli and were still attracted, at least to a certain extent, by diacetyl.

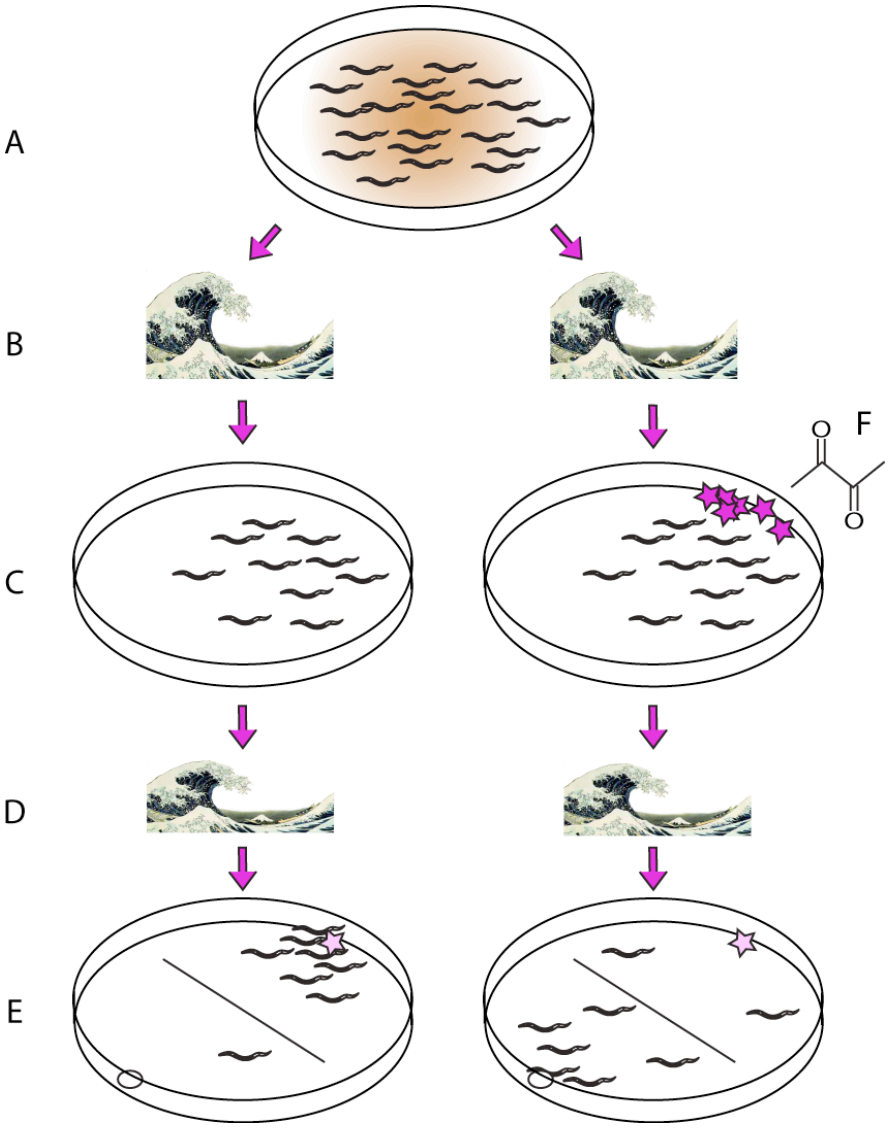

Figur2. Schematic representation of the chemotactic memory assay. Adult hermaphrodites on food (A) are washed to deliberate the worms from traces of bacteria and to starve them (B). (C) The worms are conditioned on without bacteria. One plate has a patch with pure diacetyl (pink stars) on the top of the lid (Glodowski et al.). The other plate (left) contains no odorant. (D) The worms are washed to deliberated them from traces of diacetyl. (E) Chemotaxis assay; wild-type worms that have been conditioned with diacetyl avoid the source of 0.1% diacetyl (light pink star) dissolved in ethanol. They rather crawl to the control spot source (empty circle) (Glodowski et al.), whereas the worms that were starved without diacetyl are strongly attracted by the odorant. (E) chemical structure of diacetyl. The "Great Wave off of Kanagawa" by Katsushika Hokusai represents the washing steps.

There are some general points that have to be kept in mind in order to achieve satisfying results with this assay.
First, the humidity of the plates used for the experiments and the atmosphere might play a role in that the worms are able to sense the attractive chemical. Second, the worms should not be starved before starting the assay. Third, testing mutant strains, the locomotory and the sensory abilities of the worms should be examined before performing the memory assay. Moreover, it might be of advantage to change to a new source diacetyl, in case the experiments do not work.
Lastly, the original manual suggests washing the worms twice in M9 buffer, followed by two washing steps of 20mins. I washed the worms longer and exchanged the M9 buffer more often (see methods) such as to completely remove remaining traces of food from the worms, to synchronise and starve them already before the actual starvations experiment (see Fig. 2). In addition, I increased the conditioning time from one hour to two hours. The disadvantages of this change are commented in the discussion. In the methods part, the protocol that I used for the further examination of the mutant strains is described.
The results displayed hereafter all derive from experiments performed with 100 to 150 worms per plate. The calculation of the chemotactic index was calculated as follows: Chemotactic index (CI)=((N worms at diacetyl)-(N worms at ethanol))/(N total number of worms). Learning index (LI) =(CI naïve worms)-(CI conditioned worms)/(CI naïve worms)*100.

2.2 GLR-1 is Involved in Associative Memory in *C. elegans*

I reproduced Frédéderic Hörndli's Data obtained with *glr-1(n2461)* mutants (see graph1/2). The experiment was performed on three different days. Every day the worms were analysed for chemotaxis on three independent chemotaxis plates. Thus, the results were obtained from nine independent chemotaxis experiments. The *glr-1(n2461)* defective worms show a slight chemosensory defect as their chemotaxis index is at 0.52 in contrast to control wild-type animals that have chemotaxis index of 0.8. Nevertheless, studying the results obtained from conditioned worms, the difference between the chemotaxis index of the *glr-1(n2461)* mutants (0.29) and the chemotaxis index from wild-type animals (0.008), shows a clear memory defect of

glr-1(n2461) defective animals. The learning index form wild-type animals is at 99% and the learning index of *glr-1(n2461)* mutants is at 42%.

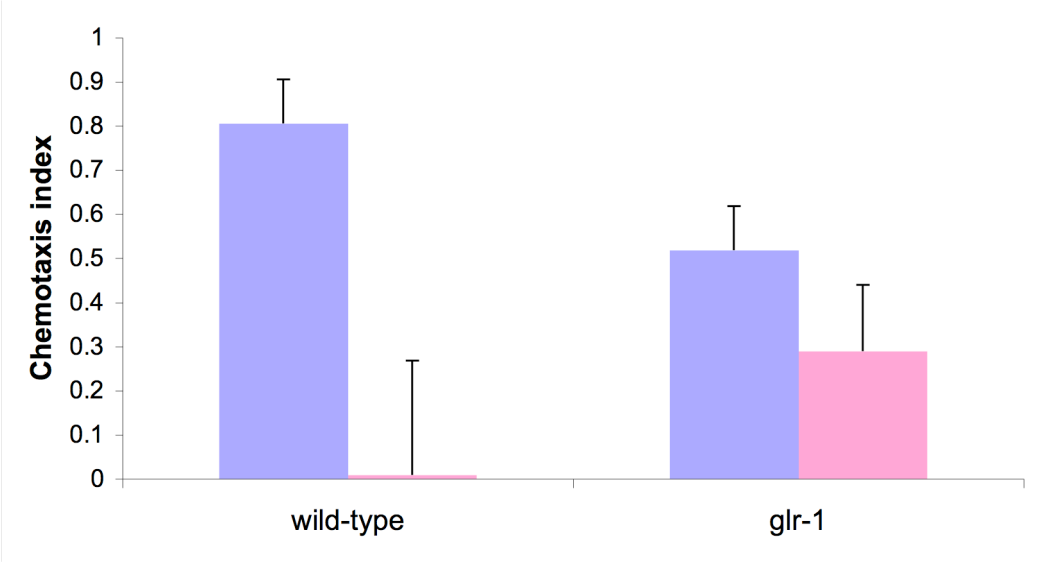

Graph 1. Comparison of diacetyl starving conditioning performance of wild-type and *glr-1*(n2461) animals. The chemotaxis index was calculated as (CI)=((N worms at diacetyl)-(N worms at ethanol))/(N total number of worms). The experiment was performed three times in triplicates (N=9), the amount of worms is 100<n<150. Blue defines the results form unconditioned worms and pink defines the results from conditioned worms. Error bars indicate the standard error of mean.

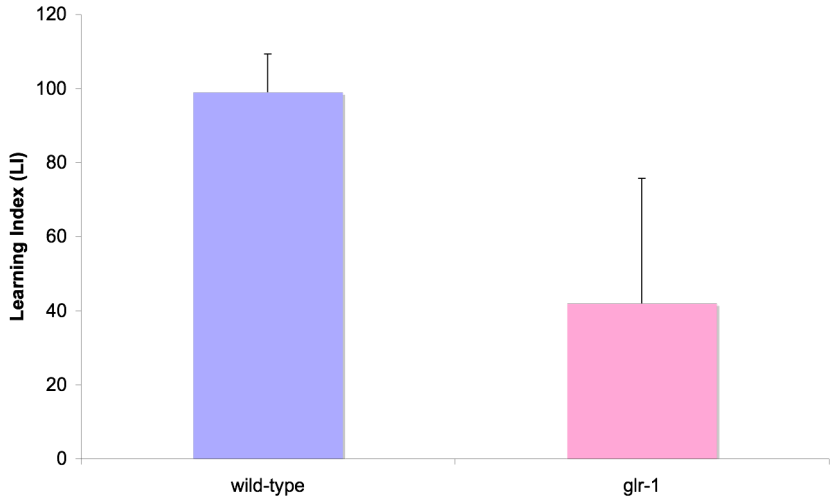

Graph 2. Comparison of diacetyl starving conditioning performance of wild-type and *glr-1*(n2461) animals. The learning index was calculated as Learning index (LI) =(CI naïve worms)-(CI conditioned worms)/(CI naïve worms)*100. The experiment was performed three times in triplicates (N=9), the amount of worms is 100<n<150. Blue defines the results form unconditioned worms and pink defines the results from conditioned worms.

2.3 The Candidate Proteins LIN-10, LIN-7 and LIN-2

To examine the effect on associative learning of LIN-10, LIN-2 and LIN-7, *lin-10(n1439) lin-7(n1449)* and *lin-2(n397)* animals were submitted to a chemotactic learning assay. The experiment was performed on three different days for each mutant. Every day, the conditioned worms were analysed for chemotaxis on threindependent chemotaxis plates. Thus, results originate from nine independent chemotaxis experiments, performed on three different days in parallel.

To test *lin-7(n1449)* defective animals, the experiment was performed in contrast to previous experiments on two different days only. On both days, the conditioned worms were analysed for chemotaxis on three independent chemotaxis plates. Thus, the results origin from six independent chemotaxis experiments.

Note, that in my hands, cd synchronized for conditioning experiments were not as accurately synchronized as wild-type worms. While most animals reached adulthood

by the expected time, others had reached L4 or sometimes even less. I did not count the animals that had not reached adulthood.

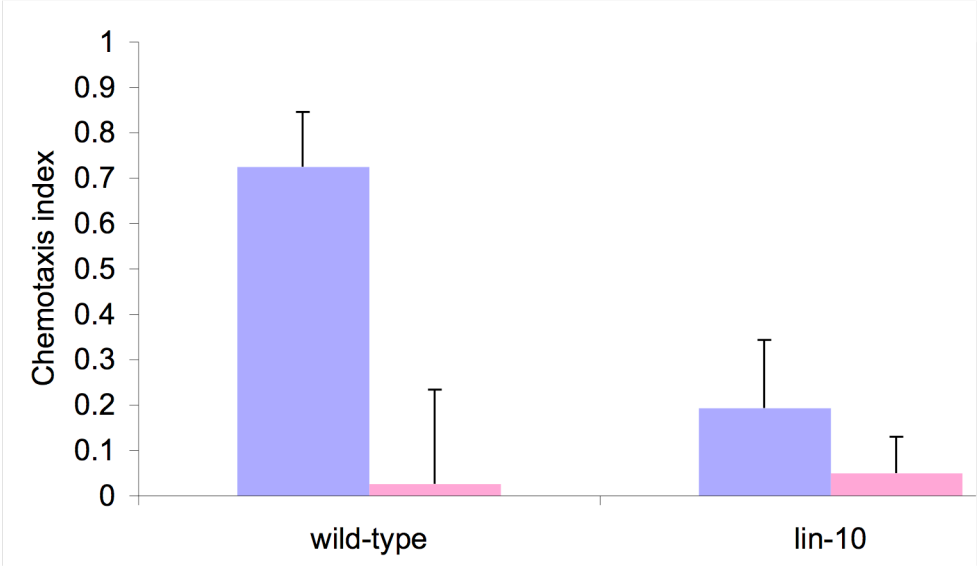

Graph 3. Comparison of diacetyl starving conditioning performance of wild-type and *lin-10(n1439).* Scoring and quantifications were done as described in graph legend 1. Blue defines the results form unconditioned worms and pink defines the results from conditioned worms.

In these studies, the unconditioned *lin-10(n1439)* defective worms displayed a strong chemosensory defect since their chemotaxis index is of 0.19. This result is in contrast to control wild-type animals that exhibit a chemotaxis index of 0.72. However, conditioned *lin-10(n1439)* defective animals showed a chemotaxis index of 0.05 that is higher than the results obtained with conditioned wild-type worms (0.03).

lin-2(n397) animals were also less attracted to diacetyl. While the wild-type control animals had an chemotactic index of 0.73 in this experiment, the index obtained by *lin-2(n397)* mutants reached 0.25. Conditioned wild-type animals had a chemotaxis index of 0.02 whereas the conditioned *lin-2(n397)* animals showed an index of 0.04.

Similar results were obtained with *lin-7(n1449)* defective worms. Unconditioned *lin-7(n1449)* defective worms seem to have a very strong chemosensory defect as their chemotaxis index is at 0.05 in contrast to the control wild-type animals that showed a

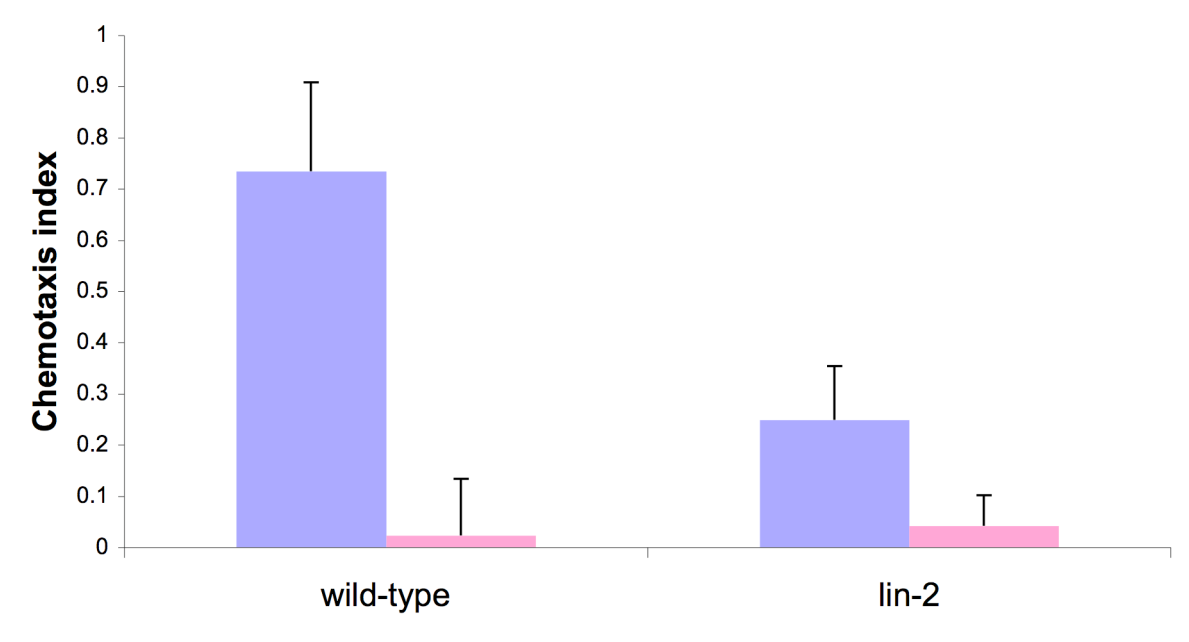

Graph 4. Comparison of diacetyl starving conditioning performance of wild-type and *lin-2(n397)* animals. Scoring and quantifications were done as described in graph legend 1 Blue defines the results form unconditioned worms and pink defines the results from conditioned worms.

chemotaxis index of 0.82 in this case. Conditioned *lin-7(n1449)* defective animals show a chemotaxis index of 0.1 that is higher than the results obtained with conditioned wild-type worms (0.04).

Confusingly, the results obtained with conditioned *lin-7(n1449)* mutants indicate an increased interest in diacetyl in contrast to unconditioned worms. This is the exact opposite of the expected outcome. However this finding must be moderated by the fact that these animals have a very reduced capacity of sensing the cue diacetyl.

Since *lin-10(n1439)* *lin-7(n1449)* and *lin-2(n397)* worms show already a defect in chemosensory, I the learning index of these strains was not investigated.

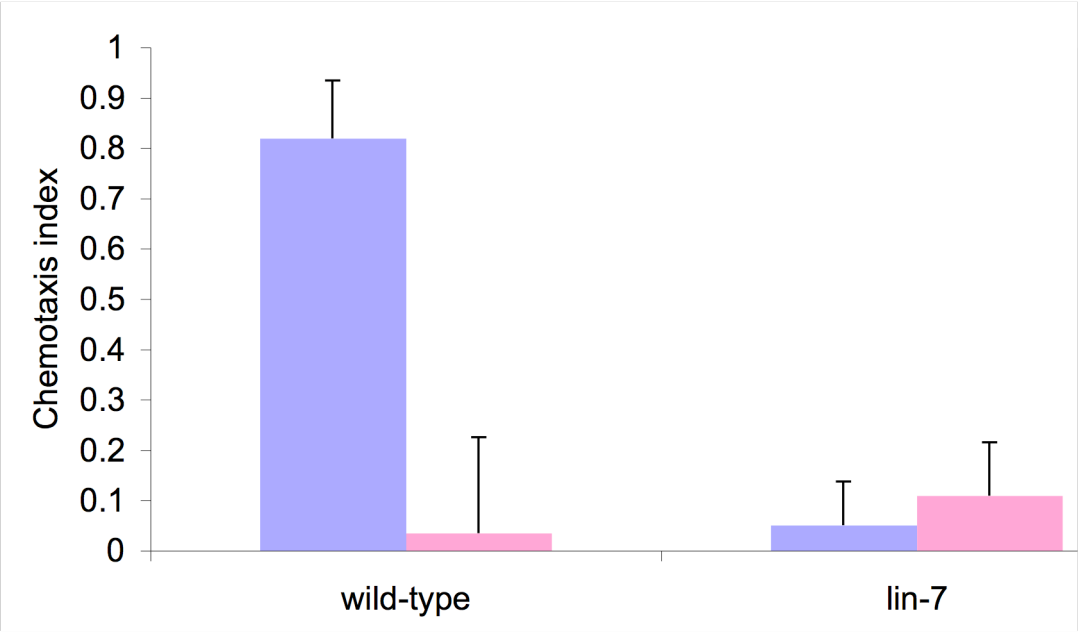

Graph 5. Comparsion of diacetyl starving conditioning performance of wild-type and *lin-7 (n1449)* animals. N=6, 100<n>150. Scoring and quantifications were done as described in graph legend 1. Blue defines the results form unconditioned worms and pink defines the results from conditioned worms.

3 Discussion

Recently, it was shown in our laboratory that *casy-1* and *glr-1* mutated worms exhibit a defect in associative memory (Fred Hörndli, unpublished results).

Moreover, moreover Rongo et al. showed that LIN-10 contributes to the receptor localisation complex that is involved in glutamate receptor localisation during associative learning in *C. elegans* (Rongo et al., 1998).

It is known that LIN-10, a PDZ domain protein interacts with GLR-1 in neurons of *C. elegans*, but so far, it remains to be elucidated in what specific processes both proteins are interacting with each other. Furthermore, it was identified that LIN-10, LIN-7 and LIN-2 form a complex that mediates basolateral membrane localization of the *C. elegans* LET-23 EGF receptor in vulval epithelial cells.

Based on this knowledge, LIN-2, LIN-7 and LIN-10 were examined for their involvement of GLR-1 localisation in a specific role during associative learning.

Unlike *glr-1* defective worms*,* worms defective for *lin-10, lin-2* and *lin-7* seem to have a very strong chemosensory defect.Whereas the chemosensory index of wild-type animals is usually around 0.8, the chemosensory index of *glr-1(n2461)* defective worms is at 0.52, which is reduced but to such an extent as is seen in *lin-10(n1439)* defective worms. *lin-10(n1439)* have a chemotactic index of 0.19, *lin-2(n397)* a chemotactic index of 0.25 and *lin-7(n1449)* a chemotactic index of 0.05.

In conclusion, due to the strong diacetyl dependent chemotactic phenotypes, an additional role in associative learning could not been examined.

Nevertheless, this suggests that LIN-10/LIN-7 and LIN-2 are involved in the establishment of olfaction. I propose three different models to explain the observed phenotype.

First of all, the proteins might belong to the scaffolding protein complex that localises ODR-10. ODR-10 is a GPCR protein that specifically senses diacetyl (Sengupta et al., 1996). ODR-10 receptor is specifically expressed in the AWA neurons (Sengupta, 1996 #59; Brenner, 1974 #146).

Second, the general functionality of the AWA neurons might be dependent on LIN-10, LIN-2 and LIN-7, but not only by their specific involvement in the localisation of ODR-10 There might be other proteins that are dependent on such a protein complex to establish the functionality of the AWA neuron.

Finally, there might be a role for LIN-10, LIN-2 and LIN-7 in recruiting proteins that are involved in establishing the overall functionality of sensory neurons.

To sort out the different models, and define the specificity of the proteins, *lin-10, lin-2* and *lin-7* defective animals should be examined for their ability to sense other chemicals then diacetyl such as benzaldehyde and trimethylthiazole. Benzaldehyde trimethylthiazole are diacetyl are recognised by receptors expressed in AWA neurons.

If *lin-10*, *lin-2* and *lin-7* defective animals can sense these two chemicals, this would suggest that the problem is diacetyl and ODR-10 specific. In contrast, if the two additional odorants are not recognised by the above-mentioned mutants, this would point to an indirect involvement of LIN-10, LIN-2 and LIN-7 in the establishment of the general functionality of the AWA neurons.

Moreover, the *lin-10, lin-2* and *lin-7* mutants could be tested for sensing chemicals that are recognised by different neurons, such as for example, the AWB neurons. AWB neurons allow the animals to sense different chemicals such as octanol and nonanol.

If *lin-10, lin-2* and *lin-7* mutant animals exhibit defects in sensing octanol, the AWA specificity is ruled out and a rather broad role of the three proteins in neuron functionality would be suggested.

Unfortunately, olfaction defect of these mutants makes it impossible to study memory based on diacetyl sensing assays. To circumvent this problem, different associative learning experiments such as thermotaxis assays should be performed to further explore the role of these proteins in memory.

Another suggestion that might explain the results of the chemotaxis assays with *lin-10*, *lin-2* and *lin-7* defective animals is that the effect does not result form an inability to sense the attractive source but simply results form a locomotor defect. This implies that the animals cannot reach the source of diacetyl due to the unlaid eggs that cripple them (see explanation below).

In effect, as was mentioned before, LIN-10, LIN-2 and LIN-7 are involved in basolateral membrane localization of the *C. elegans* LET-23 EGF receptor in vulval precursor cells, key actors of vulval induction (Kaech et al., 1998). As a result, *lin-2,* and *lin-7*, *lin-10* animals have a defective vulval development that results in a vulvaless (Vul) phenotype. This leads to a severe egg-laying defect. The developed

eggs accumulate and eventually even hatch inside of the mother's body. It is known that old animals with an accumulation of eggs are hampered in their movements.
Nevertheless, an argument that states against this explanation is that the experiments were performed with young animals. Young animals carry only a few eggs and their locomotion is not visibly disturbed. More striking, after one hour of incubation time, the young mutants were found to spread uniformly on the plate, able to reach any position.
As a precautionary measure, nonetheless, *lin-10*, *lin-2* and *lin-7* defective worms should be tested for their general locomotory capabilities (bends per minute in liquid).
In case that the worms display a locomotory defect the problem I suggest that the problem could be circumvented by rescuing the vulval specific phenotype in a cell type specific manner.
In addition I suggest that the difference between a loss of associative learning and a habituation defect should be examined when working with mutants.
To do so, the strains are exposed to diacetyl in the presence of food instead of conditioning the animals on plates with diacetyl under starvation conditions. If the mutants and the wild-type animals show a similar chemotaxis index in contrast to the starved mutated animals, the results would suggest that the mutant strain is not defective for habituation.
In our laboratory, animals defective for *glr-1* have not been tested for an additional habituation defect so far. Nevertheless, *glr-1* defective worms were identified in other laboratories as exhibiting a habituation phenotype by performing tapping experiments (Rose et al., 2003). It would be interesting to examine whether the *glr-1* mutants are defective in habituation in an experiment such as I described or whether the phenotype is tap specific.

An important point that should be discussed here is the change of the conditioning time from one to two hours, as was already mentioned in the results.
Recently, it has been speculated that if the worms are conditioned during a longer period the results of the mutant strains change. We speculated that despite the fact that our mutants had a defect in memory performance, they would be able to memorise more efficiently in two hour than in one due to the increased length of the stimuli. Nevertheless the assays that I performed with the *glr-1* deficient worms with a conditioning time of two hours gave similar results to those performed by Frederic

Hörndli in which the animas were conditioned only for one hour, thereby stating against our previous assumption.

I suggest that these experiments should be carried in parallel with different incubation times at least once, in order to distinguish whether doubling the incubation time from one to two hours, does in fact result in increased memorisation in the mutants.

In summary, due to a chemosensory defect, the associative memory performance of the mutants *lin-10*, *lin-2* and *lin-7* could not be addressed by the method employed. Moreover, the used method is not reproducible enough in our laboratory to obtain trustful results. Other assays such as salt chemotaxis learning should be used instead (Ikeda et al., 2008).

Finally, as a last remark, CLSTN2 was identified to be involved in episodic memory in human and its homolog CASY-1 then tested for its involvement in associative learning in the worm.

It is interesting to mention here that there is a difference between associative and episodic memory described in literature (Zentall et al., 2001). Here are two examples that described the difference: If I see a friend and ask him unexpectedly what he had for dinner last night, he reflects searching for the episode to answer (episodic memory). If I ask him the same question every morning, he already associates during the dinner what he will answer the next day. This would be more an example for semantic or associative memory. Furthermore, episodic memory is defined as a trait that depends on consciousness, and is therefore not found in nematodes (Perner and Ruffman, 1995).

It seems clear to everyone that the worm has probably not such an evolved system to memorise things and emotions and it is not wrong to test candidates for episodic memory in worms performing experiments that are test associative memory. Nevertheless, the limits to study episodic memory in the worm also display a general limit of the use of the worm studying more profound details in memory performance in human.

4 Material and Methods

4.1 Strains and general methods

For maintaining and manipulating, *C. elegans*, standard methods were used (Brenner, 1974). Unless otherwise mentioned, the variety Bristol, strain N2 was used as the wild-type reference strain. The experiments were all performed at 20° C.

4.2 Genes and Alleles used in this Project

LGI *lin-10(n1439)*I
LGII *lin-7(n1449)*II
LGIII *glr-1(n2461)*III
LGX *lin-2(n397)*X

4.3 Pouring the Conditioning and Chemotaxis Plates (CTX plates)

The chemotaxis and conditioning plates were prepared at least three days in advance to ensure ideal dryness of the plates.

CTX agar:
20g agar
1 L ddH_20
5ml 1M KPO_4^-
1ml 1M $MgSO_4$
1ml 1M $CaCl_2$

The agar and water were autoclaved together, while the 1M solutions (KPO_4^-, $CaCl_2$ and $MgS0_4$) were autoclaved separately and added to the dissolved agar once it reached ~50°C. 20ml CTX agar solution was poured in Petri dishes (10cm diameter). The accuracy here is possibly of importance. The plates were left to dry 3 days at room temperature on the bench prior to the conditioning and chemotaxis assay.

4.4 Synchronising the Worms by Bleaching

Worms were washed from 4 to 6 small plates with a mixed population containing many adults into a 13ml Falcon tube by using M9 buffer. They were settled by centrifugation and the liquid supernatant was discarded to reduce the volume to 3ml H_2O. 1ml 1.5% hypochlorite and 1ml 2M NaOH is added, the tube was manually shaken for 10mins or until the adult worms had bleached away and only the eggs were visible. Next, the worms were centrifuged down for 1min at 2000 rpm. The supernatant was discarded and the worms were washed once by refilling the tube with sterile M9 and repeating the centrifugation step. The M9 was discarded and the worms were dispensed on empty CTX plates without food. The eggs hatched over night and the L1 worms were collected the next day, by washing them from the empty plates with sterile M9. The period over night should not be less then 13 hours to obtain synchronised L1 animals. The L1 animals were collected in a Falcon tube and were spun down and distributed on 10-20 plates containing much OP50. It is important not to create a dense worm population to avoid that the worms eat all *E.coli* before having reached adulthood. Starved worms are not optimal for good results. The animals were let growing at 20° C for three days to reach adulthood.

4.5 Conditioning the Worms

The synchronised worms were washed from the plates with M9 and collected in 50ml glass tubes. They were settled by gravity, taken off the tube with Pasteur pipettes and transferred in a second 50ml glass tube filled to the brim with M9. While the worms settled in the second tube, the first was emptied and filled up again with M9 for the third washing round. After five rounds, the tubes were sealed with Parafilm, manually shaken and shaken on the table shaker for about five minutes to release them from all the traces of bacteria and to starve them. After this step, the worms were transferred again to a new tube and the shaking step is repeated. In summary, the worms were transferred seven times to fresh M9 during 70mins. While keeping the washing time 70mins, the shaking during was most probably more monkey business then anything else.

After the last washing step, the worms were transferred to a empty tube and the worm density was adjusted to 8000 worms/ml of M9 before plating 0.3 ml on each plate. This step was carried out under the aspiration hood. Two plates per tested

strain were prepared: one for the control experiment and one for the conditioning experiment. The worms were dispensed to the plates synchronously taking care to spread the liquid to maximum. The control worm plates were sealed with paraffin and removed from aspiration hood. 2µl of pure diacetyl was dispensed on a small Whatman paper slip attached to the lid of the conditioning plate using double faced adhesive tape. To avoid every contact of the pipette with diacetyl, filtered tips were used. The plates were sealed with Parafilm and taken out of the hood. The worms were left in the conditioning plates for 2hrs at room temperature. Note that in the classical manuals for conditioning, the worms were incubated for 1hr for conditioning (personal communications with Frederic Hörndli).

4.6 Chemotaxis Assay

During the conditioning step, the chemotaxis testing plates were prepared and the diluted diacetyl was prepared. The diacetyl dilution was prepared by serial dilutions to obtain an accurate result. First, 10µl pure Diacetyl was dissolved in 90µl 100% EtOH and mixed. From this dilution, 10µl were dissolved further in 990µl 100% EtOH.
3 day old CTX plates were drawn using a mold so that 1cm radius circles 6cm equidistant from the center of the plate and a middle line were drawn. The following steps were performed under the aspiration hood.
The worms were washed down from the conditioning plates with ddH_20 and 15ml glass tubes were filled to 10ml with ddH_20. The worms were left to settle by gravity. This procedure was repeated once to wash traces of chemoattractant from the worms. After the last wash step, the liquid was discarded remaining diluted worms of a concentration of 2000 worms/ml in the glass tube.
5 mins before the worms were plated on the chemotaxis plates, 1µl of 1M sodium azide was added to the middle of both circles on all plates.
Just before plating the worms, 2µl 100% EtOH and 2ul 0.1% diacetyl dissolved in EtOH were added to the specified circles.
50µl of prepared worm suspensions were distributed to the line in the middle of the plates and the plates were closed. The liquid was dispensed along the middle line to speed up the worm release from liquid medium. The worms were incubated to migrate for 1hr at room temperature.

4.7 Counting the Worms

After 1hr incubation time at room temperature, the worms were counted. The worms in the circles or with rigor appearance outside the circle are counted for either chemo attractant or control attraction.
The worms elsewhere on the plate were counted as neutral. This step has to be accomplished as fast as possible, due to a difference of incubation time of the different plates.
After counting, the following formulae were used to calculate the chemotactic index and the learning index of the mutants.

Chemotactic Index (CI) = (N attractant-N EtOH)/N TOTAL

Learning Index (LI)= =((CI naïve-CI conditioned)/CI naive)*100

Generally, the used memory assays seem to be very tricky to establish, the variability of the results is high and often not considered being statistically significant concluding that there has to be investigated much of time to establish the assays under stable conditions such as stable temperature, light factor and even air humidity. I suggest that stable conditions are applied during growth of the worms and kept stable during the experiments themselves. Further, the plates are suggested to be poured not manually to avoid small differences and should be stored as well under stable conditions. These provisions might help to reduce the variability.

5 References 2

Araki, Y., et al., 2003. Novel cadherin-related membrane proteins, Alcadeins, enhance the X11-like protein-mediated stabilization of amyloid beta-protein precursor metabolism. J Biol Chem. 278, 49448-58.

Bargmann, C. I., et al., 1993. Odorant-selective genes and neurons mediate olfaction in C. elegans. Cell. 74, 515-27.

Bargmann, C. I., Horvitz, H. R., 1991. Chemosensory neurons with overlapping functions direct chemotaxis to multiple chemicals in C. elegans. Neuron. 7, 729-42.

Bargmann, C. I., Kaplan, J. M., 1998. Signal transduction in the Caenorhabditis elegans nervous system. Annu Rev Neurosci. 21, 279-308.

Battu, G., et al., 2003. The C. elegans G-protein-coupled receptor SRA-13 inhibits RAS/MAPK signalling during olfaction and vulval development. Development. 130, 2567-77.

Brenner, S., 1974. The genetics of Caenorhabditis elegans. Genetics. 77, 71-94.

Brockie, P. J., et al., 2001a. Differential expression of glutamate receptor subunits in the nervous system of Caenorhabditis elegans and their regulation by the homeodomain protein UNC-42. J Neurosci. 21, 1510-22.

Brockie, P. J., et al., 2001b. The C. elegans glutamate receptor subunit NMR-1 is required for slow NMDA-activated currents that regulate reversal frequency during locomotion. Neuron. 31, 617-30.

Chao, M. Y., et al., 2004. Feeding status and serotonin rapidly and reversibly modulate a Caenorhabditis elegans chemosensory circuit. Proc Natl Acad Sci U S A. 101, 15512-7.

Cooke, S. F., Bliss, T. V., 2006. Plasticity in the human central nervous system. Brain. 129, 1659-73.

Glodowski, D. R., et al., 2005. Distinct LIN-10 domains are required for its neuronal function, its epithelial function, and its synaptic localization. Mol Biol Cell. 16, 1417-26.

Hills, T., et al., 2004. Dopamine and glutamate control area-restricted search behavior in Caenorhabditis elegans. J Neurosci. 24, 1217-25.

Hintsch, G., et al., 2002. The calsyntenins--a family of postsynaptic membrane proteins with distinct neuronal expression patterns. Mol Cell Neurosci. 21, 393-409.

Ikeda, D. D., et al., 2008. CASY-1, an ortholog of calsyntenins/alcadeins, is essential for learning in Caenorhabditis elegans. Proc Natl Acad Sci U S A. 105, 5260-5.

Kaech, S. M., et al., 1998. The LIN-2/LIN-7/LIN-10 complex mediates basolateral membrane localization of the C. elegans EGF receptor LET-23 in vulval epithelial cells. Cell. 94, 761-71.

Kim, E., Sheng, M., 2004. PDZ domain proteins of synapses. Nat Rev Neurosci. 5, 771-81.

Konecna, A., et al., 2006. Calsyntenin-1 docks vesicular cargo to kinesin-1. Mol Biol Cell. 17, 3651-63.

Maricq, A. V., et al., 1995. Mechanosensory signalling in C. elegans mediated by the GLR-1 glutamate receptor. Nature. 378, 78-81.

Massie, M. R., et al., 2003. Exposure to the metabolic inhibitor sodium azide induces stress protein expression and thermotolerance in the nematode Caenorhabditis elegans. Cell Stress Chaperones. 8, 1-7.

Melkman, T., Sengupta, P., 2004. The worm's sense of smell. Development of functional diversity in the chemosensory system of Caenorhabditis elegans. Dev Biol. 265, 302-19.

Mellem, J. E., et al., 2002. Decoding of polymodal sensory stimuli by postsynaptic glutamate receptors in C. elegans. Neuron. 36, 933-44.

Mohri, A., et al., 2005. Genetic control of temperature preference in the nematode Caenorhabditis elegans. Genetics. 169, 1437-50.

Nuttley, W. M., et al., 2002. Serotonin mediates food-odor associative learning in the nematode Caenorhabditiselegans. Proc Natl Acad Sci U S A. 99, 12449-54.

Nuttley, W. M., et al., 2001. Regulation of distinct attractive and aversive mechanisms mediating benzaldehyde chemotaxis in Caenorhabditis elegans. Learn Mem. 8, 170-81.

Papassotiropoulos, A., et al., 2006. Common Kibra alleles are associated with human memory performance. Science. 314, 475-8.

Perkins, L. A., et al., 1986. Mutant sensory cilia in the nematode Caenorhabditis elegans. Dev Biol. 117, 456-87.

Perner, J., Ruffman, T., 1995. Episodic memory and autonoetic consciousness: developmental evidence and a theory of childhood amnesia. J Exp Child Psychol. 59, 516-48.

Rongo, C., et al., 1998. LIN-10 is a shared component of the polarized protein localization pathways in neurons and epithelia. Cell. 94, 751-9.

Rose, J. K., et al., 2003. GLR-1, a non-NMDA glutamate receptor homolog, is critical for long-term memory in Caenorhabditis elegans. J Neurosci. 23, 9595-9.

Rose, J. K., Rankin, C. H., 2001. Analyses of habituation in Caenorhabditis elegans. Learn Mem. 8, 63-9.

Sengupta, P., et al., 1996. odr-10 encodes a seven transmembrane domain olfactory receptor required for responses to the odorant diacetyl. Cell. 84, 899-909.

Sharma-Kishore, R., et al., 1999. Formation of the vulva in Caenorhabditis elegans: a paradigm for organogenesis. Development. 126, 691-9.

Sheng, M., Sala, C., 2001. PDZ domains and the organization of supramolecular complexes. Annu Rev Neurosci. 24, 1-29.

Tulving, E., 1987. Multiple memory systems and consciousness. Hum Neurobiol. 6, 67-80.

Zentall, T. R., et al., 2001. Episodic-like memory in pigeons. Psychon Bull Rev. 8, 685-90.

Zheng, Y., et al., 1999. Neuronal control of locomotion in C. elegans is modified by a dominant mutation in the GLR-1 ionotropic glutamate receptor. Neuron. 24, 347-61.

6 Acknowledgements

First of all, I would like to thank Prof. Dr. Hajnal for giving me the opportunity to do my PhD in his laboratory.
Further, I am grateful to the members of my thesis committee, Prof. Dr. Michael Hengartner, Prof. Dr. Urs Greber and Dr. Michel Labouesse for attending the meetings during my PhD to find new ideas and directions about my work.
A special thank goes to current and past members of the laboratory. I am really grateful about all the support during my PhD. Thanks a lot for all the joyful and happy hours we spent together the past four years, but also the time during the more difficult periods.
Thanks go also to Irene Hofmann for logistics and her smile and Raymond Grunder for sequencing my plasmids.
I wish further to thank Erika Fröhli, not only for technical support but also for the so many nice chats and discussions.
In addition, I would like to express my thanks to Charlotte Chaine. Lucky me, that Paris sent me such a congenial and clever summer student!
Further, I would like to mention Jonathan Audebourg that gave me a hand during my screening procedures and Alexandra Wegmann and Walther Haenseler for their help.
The quality of the thesis was greatly enhanced by Simon Restrepo, Juan Miguel Escobar-Restrepo, Ivo Rimann, Peter Gutierrez and also by Corina Freudiger, Tobias Schmid and Michael Walser correcting parts of the thesis thereby “endowing” me to hand in my thesis in time. ☺
Last but for sure not least, I would like to thank my parents, my brother Tobias and my friends for their support during the last four years. Thank you so much!!!!

Zürich, August 2008

7 Curriculum Vitae

Personal information

Last name:	VASSALLI
First names:	Sara Martina
Date of birth:	07.01.1978
Home town, Canton:	Riva San Vitale, TI
Country:	Switzerland

Education:

2004-2008	PhD student in the laboratory of Prof. Dr. Hajnal, University of Zurich, molecular life science (MLS) PhD program, University of Zurich and ETH Zurich, Switzerland
2003-2004	Master thesis (Diploma) in plant developmental genetics (Dipl. Bot.) University of Zurich, Switzerland in the laboratory of Prof. Dr. Ueli Grossniklaus under the supervision of Prof. Dr. Ueli Grossniklaus and Dr. Mark Curtis. Title: Activating Randomly Tagged Genes in Trichome Cells
1999-2003	Studies of Biology at University of Zurich, Switzerland Main subjects: botany; ancillary: phytochemistry.
1994-1999	Matura Typus D, (French, Italien and English), Kantonsschule Stadelhofen, Zürich, Switzerland.

Conferences:

2008	-European *C. elegans* meeting, Sevilla, Spain
2007	- International *C. elegans* meeting, Los Angeles, USA
2006	-3rd MLS retreat (Zurich Ph.D Program in Molecular Life Sciences), Candolin, Switzerland, 2006 -*C. elegans* Development and Evolution Meeting, Wisconsin-Madison, USA -European Worm Meeting, Hersonissos, Crete, Greece -2nd MLS retreat, Lenk, Switzerland
2005	-International *C. elegans* meeting, Los Angeles, USA
2004	-1st MLS, Einsiedeln, Switzerland

Publication:

Brand L, Horler M, Nuesch E, **Vassalli S**, Barrall P, Yang W, Jefferson RA, Grossniklaus U. Curtis MD (2006 Aug) A versatile and reliable two-component system for tissue-specific gene induction in Arabidopsis. ***Plant Physiol***. 4,1194-204

8 Appendix

FLP mapping data *zh68*(IV)

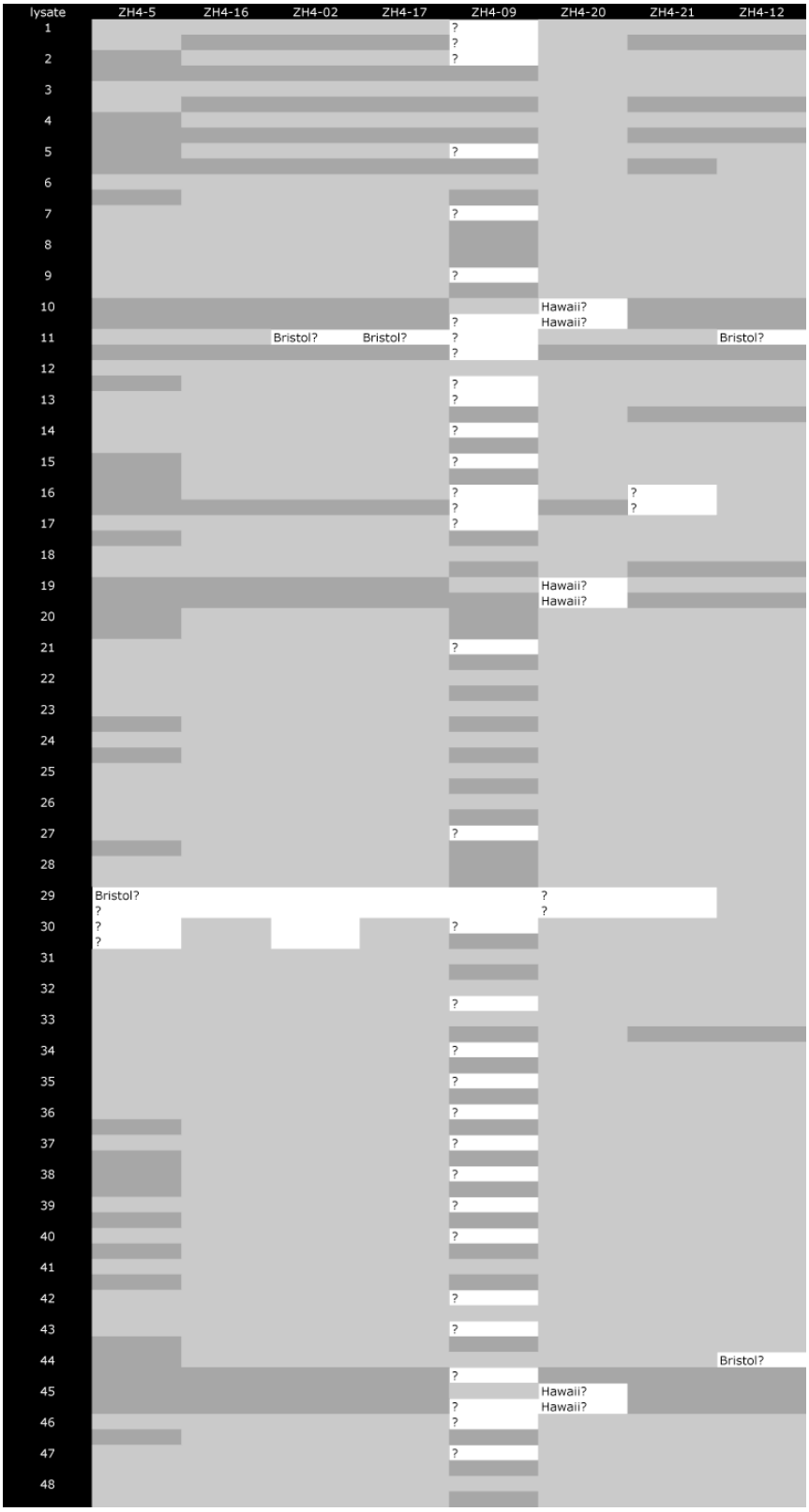

FLP mapping data *zh69*(IV)

FLP mapping data *zh69*(IV)

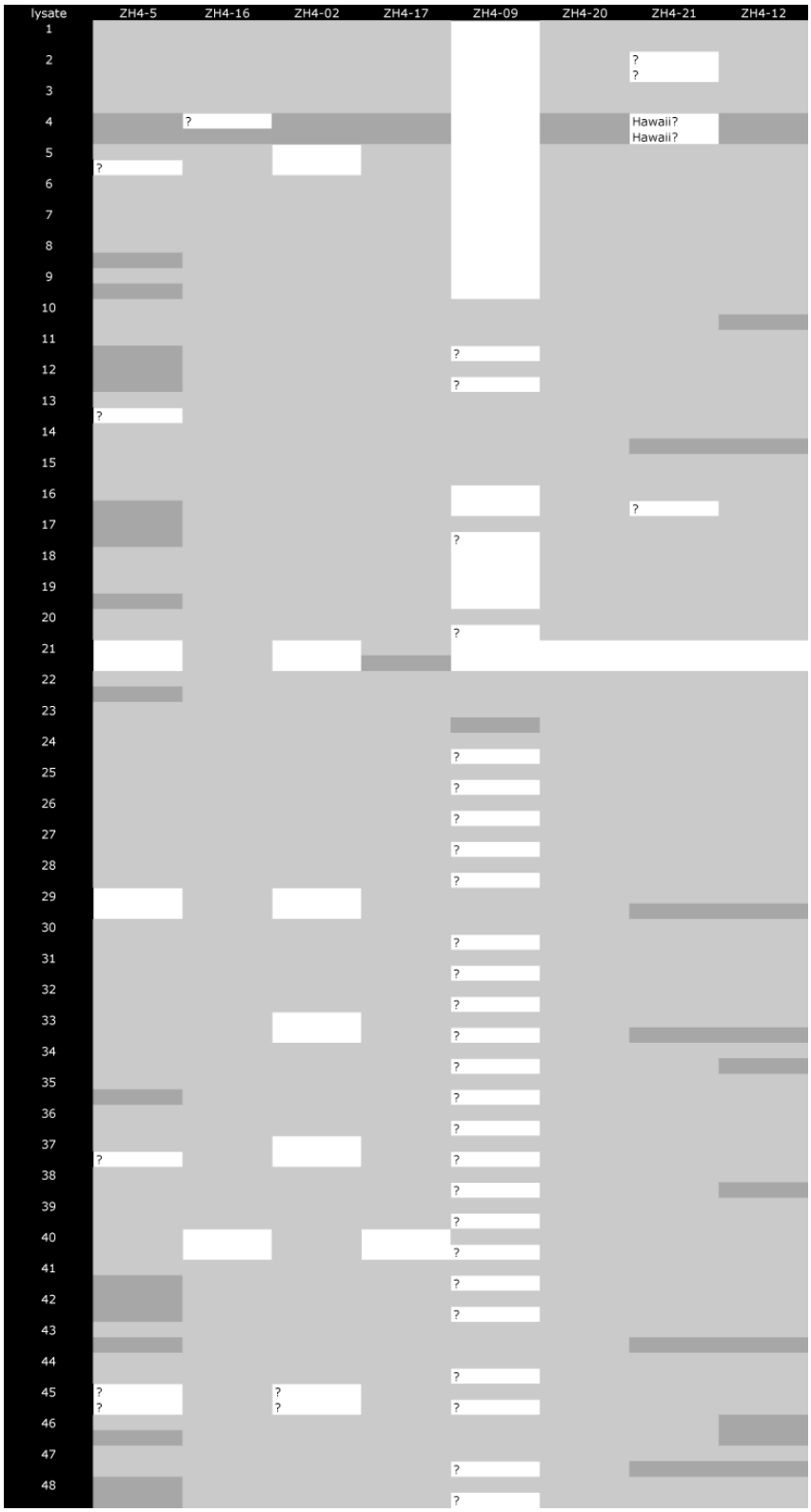

FLP mapping data *zh72*

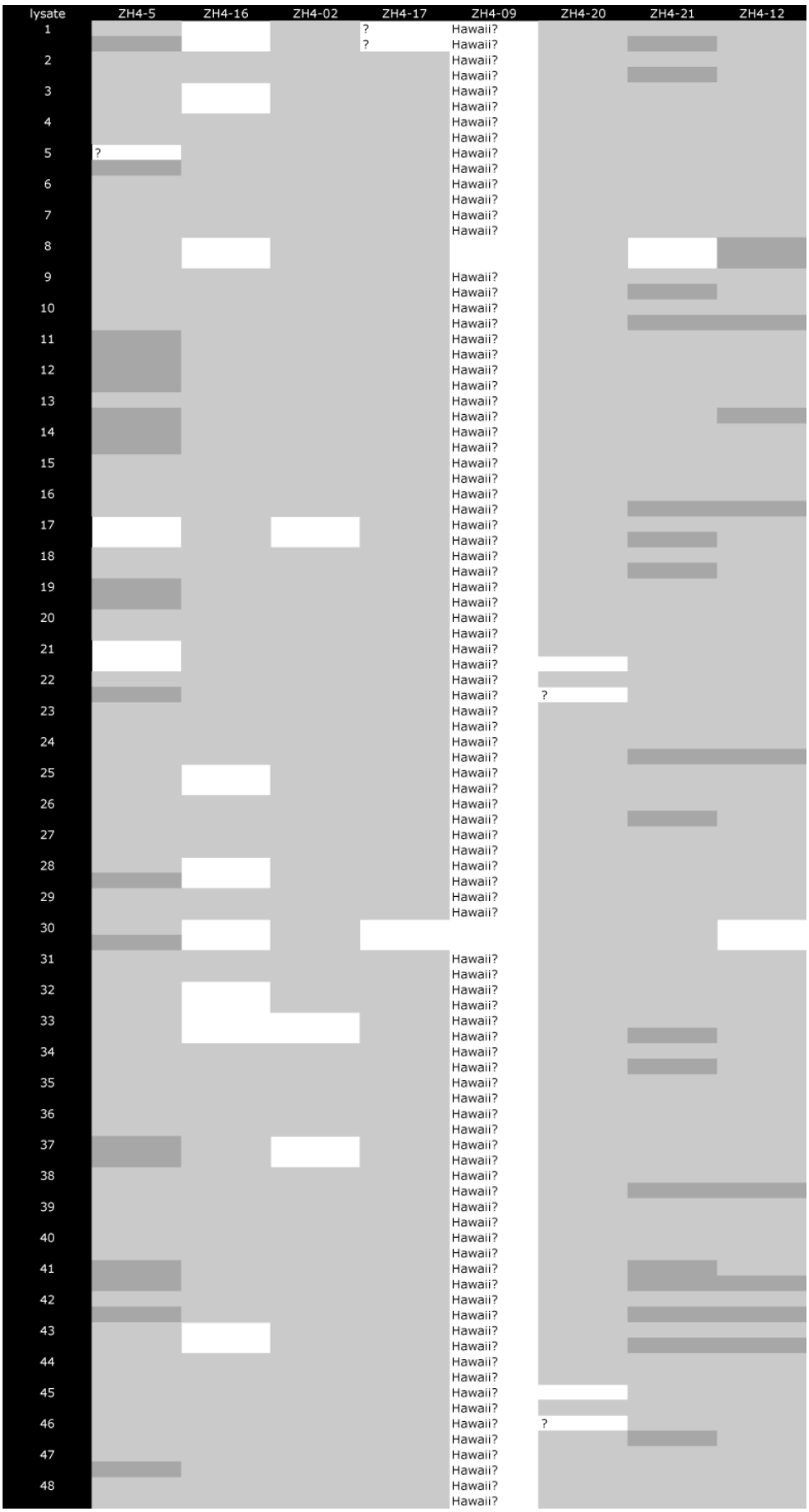

FLP mapping data *zh73*(I)

FLP mapping data *zh74* (II)

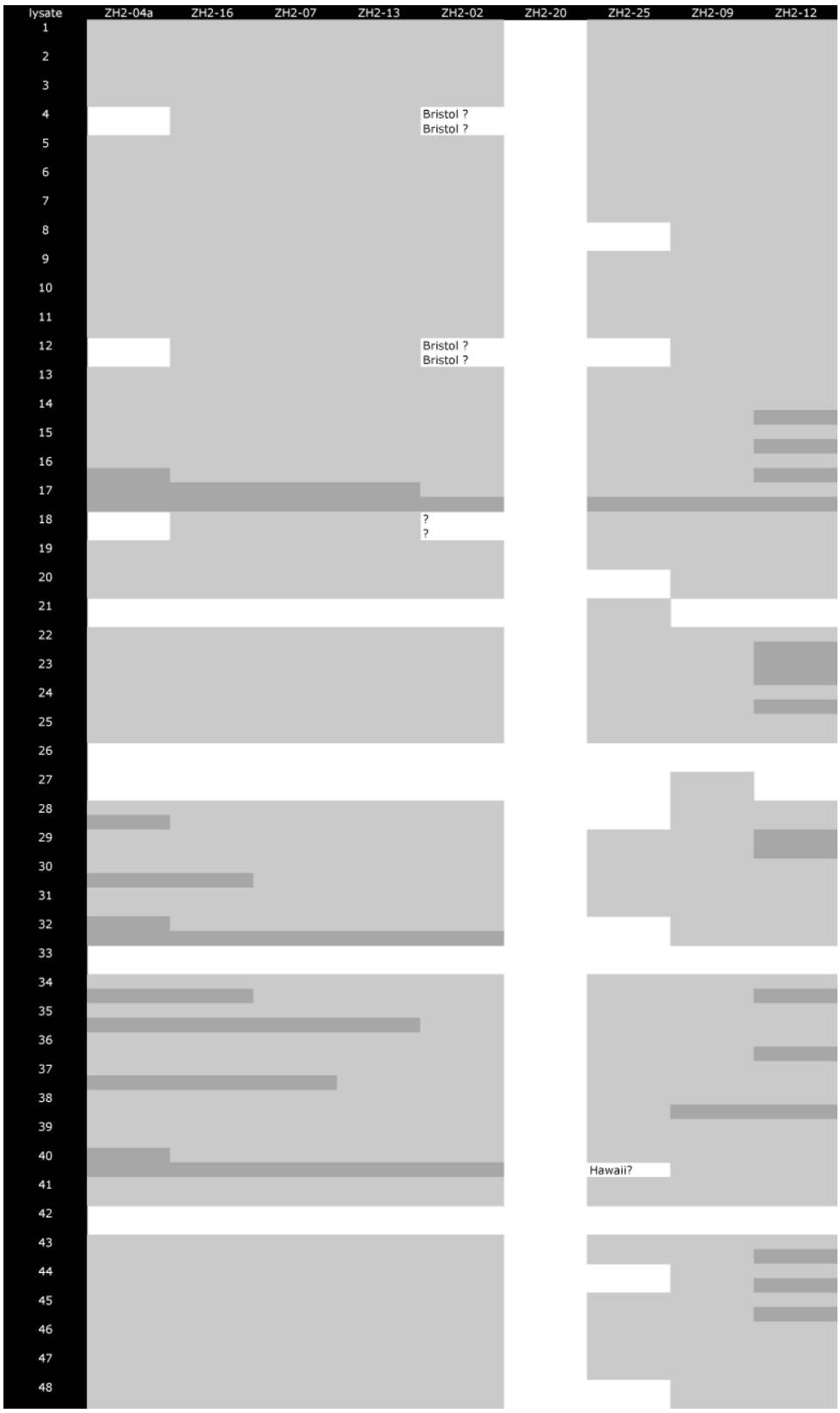

FLP mapping data *zh76*(IV)